LWP - 799
Copy No.

LANGLEY WORKING PAPER

THE LANGLEY TRANSONIC DYNAMICS TUNNEL

By Staff of the Aeroelasticity Branch

Langley Research Center
Hampton, Virginia

NOTICE

This document is provided for reference only. Although the information contained herein is generally correct, tunnel performance may be different from that shown and certain hardware items may no longer exist. Prospective users of this facility should contact the Head, Configuration Aeroelasticity Branch, MS-340, NASA, Langley Research Center, Hampton, VA 23665-5225, Area Code: (804) 864-1207, early in any proposed model program to obtain the latest information.

~~This paper is given limited distribution and is subject to possible incorporation in a formal NASA report.~~

NATIONAL AERONAUTICS AND SPACE ADMINISTRATION

September 23, 1969

Last Printing 7/92

LWP - 799
Copy No.

LWP -799

LANGLEY WORKING PAPER

THE LANGLEY TRANSONIC DYNAMICS TUNNEL

By Staff of the Aeroelasticity Branch

Langley Research Center
Hampton, Va.

This paper is given limited distribution
and is subject to possible incorporation
in a formal NASA report.

NATIONAL AERONAUTICS AND SPACE ADMINISTRATION

September 23, 1969

LWP - 799

September 23, 1969

LANGLEY WORKING PAPER

THE LANGLEY TRANSONIC DYNAMICS TUNNEL

Prepared by

Staff of the Aeroelasticity Branch

Approved by I. E. Garrick

I. E. Garrick
Chief, Dynamic Loads Division

Approved for distribution by Reage H. Barker

LANGLEY RESEARCH CENTER

NATIONAL AERONAUTICS AND SPACE ADMINISTRATION

TABLE OF CONTENTS

	PAGE
TABLE OF CONTENTS	i
LIST OF FIGURES	iii
INTRODUCTION	1
DESCRIPTION	1
AIRSTREAM OSCILLATOR SYSTEM	3
MODEL SUPPORT SYSTEMS	4
NONELECTRICAL UTILITIES FOR MODEL	6
INSTRUMENTATION, CONTROLS, AND DATA HANDLING	6
MODELS	10
REFERENCES	12
APPENDIX I - MEASUREMENT OF TUNNEL FLOW CONDITIONS	14
Total head pressure (H)	14
Static pressure (P)	14
Differential pressure (H-P)	14
Stagnation temperature (T_t)	14
Freon purity (X)	14
Mach-q Meter	15
Input	15
Computer operation	15
Accuracy	15
Estimation of Flow Characteristics	16
Air	16
Freon-air mixture	16
Equations for Flow Characteristics	16
Air	16
Air-Freon mixtures	16
Ratio of specific heat, γ	16
Speed of sound	17
Mass density	17
Viscosity, μ	17
Calculation of Tunnel Parameters	18
Equations	18

PAGE

APPENDIX II - TUNNEL DRIVE 22
Motor performance 22
Speed control 23

APPENDIX III - TUNNEL CALIBRATION 24
Mach number distribution 24
Wall boundary layer survey 25
Turbulence 25
Bypass valve operation 25
Airstream oscillator characteristics 25

LIST OF FIGURES

Figure 1.- General operating characteristics of the Langley transonic dynamics tunnel.

(a) Operating envelope using air or Freon-12 based on $T_t = 130^{\circ}F$ with no model in test section.

(b) Operation with Freon.

(c) Operation with air.

Figure 2.- General arrangement of the Langley transonic dynamics tunnel.

Figure 3.- Cross section through laboratory building, test chamber, control room, and test section.

Figure 4.- Representative variation of tunnel stagnation temperature with drive system power. Cooling system on above 100°F.

Figure 5.- General arrangement of test section.

Figure 6.- Cross section views through test chamber and test section.

Figure 7.- Control room floor plan.

Figure 8.- Sketch of airstream oscillator vanes and model, with cutaway showing schematic of mechanism.

Figure 9.- Approximate Mach number decrease caused by models, struts, and other objects in test section.

Figure 10.- Sting support system.

Figure 11.- Path of travel with angle of attack of two stations on a sting.

Figure 12.- Stings and adapters.

Figure 13.- Sidewall mounting plate.

Figure 14.- Crossbar support.

Figure 15.- Turntable installation.

Figure 16.- Bolt hole locations in turntable.

Figure 17.- Two-cable mount.

Figure 18.- Model on two-cable mount.

Figure 19.- Schematic diagram of typical two-cable mount systems and snubbers.

Figure 20.- Schematic diagram of aeroelastic buffet model support system.

Figure 21.- Layout of utilities.

Figure 22.- Model leads layout.

Figure 23.- NASA 36-bit time code (modified for point number).

Figure 24.- General block diagram of telemetry system.

Figure 25.- Dimensions and mass properties of telemetry components.

Figure 26.- Variation of Reynolds number per unit length with Mach number for air.

Figure 27.- Compressible flow relations for a 95-percent Freon-12 air mixture.

Figure 28.- Speed of sound for 95-percent Freon-12 air mixture.

Figure 29.- Mass density of 95-percent Freon-12 air mixture.

Figure 30.- Absolute viscosity of 95-percent Freon-12 air mixture.

Figure 31.- Variation of Reynolds number per unit length with Mach number for 95-percent Freon-12 air mixture.

Figure 32.- Longitudinal Mach number distribution.

(a) Tunnel centerline. Test medium, air.

(b) Tunnel sidewalls. Test medium, air.

(c) Tunnel top. Test medium, air.

(d) Tunnel sidewalls. Test medium, Freon.

(e) Tunnel top. Test medium, Freon.

Figure 33.- Maximum static variation from average value of local Mach number between stations 64 feet and 78 feet.

Figure 34.- Approximate maximum deviation from reference Mach number of average Mach number between stations 64 feet and 78 feet.

Figure 35.- Sample test section wall boundary layer velocity profiles. (Station 69.5 feet, center, east sidewall.)

Figure 36.- Test section wall boundary layer thickness. (Station 69.5 feet, center, east sidewall.)

(a) Freon-12.

(b) Air.

Figure 37.- Preliminary turbulence survey. Station 72-0, centerline, Freon. X-hot wire probe.

Figure 38.- Effect of bypass valve operation.

Figure 39.- Representative characteristics of airstream oscillator at Sta. 72.0 ft., M = 0.22, q = 53 psf, Freon-12, oscillator vane angle ± 5.93 deg., vanes in phase.

Figure 40.- Variation of vertical and horizontal components of gust angle across stream along axes through tunnel centerline. Vanes 180° "out of sync," vane angle ± 6°, Mach number 0.23.

NATIONAL AERONAUTICS AND SPACE ADMINISTRATION

THE LANGLEY TRANSONIC DYNAMICS TUNNEL

by Staff of the Aeroelasticity Branch

INTRODUCTION

The Langley transonic dynamics tunnel was designed to fill the need for a transonic wind tunnel capable of testing dynamic models of a size large enough to allow simulation of important structural properties of aircraft or spacecraft. Aeroelastic research conducted in this facility includes the study of flutter, aerodynamic loads, and input response. The wind tunnel is a continuous-flow tunnel which operates from Mach numbers near 0 to 1.20 at pressures ranging from about 0.2 psia to atmospheric pressure within the limits shown in figure 1 for the tunnel empty condition. Either air or Freon-12 is used as a test medium. Freon-12 (dichlorodifluoromethane) is a heavy gas with a low speed of sound. It has advantages over air in aeroelastic research such as making possible less difficult model construction, of simplifying data read-out because of slower time scale, of permitting closer simulation of Froude number, and of higher Reynolds numbers for a given amount of drive motor power. More detailed information on Freon-12 properties and computing procedures applying to its use is given in Appendix I. The use of Freon-12 as a test medium is discussed in references 1-4. The tunnel is located at building 648, on the corner of Dodd Boulevard and Mathis Road, in the east area of Langley Air Force Base, Hampton, Virginia.

DESCRIPTION

The major elements of the Langley transonic dynamics tunnel, as shown in figures 2 and 3, are the pressure-tight steel shell, electric motor drive system, cooling system, gas-handling system, tunnel control room and observation chamber, transonic test section, and model calibration laboratory.

The drive system consists of a two-speed range wound-rotor induction motor directly connected to a single stage fan, adjustable prerotation and stator vanes, and motor speed control system. The fan speed ranges are about 15 to 235 rps for operation in Freon-12 and 15 to 470 rps for operation in air. Motor speed is automatically controlled by the use of a liquid rheostat and eddy current brake to better than $\pm$ 1/4 percent. In each speed range the maximum shaft output is 20,000-horsepower continuous rating. Test section Mach number, which depends on compression ratio across the fan, is controlled

by varying the motor rpm and/or remotely varying the angle of prerotation vanes located ahead of the fan. A more detailed description of the drive system is given in Appendix II.

The tunnel cooling system consists of a cooling tower, pumps, and a two-row, vertical-finned tube cooler across the wind stream (fig. 2), through which water is circulated to maintain a test section stagnation temperature of less than 140° Fahrenheit. Representative tunnel stagnation temperature variation with power is shown in figure 4.

A large capacity pumping and gas separating system is used to vary tunnel pressure and change test medium. Valves are located upstream and downstream of the test section, as shown in figure 2, which may be closed to isolate the test section and surrounding chamber, thereby permitting more rapid access to the model by reducing the volume of gas which must be handled. Average times for performing these operations are shown in Table I. It should be noted that these gas-handling operations can extend testing time considerably for programs requiring frequent model adjustments. A typical flutter run, for example, may take two to four hours overall time when Freon-12 is used and tunnel access is required between runs.

The test section and surrounding 60-foot-diameter test chamber are shown in figures 2, 3, 5, and 6. The test section is about 16-feet square with filleted corners, giving a nominal cross-sectional area of 248 square feet. The ratio of area contraction of the entrance section is 8.9:1. The test section has a fairly uniform flow region which varies in length from about 30 feet at the lower subsonic Mach numbers to about 10 feet at the highest Mach numbers. Through this region the centerline Mach number variation is, at most, about $\pm$ 0.014 above Mach 1.0 and is generally less than $\pm$ 0.005 below Mach 1.0. A description of flow characteristics and calibrations is given in Appendix III. Transonic flow is generated by means of three slots in both the ceiling and the floor of the test section giving an open area of 2.1 percent in the test region. To alleviate model blockage effects, two short auxiliary slots are located on each of the two sidewalls giving an additional 2.3 percent open area. Tunnel wall corrections based on methods of reference 5 for the average model in this test section are small and are usually disregarded. Correction factors to the measured stagnation and static pressures are also relatively small and are usually not applied (see Appendix III). Double-hinged diffuser flaps across the width of the test section at the downstream ends of the slots in both the floor and the ceiling control flow reentry. The lower slots may be closed along the downstream 20 feet of their length when work on a model is in progress to prevent personnel from stepping through. For model and equipment installation a section of the test section floor, 12 x 35 feet in size, may be lowered as an elevator to the level of the second floor shop. A 6.4 x 14-foot hatch gives entrance through the tunnel shell. To facilitate handling of heavy equipment and models, a 6-ton crane is provided in the test chamber above the test section.

A device has been provided to quickly reduce the test section Mach number and dynamic pressure. This device consists of four quick-opening valves located in bypass lines which connect the test chamber and the tunnel

return leg downstream of the drive motor nacelle (figs. 2 and 3). Information on the reduction to be expected is given in Appendix III.

All tunnel controls are mounted in a 32-foot-long, 15-foot-diameter control room located within the test chamber alongside the test section (fig. 2). The control room is connected to the third floor of the building by a corridor and remains at atmospheric pressure. During tests the model controls and instrumentation are located in the control room or in the data instrument room on the third floor. A floor plan of the control room, drawn to the scale indicated, is given in figure 7 to facilitate instrument location planning. Direct visual observation of the model from the control room is provided from the side by eleven windows, each 18 x 24 inches, from a 3/4 front position by a 12-inch-diameter window, and from a 7/8 rear view by a small observation dome projecting into the airstream just forward of the downstream isolation valve.

To permit movie photography, the test section has 60 kilowatts of built-in lighting to provide up to 600 foot-candles of illumination from the front, rear, and side in the volume occupied by the usual model. Several 16 mm cameras using 400-foot reels are available for taking movies at several frame rates from 24 to 400 frames per second. Specialized cameras can be made available when required.

AIRSTREAM OSCILLATOR SYSTEM

A simulated gust field may be applied to the test section flow in the form of a sinusoidal oscillation of the flow direction. This oscillating flow is generated by a biplane arrangement of vanes on either side of the entrance section as shown in figures 2 and 8. Frequency is variable from 0 to 20 cps, and the two sides may be operated either in phase or up to 180° out of phase. Vane amplitude is manually adjustable (vanes not operating) from 0° to 12°. The operation of the vanes is power limited such that at 20 cps the maximum tunnel dynamic pressure is about 60 psf for 12° vane angle and about 350 psf for 3° vane angle. The variation of gust characteristics with frequency and position is discussed in Appendix III. In general, more specific information on airstream inputs for a given gust research program will be obtained from measurements during the investigation at applicable test conditions. More detailed information about the use of the system is also given in reference 6.

MODEL SUPPORT SYSTEMS

The wide variety of model configurations which have been investigated in this wind tunnel has required the use of numerous different support systems to meet the special requirements of each model. Several of the most frequently used systems are described in the following paragraphs. Model configurations which require support in some other manner (rods, wires, etc.) may also be tested but approval of the design prior to construction is required. Stress analysis of all mounting systems, where applicable, must be submitted prior to testing. For all dynamic models supported in a manner which permits body freedoms, a stability analysis of the model on the mount system must also be submitted prior to testing. If the mounting incorporates a snubbing system for emergency restraint, this condition must also be included in the analysis. These requirements are described in detail in a document available from this facility, entitled "Requirements for a 'Model Integrity Report' for Models to be Used in the Langley Transonic Dynamics Tunnel." This model integrity report must be submitted prior to construction of models and support systems to be tested in this wind tunnel.

Although not a critical consideration for many tests, support systems and model configurations having unusually high drag characteristics will appreciably decrease the tunnel Mach number capabilities and increase power requirements. This is especially evident with bluff or cylindrical supports and struts perpendicular to the windstream at supercritical Mach numbers. An estimate of the decrease in Mach number to be expected below that of the corresponding tunnel empty valve shown in figures 1(b) and 1(c) may be made from figure 9. This figure shows the approximate Mach number decrease, ΔM, vs. a drag parameter, $\Sigma C_D A$, where Σ represents the sum of each area multiplied by the respective drag coefficient for all of the objects installed in the test section. Allowance should be made, of course, for the effects of wake on those objects directly downstream of bluff bodies. The drag parameter $\Sigma \frac{D}{q}$, which is the sum of the drags of the various objects divided by dynamic pressure, may be used instead of $\Sigma C_D A$ if more convenient since these parameters are equivalent. Reference 7 is a useful source of information on drag coefficients for many kinds of objects. Several iterative steps may be necessary to determine reasonable values of drag coefficients in the range of Mach number where large variations occur. Power requirements are increased over those shown in figures 1(b) and 1(c) at corresponding Mach number and dynamic pressure conditions up to about 20 percent over the range of $\Sigma C_D A$ shown in figure 9.

One model support system for the transonic dynamics tunnel consists of a movable cantilevered sting, mounted on a vertical strut located downstream of the test section (fig. 10). The sting may be traversed vertically to maximum displacements of 62-5/8 inches above and 64-1/8 inches below the tunnel centerline, and may be rotated through an angle of attack range of about $\pm$ 15 degrees, the center of rotation being about a fixed point in the test section at station 71'-11.7". Streamwise and vertical displacements of two points on the sting from zero angle of attack positions are shown in figure 11.

The motion of other points along the sting may be determined using this plot. Figure 12 is a sketch of some of the stings and mounting adapters available. Detailed drawings, gages, and jigs for butt taper and threads and model-mount details can be furnished.

A rotatable plate one-inch thick by 16.47 inches in diameter is located in the east side wall of the test section at station 72'-0 opposite the control room, as indicated in figure 6. It can be rotated by motor drive through an angle range of 90°. Details of existing holes in this plate are shown in figure 13. Semispan wing models, for example, may be attached to this plate by bolting on a suitable mounting butt.

A crossbar support is available, as shown in figure 14, which can be attached to the semispan support on one end and pivoted on the opposite wall on the other end. This support provides high angle capability for relatively small sting mounted models, within the load range shown in figure 14. The high drag of the crossbar support, however, limits tunnel capability to a maximum Mach number of about 0.9 and reduces maximum dynamic pressure by about 20 to 25 percent.

A remotely operated turntable, shown in figure 15, is available for installation on the tunnel floor with the center of rotation at station 57'-0. The turntable can be rotated continuously in either direction through 360° at the rate of 250 degrees/minute. Angle is digitized for readout and recording. The turntable is a massive steel plate, 8 feet in diameter, and is equipped with a pneumatic system which applies pressure for an air bearing when the turntable is rotating and vacuum hold down when rotation is stopped. The location of existing holes in the turntable surface is shown in figure 16, however, other patterns may be used as necessary. In order to cover the 5-1/4-inch projection of the turntable above the tunnel floor a fairing is installed from about station 45 to 69.

A two-cable mounting system (ref. 8) for dynamic models of complete airplanes is often used in this tunnel. This system allows relatively large amplitudes of body motion. In this two-cable system, shown schematically in figures 17 and 18, the model is held by two cable loops, one extending to the tunnel walls in the upstream direction and the other in the downstream direction. One loop lies in a vertical plane (either upstream or downstream) and the other loop in a horizontal plane. Each cable loop passes through pulleys located within the fuselage contour. The cables are kept under tension by stretching a soft spring in the rear cable. Remotely operated trim control is provided in the model to keep it centered in the tunnel and is usually operated by a single "pilot" using a miniature airplane-type control stick. A lift counterbalancing device with a low spring rate and low mass is also available for use with the cable mount if high lift flight conditions need to be simulated. The device is capable of lift counterbalancing forces up to about 1200 lb. (see ref. 9). A snubber system is provided for emergency restraint. Although cable configurations vary with model requirements, some representative dimensions are shown in figure 19. The dynamic characteristics of the suspension system vary with model configuration and to assure adequate stability and satisfactory flying qualities, an

analysis (Fortran program available) is required before a test program is undertaken. Experience has also shown it advisable in investigations of expensive and complex dynamic and elastic models, to first check out the system with a relatively inexpensive simplified "dummy" model which is approximately geometrically scaled but with only the overall mass and inertia properties represented.

An example of a mounting system which provides the freedom necessary for a simulation of free-free modes of launch vehicles is shown schematically in figure 20. This system, which was used successfully in one investigation, is described in reference 10. Briefly, it consists of a sting on which the model is supported through a system of cables and springs. Leaf springs support the model at the forward and rear node points through pulleys to support the weight. The cables run outside to adjustable torque springs which provide the remaining part of the pitch stiffness. The pneumatically operated snubbers were used to restrain model motion with respect to the sting when necessary. Another feature is the electromagnetic shaker used to excite the model in its elastic vibration modes in order to determine the aerodynamic damping in each mode. Since mounting systems of this type are highly dependent upon the particular model configuration, extensive modifications to existing hardware would probably be necessary before it could be used again.

NONELECTRICAL UTILITIES FOR MODEL

Stainless steel tubing has been installed in the wind tunnel, terminating near both the sting support and the semispan mount, and in the calibration lab, terminating near the backstop, and may use air, water or hydraulic fluid to operate mechanisms such as shakers or motors in the models. Provisions are made for routing this tubing through the tunnel control room if manual valve control is required. Details are given in figure 21. A pump is installed for pumping 150 gpm of treated water at approximately 90°F. Chilled water (about 40°F) is available through a heat exchanger cooled by water from a central system.

INSTRUMENTATION, CONTROLS, AND DATA HANDLING

Readout and recording equipment and model controls are normally assembled from portable components, and are located in the tunnel control room or data instrument room during tests. Space is provided in the shop area adjacent to the control room for any equipment that cannot be placed in these rooms. Equipment cabinets to go into the control room cannot be larger than 60 inches long by 30 inches wide by 80 inches tall.

Power available in the control room includes 6 regulated 115 V ac circuits and 11 unregulated 115 V ac circuits (including seven night circuits), with provisions for additional power supplies as required. Details of the power available are given in figure 22.

Permanent, 4-conductor shielded electrical leads are installed in the wind tunnel running from the control room to points in the sting support and near the semispan mount. The sting base contains seven 32-prong connectors plus four iron-constantan thermocouple leads. A junction box adjacent to the semispan mount contains 48 4-pin connectors. Details of the plugs required to fit these connectors are shown in figure 22. Provisions are available for bringing other leads or piping into the control room from the test chamber by potting through utility pipes which terminate below the control room floor.

Data readout during tests includes both tunnel operating conditions and model data. Tunnel static and stagnation pressures and stagnation temperature are displayed continuously, and test section Mach number and dynamic pressure are computed by an analog computer and displayed continuously. Instrumentation for measuring these quantities is described in Appendix I. The displayed tunnel conditions are automatically printed for each data point by an IBM tabulator (Model 419) and summary card punch (Model 523). In addition, provision is made for printing and punching up to 78 manually preset digits.

Strain gage signals and other outputs from the model are read out in various ways to suit test conditions. Static data may be read out on automatic, resistive, balance-type indicators and the signals can be digitized and printed on the typewriter and card punch. For these indicators, 2,000 micro-inch/inch strain gives a full-scale reading of 2,000 counts. Normally 120 ohm gages are used but other resistance gages are permitted. Tunnel parameters and other data on the punched cards are reduced by a Fortran IV program through a remote terminal station located in the building by the facilities of the LRC Data Reduction Center.

A 100-tube liquid manometer (120-inches tall) is available for general purpose static pressure measurements. Tubes are connected to a central patch board in the test chamber beneath the test section. The manometer is backlighted for photographing with a K-22 camera. Manometer liquid is butyl phthalate (sp. gr. 1.045 at 75°F). Use of this manometer for numerical data acquisition purposes, however, has been almost entirely superseded by scanivalves and machine data processing equipment.

Methods of handling dynamic data vary with the particular investigation. Some of the specialized equipment listed in the following paragraphs is used in data acquisition and reduction:

A Hyperion Model HI-150-591 time-code generator-monitor generates a precise time reference in modified NASA 36-bit code (fig. 23) and provides output and display for point number (000-999) and time in hours, minutes, and seconds. As a monitor it will demodulate time-code signals from magnetic tape (using compatible components) for transferring to a visual time and point number display and/or search mode. Using generator mode and translator control unit, point number and time may be recorded on command by the IBM data typewriter and card punch.

A wide variety of small instrumentation such as scopes, power supplies, amplifiers, various kinds of filters, recorders, and other readout instruments can be drawn as needed from an instrumentation pool. Such equipment is usually obtainable on demand or is on long-term assignment to the facility. To insure availability at a particular time, however, a list of the specific items should be submitted in advance.

Specialized instruments presently available at the tunnel are as follows:

(a) Ampex Corporation
401 Broadway
Redwood City, California 94063

Tape recorder systems:

Transports				
Model	FR 100C	FR 600	FR 1200	FR 1200
Rec/Play	1	1	1	
Play				1

Electronics										
Mode	Dir. Rec.	Dir. Repro	FM Rec.	FM Repro	PDM Rec.	PDM Repro	Equalizers			
							1 7/8	7 1/2	15	60
Number chan.	11	16	13	27	2	2	8	6	16	1

(b) Boonshaft and Fuchs, Inc.
Hatboro Industrial Park
Hatboro, Pennsylvania 19040

Six No. 711 analog transfer function analyzers.

(c) Technical Measurement Corporation
441 Washington Avenue
North Haven, Connecticut 06473

One CAT 400C computer of average transients; one model COR 256 correlation computer; one model 600 computer accessory unit. This equipment can be used for real-time computation of statistical quantities such as correlation functions and probability density.

(d) Flow Corporation
205 Sixth Street
Cambridge, Massachusetts 02138

Two computerized model DFA X-array constant-temperature hot-wire anemometer systems for measuring instantaneous stream flow angles and turbulence.

(e) Data Control Systems, Inc.
Danbury
Connecticut 06810

One subcarrier discriminator, model GFD-5. Model GFD-5 is a transistorized, pulse-averaging discriminator designed for use in Data Control System's UNIDAP data systems. Interchangeable, plug-in tuning units and low pass filters may be selected for the subcarrier channel and filter characteristics desired. Bandpass filters may be modified to handle a constant percentage deviation system (standard IRIG) or a DCS constant frequency system. The DCS employs a constant bandwidth using five discrete channels for each system.

(f) Hewlett-Packard Company
395 Page Mill Road
Palo Alto, California 94306

One Dymec DY-6664 data acquisition system with IBM 526 card punch. System will sequentially measure 25 data channels at selectable (3) sampling rates. The system uses an integrating digital voltmeter which measures dc voltages in five ranges from $\pm$ 0.1 volt to $\pm$ 1000 volts. In addition to voltage measurements, direct-frequency measurements from 5 cps to 300 kc can be made. In addition to the 25 data channels, 10 manually set constants may be put into the cards by thumbwheel switches. The output of an IBM typewriter may also be put into the cards.

(g) A microelectronic telemetry system is available for installation in models which require minimum size of the electrical cable bundle. Features of this system are described in reference 11. As illustrated in the general schematic layout of figure 24, the system receives commands and transmits data signals using a single 1/16-inch-diameter coaxial cable. Power is supplied through two 28 V dc power cables (copper-clad snubber cables may be used for this purpose). The system will transmit simultaneously up to 20 channels of analog data from transducers within the model. A remotely actuated 6-position transducer selector allows use of up to 120 transducers with the 20 channels on a time-shared basis. In addition, the coaxial cable is used to transmit coded gain and offset commands to on-board signal conditioning units in each channel, switch commands to transducer selector unit, operate commands for each of three trim control motors, and programmed

operate commands to three variable speed motors. The outputs of signal control and conditioning units modulate 20 voltage controlled FM oscillators (200 cps capability) grouped in four blocks of five oscillators each, giving a modular arrangement such that 5, 10, 15 and 20 channels may be used as required. Each of the four blocks is recorded on a separate tape channel. The system provides amplification to a 5-volt full-scale output for each of four remotely selectable ranges of transducer input (5, 10, 25, and 50 millivolts full scale). Transducer power is furnished by power converters of the required voltage and number to supply the necessary current. Current capacities of the converters and requirements of the data modulators is shown on figure 24 to aid in determining unit requirements. Gyro instrumentation requiring ac power (such as 400 or 800 cycle) may be powered by suitably matched 28 V dc/ac power converters on-board or else supplied through additional cables from external power sources. Physical dimensions and mass properties for each of the on-board telemetry components are given in figure 25 for model layout purposes.

MODELS

The use of aeroelastically and dynamically scaled models is reviewed extensively by Regier (ref. 12) and Guyette (ref. 13). These papers also make reference to numerous treatments of similitude relationships. Several charts in Appendix I give approximate values of compressible flow relationships and physical properties of a typical 95-percent mixture of Freon 12 and air for use in extimating tunnel parameters in scaling models when this test medium is to be used.

Because of flow considerations and other problems of technique, discussed to some extent in reference 14, it is recommended that model wing spans be limited to about 8 or 9 feet for flutter models and to about 6 feet for gust models. Low-speed aerodynamic-type models may be considerably larger. Body lengths greater than about 12 feet may involve some compromises in flow uniformity, range of movement, and support configuration. Models mounted vertically on the turntable, as in ground wind loads investigations, should be limited to 14 feet in height.

As mentioned previously under Model Support Systems, model integrity requirements are defined in a document available from this facility. A model integrity report must be submitted before construction of any model to be tested in this wind tunnel. In addition to stability analysis requirements, this specification states that strength requirements for models vary with the kind of model. Nonelastic models, mountings, attachments, etc., should, in general, have a minimum factor of safety of 3 on the yield or 4 on the ultimate for all critical structural parts at the most severe load conditions. Screw-fastened joints should be capable of sufficient torque to provide greater holding force than maximum expected loads. No specific strength requirements are defined for the structures of elastically and

dynamically scaled models since stiffness and mass considerations usually dictate the structural configuration. Such structures, however, must be shown to have adequate strength to meet test objectives. Experience has shown that failures due to inadequate engineering of covering sections, stores, nacelles, fairings, and other sometimes seemingly minor parts have caused numerous delays in the test programs and on some occasions triggered off major failures. For this reason a strength analysis should be made of all external covering sections and other parts in contact with the windstream. This analysis should be based upon a reasonable estimate of local differential pressures and should show that the part has adequate strength and stiffness for the maximum test conditions (conditions of instability such as flutter excepted).

In addition to strength considerations, materials should be compatible with the required tunnel environmental conditions, both during testing and during processing (Freon-air interchange). Stagnation temperatures may be estimated from figures 4 and 1(b) or 1(c). Between runs and at the beginning of runs, temperatures may tend to approach outdoor temperatures because of the steel tunnel shell. During Freon processing, pressures in the test chamber are usually reduced for short periods of time to about 1 psia. Interior spaces should be sufficiently vented and materials such as foamed plastics should allow such pressure variation without damage. Dry Freon-12 vapor as used in this tunnel generally causes no problems in the use of conventional model materials. There may be, however, a small quantity of oil vapor present in the windstream when operating with Freon. Discharge of contaminates from the model into the tunnel cannot be permitted during Freon operation. Model surfaces should also permit flourescent oil flow studies where applicable.

Models submitted for testing in this wind tunnel should be addressed as follows:

Head, Aeroelasticity Branch
National Aeronautics and Space Administration
Langley Research Center
Building 648, Mail Stop 340
Hampton, Virginia 23365

Telephone number: Area Code 703, 827-2665

REFERENCES

1. Huber, Paul W.: Use of Freon-12 as a Fluid for Aerodynamic Testing. NACA TN 1024, 1946.

2. Von Doenhoff, Albert E.; Braslow, Albert L.; and Swartzberg, Milton A.: Studies of the Use of Freon-12 as a Wind-Tunnel Testing Medium. NACA TN 3000, 1953.

3. Yates, E. Carson, Jr.; Land, Norman S.; and Foughner, Jerome T., Jr.: Measured and Calculated Subsonic and Transonic Flutter Characteristics of a 45° Sweptback Wing Planform in Air and Freon-12 in the Langley Transonic Dynamics Tunnel. NASA TN D-1616, 1963.

4. Pozniak, D. M.: Investigation Into the Use of Freon-12 as a Working Medium in a High-Speed Wind Tunnel. College of Aeronautics, Cranfield (Great Britain), Note No. 72, Nov. 1957.

5. Davis, Don D., Jr.; and Moore, Dewey: Analytical Study of Blockage- and Lift-Interference Corrections for Slotted Tunnels Obtained by the Substitution of an Equivalent Homogeneous Boundary for the Discrete Slots. NACA RM L53E076, June 1953.

6. Gilman, Jean, Jr.; and Bennett, Robert M.: A Wind-Tunnel Technique for Measuring Frequency-Response Functions for Gust Load Analysis. AIAA J. of Aircraft, Vol. 3, No. 6, Nov.-Dec. 1966.

7. Hoerner, Sighard F.: Fluid-Dynamic Drag. Published by the author, Dr.-Ing. S. F. Hoerner, 148 Busteed Drive, Midland Park, N. J., 1958.

8. Reed, Wilmer H., III; and Abbott, Frank T., Jr.: A New "Free-Flight" Mount System for High-Speed Wind-Tunnel Flutter Models. Proceedings of the Symposium on Aeroelastic and Dynamics Modeling Technology, U.S. Air Force Systems Command, RTD-TDR-63-4197, Pt. I (1964).

9. Rainey, A. Gerald; and Abel, Irving: Wind-Tunnel Techniques for the Study of Aeroelastic Effects on Aircraft Stability, Control, and Loads. Paper presented at the AGARD Flight Mechanics Panel Meeting, Marseilles, France, April 21-24, 1969.

10. Hanson, Perry W.; and Jones, George W., Jr.: The Use of Dynamic Models for Studying Launch Vehicle Buffet and Ground-Wind Loads. Proceedings of Symposium on Aeroelastic and Dynamic Modeling Technology, RTD-TDR-63-4197, Pt. I, March 1964.

11. Schrader, J. H.; Nichols, C. H.; Shriver, C. L.; and Taylor, L. V.: A Microelectronic Data and Control System for Wind Tunnel Applications. NASA LWP-691, Dec. 12, 1968.

12. Regier, Arthur A.: The Use of Scaled Dynamic Models in Several Aerospace Vehicle Studies. Paper presented at a colloquium on the use of models and scaling in shock and vibration, Winter Annual Meeting of the ASME, Nov. 19, 1963.

13. Guyette, P. R.: The Use of Flexible Models in Aerospace Engineering. RAE Technical Rept. No. 66335, Nov. 1966.

14. Goethert, Bernhard H.: Transonic Wind Tunnel Testing. Pergamon Press, 1961.

15. Ames Research Staff: Equations, Tables, and Charts for Compressible Flow. NACA TR 1135.

16. Thermodynamics and Physics of Matter. Vol. 1, High Speed Aerodynamics and Jet Propulsion, Princeton University Press, 1955.

17. Tables of Thermodynamic and Transport Properties of Air, Argon, Carbon Dioxide, Carbon Monoxide, Hydrogen, Nitrogen, Oxygen, and Steam. Pergamon Press, 1960.

18. Masi, J. F.: Thermodynamic Properties of Gaseous Dichlorodifluoromethane. Journal American Chemical Society, Vol. 74, pp. 4738-4741, 1952.

19. Article by Kinetic Chemicals, Inc.: Refrigerating Engineering. April 1939.

20. Brokaw, Richard S.: Alignment Charts for Transport Properties, Viscosity, Thermal Conductivity, and Diffusion Coefficients for Nonpolar Gases and Gas Mixtures at Low Density. NASA TR R-81, 1961.

APPENDIX I

MEASUREMENT OF TUNNEL FLOW CONDITIONS

Total head pressure (H).- Total head is obtained from a total head tube located on the west side of the tunnel entrance cone on the centerline, at station 0, and which extends about 24 inches out from the wall. Pressure is measured by an Ideal-Aerosmith mercury manometer with an automatic tracker linked by servo to a counter on the control room desk and digitized to print on the IBM tabulator and card punch. The manometer has a range of 0 to 2200 psf. Absolute accuracy usually is ± 0.5 psf. Relative accuracy of the instrument after correcting for wind-off zero shift is about ± 0.3 psf. The pressure reading is displayed, punched, and printed to 0.1 psf.

Static pressure (P).- The static pressure is picked up in the test chamber. It is measured with instruments identical to those used for total head.

Differential pressure (H-P).- Two other Ideal-Aerosmith mercury manometers similar to that described under "total head pressure" are connected to alternate total head and static pressure sources. The outputs of these manometers are interconnected to display and read out differential pressure (H-P) as described above. For very small values of differential pressure, a liquid (such as water) micromanometer can be connected to an alternate total head tube and static orifice. Accuracy is about 0.05 psf and range of differential pressure is up to 115 psf. This manometer is manually read and logged.

Stagnation temperature (T_t).- The stagnation temperature is measured with thermocouples located between the turning vanes a few feet downstream of the tunnel cooling coil. The cooling coil is divided into six banks with the flow of water to each bank adjusted to maintain reasonably uniform temperature across the span of the coil. Behind each bank is a thermocouple originally installed to balance the coil. These thermocouples read out individually by means of a selector switch to a Honeywell-Brown indicator. A thermocouple indicating an average value is selected. An accuracy of about ± 2°F is expected for average stagnation temperature. A digitizer connected to this instrument permits recording temperature from the selected thermocouple on the IBM tabulator and punch. In addition to these six thermocouples, there are four more thermocouples located behind the cooling coil whose average signal is indicated on a Swartwout meter (located on the upper part of the control room desk) and used to automatically control tunnel temperature.

Freon purity (X).- Freon purity is obtained by measuring the oxygen content of the gas mixture and assuming that the mixture is comprised only of air containing 20-percent oxygen by volume and of Freon. A Beckman Model F3 oxygen analyzer measures the amount of oxygen. The zero oxygen point is adjusted by passing pure Freon through the meter. The meter, which operates at atmospheric pressure, is supplied with the sample gas mixture by 2 two-stage diaphragm-type pumps which do not contaminate the sample and which operate at tunnel pressures as low as 70 psf. Air in-leakage to the system amounts to

2 percent at 500 psf and 4 percent at 70 psf. At low pressures the zero oxygen point is adjusted to compensate for this in-leakage. The tunnel gas is sampled a few feet downstream of the test section butterfly valve. Freon purity can be read to 0.1 percent by volume.

Mach-q Meter

Input.- Because of the dependence of both Mach number and dynamic pressure on four measured variables, H, P, T_t and X, it was necessary to construct a computer to provide a running check on M and q during operation of the tunnel. The computer is an analog device into which are fed electrical signals proportional to the measured variables. Since it has been found impractical to connect the Beckman instrument directly to the computer to provide a continuous signal of X for obtaining γ, a value of γ is inserted into the computer manually.

Computer operation.- The computer contains circuits to add, subtract, multiply, and divide, plus three diode function generators. One generator produces a signal of M as a function of $\frac{H-P}{H}$ for a constant γ value of 1.01 with the curve divided into 30 straight line elements. The other two generators insert corrections to the M signal as a function of $(\gamma_{true} - 1.01)$. Dynamic pressure is computed as the product of $\frac{\gamma}{2} M^2 P$. Signals of M and q are transmitted for display in the control room and are digitized for the IBM data recording system.

Accuracy.- Within the pressure range from 0.5 psia to 14.7 psia and Mach number range from 0.3 to 1.4 the computer was designed to be accurate within 0.002 in Mach number and one percent in dynamic pressure. Calibration indicates errors in q as much as $\pm$ 1 psf when H is below 100 psf and $\pm$ 3 psf when H is above 1000 psf. Below Mach 0.3, sizable errors occur because a linear relation between $\frac{H-P}{H}$ and M was assumed in the circuit design.

For true M values of 0.10, and 0.20 and 0.25, computer M values are 0.03, 0.135, and 0.21, respectively. Since q is a function of M^2, errors in q are about double the errors in Mach number.

For most tests using Freon a constant value of $\gamma = 1.14$ can be used in the Mach-q meter with negligible errors; for values of X above 0.80, maximum error will be $\pm$ 0.8 percent in q.

Estimation of Flow Characteristics

Air.- Since flow quantities for air are readily estimated from available tables and charts in TR 1135 (ref. 15), these will not be given here. Figure 26 showing the variation of Reynolds number per unit length with Mach number is given, however, to cover the range of tunnel conditions in somewhat more detail than that given in chart 25 of reference 15.

Freon-air mixture.- Flow quantities for a 95-percent Freon-air mixture, which is representative of that used in many tests, may be estimated for purposes such as model scaling from the following charts:

Compressible flow relations: $\frac{P}{H}$, $\frac{T}{T_t}$, $\frac{\rho}{\rho_t}$, $\frac{q}{H}$ vs. M (fig. 27)

Speed of sound vs. temperature for various values of P (fig. 28)

Mass density vs. pressure for various values of T (fig. 29)

Absolute viscosity vs. temperature (fig. 30)

Reynolds number per unit length vs. Mach number (fig. 31)

Equations for Flow Characteristics

Air.- Equations for computing various flow quantities in the test section are obtained from reference 15. Consistent with TR 1135, the value of γ employed is 1.400 and the value of the gas constant R is 1716 $ft^2/sec^2\,{}^\circ R$. Absolute zero is considered to be - 460°F.

Air-Freon mixtures.- In deriving working equations for air-Freon mixtures, it is presumed that Freon purity is always greater than 80 percent by volume. Equations which have been simplified are not necessarily accurate at lower purities. Reference 16 was used in deriving equations for the ratio of specific heat, speed of sound, density, and viscosity.

Ratio of specific heat, γ.- In reference 16, equations of state for the gas mixture were obtained from section 3, chapter 3, by J. A. Beattie. Values of C_p and C_v as a function of temperature and pressure were obtained from references 17 and 18. The rather complicated equation derived was simplified (with a curve fitting accuracy of 0.1 percent) to the following expression:

$$\gamma = 1.4003 - 0.096X + (0.1183)10^{-3}P - (0.5197)10^{-3}T - (0.3919)10^{-6}PT + (0.3579)10^{-6}T^2 + (0.3350)10^{-9}PT^2 \qquad \text{(A-1)}$$

where

γ = ratio of specific heats

X = Freon purity, fraction by volume

P = static pressure, psf

T = static temperature, $^{\circ}R(460 + {}^{\circ}F)$

Speed of sound, a.- The speed of sound of the gas mixture is obtained from the fundamental expression:

$$a^2 = K \frac{dP}{d\rho}$$

Pressure, P, is obtained in terms of ρ from equation of state of gas mixture and an equation for a derived. This equation has been simplified (within 0.2-percent accuracy) to:

$$a = 522.7 + 0.6434T - 0.2187XT - 415.7X$$
$$164.0X^2 + \left[3.24 + 0.02584XT - 0.00387T - 18.45X\right]10^{-3}P \qquad \text{(A-2)}$$

where a is speed of sound in feet per second and X, P, and T have the same definition and units as in the γ equation.

Mass density, ρ.- The density of the gas mixture is obtained directly from the equation of state for the gas mixture. Simplifying the equation (within 0.1-percent accuracy) results in:

$$\rho = \frac{(0.3150 + X)P}{540.70T\left[1 - \left(-0.02908 + 0.01066X + \frac{13.55}{T}\right)(10^{-3})P\right]} \qquad \text{(A-3)}$$

where ρ is in slugs per cubic foot.

Viscosity, μ.- The equation for viscosity was obtained by using methods outlined in reference 16, section D, "Thermodynamics and Physics of Matter." The general equations of viscosity were obtained and values of viscosity for pure Freon were obtained from Kinetic Chemicals, Inc., work published in reference 19. The final equation for viscosity is:

$$\mu = (1.557)10^{-8}\left[\frac{332.8 - 0.1035T + \frac{X}{1 - X}(298.1 - 0.0908T)}{211.7 - 0.113T + \frac{X}{1 - X}(464.8 - 0.224T)}\right]T^{1/2} \qquad \text{(A-4)}$$

where μ is in units of lb sec/ft^2.

Since this equation was derived, a more exact method for obtaining viscosity has been developed in reference 20. Agreement appears to be good between the two methods for the range of interest of this tunnel.

Calculation of Tunnel Parameters

Recorded values	Quantity	Decimals
H	Total head pressure, lb/ft^2	0000.0
P	Static pressure, lb/ft^2	0000.0
t_t	Stagnation temperature, $^{\circ}$F	000.0
X	Freon purity, fraction	0.000
ℓ	Representative length, ft	0.000

Reduced values	Quantity	Decimals
γ	Ratio of specific heats	0.000
M	Mach number	0.0000
q	Dynamic pressure, lb/ft^2	000.00
ρ	Mass density, slugs/cu ft	0.000000
a	Speed of sound, ft/sec	0000.00
V	Velocity, ft/sec	0000.00
μ	Viscosity, lb sec/ft^2	0.0000000000
R_N	Reynolds number	0000000.

Equations.- Standard Data Reduction equations for air should be used where applicable. Equations (A-5), (A-6), and (A-7) should be used for either air or Freon data. Equations (A-8) through (A-17) are presented primarily for the reduction of data obtained in Freon. Note that the number of figures following the decimal point is given where important. When pressure data are measured in terms of (H-P) and P rather than H and P, use equations (A-18) and (A-19) to obtain H and P, then proceed by usual steps. Small differences exist between H and P values with wind-off due to instrument error. An

arbitrary assumption is made that the error exists in P and the following equation results:

$$\Delta P = H_{\text{wind off}} - P_{\text{wind off}} \quad \text{(Use initial zero for each group.)} \tag{A-5}$$

$$P_1 = P + \Delta P \tag{A-6}$$

Stagnation temperature, $^{\circ}R$

$$T_t = t_t + 460 \tag{A-7}$$

Since γ and T_1/T_t are mutually dependent, an iteration process must be used to obtain exact values. As the values are rapidly convergent it is sufficient to use an assumed $\gamma_1 = 1.14$ as follows:

$$T_1 = T_t\left(\frac{P_1}{H}\right)^{\frac{\gamma_1 - 1}{\gamma_1}} = T_t\left(\frac{P_1}{H}\right)^{0.1228} \quad \left(\frac{P_1}{H} \text{ to 4 dec., } T_1 \text{ to 3 dec.}\right) \tag{A-8}$$

$$\begin{aligned}\gamma_2 = {} & 1.4003 - 0.096X + (0.1183)10^{-3}\, P_1 - (0.5197)10^{-3}\, T_1 \\ & - (0.3919)10^{-6}\, P_1 T_1 + (0.3579)10^{-6}\, T_1^{\,2} + (0.3350)10^{-9}\, P_1 T_1^{\,2}\end{aligned} \tag{A-9}$$

$$T_2 = T_t\left(\frac{P_1}{H}\right)^{\frac{\gamma_2 - 1}{\gamma_2}} \quad \left(\frac{\gamma_2 - 1}{\gamma_2} \text{ to 4 dec., } T_2 \text{ to 3 dec.}\right) \tag{A-10}$$

To obtain the desired accuracy in the following equations, γ_2 and T_2 should be carried to 4 decimal places and 3 decimal places, respectively.

$$M = \left[\frac{2}{\gamma_2 - 1}\left(\frac{T_t}{T_2} - 1\right)\right]^{1/2} \quad (M \text{ to 4 dec.}) \tag{A-11}$$

$$q = \frac{1}{2}\gamma_2 P_1 M^2 \qquad (q \text{ to 2 dec.}) \tag{A-12}$$

$$a = 522.7 + 0.6434T_2 - 0.2187XT_2 - 415.7X + 164.0X^2$$
$$+ (3.24 + 0.02584XT_2 - 0.00387T_2 - 18.45X)(10^{-3})P_1 \qquad (a \text{ to 2 dec.}) \tag{A-13}$$

$$V = Ma \qquad (V \text{ to 2 dec.}) \tag{A-14}$$

$$\rho = \frac{(0.3150 + X)P_1}{540.70T_2\left[1 - \left(-0.02908 + 0.01066X + \frac{13.55}{T_2}\right)(10^{-3})P_1\right]}$$
$$(\rho \text{ to 6 dec.}) \tag{A-15}$$

$$\mu = (1.557)10^{-8}\left[\frac{332.8 - 0.1035T_2 + \frac{X}{1 - X}(298.1 - 0.0908T_2)}{211.7 - 0.113T_2 + \frac{X}{1 - X}(464.8 - 0.224T_2)}\right]T_2^{1/2} \tag{A-16}$$

$$R_N = \frac{\rho V \ell}{\mu} \qquad (R_N \text{ to 4 significant figures}) \tag{A-17}$$

When (H-P) is measured as one quantity:

$$(H\text{-}P)_{corr.} = (H\text{-}P)_{wind\ on} - (H\text{-}P)_{wind\ off} \tag{A-18}$$

when measured quantity is in psf.

$$(H\text{-}P)_{corr.} = K(\text{counter reading}) \tag{A-18a}$$

when 1 count = 0.01 mm on micromanometer.

Manometer fluid	K
Distilled water at 20°C	0.0020423
Butyl phthalate at 20°C	0.0021409

$$H = (H-P)_{corr.} + P \tag{A-19}$$

APPENDIX II

TUNNEL DRIVE

Motor performance.- The wound rotor induction motor was designed to be operated over a low speed range of 23 to 235 rpm and a high speed range of 47 to 470 rpm and deliver 20,000 hp at the top rpm in each range. The motor will operate at speeds somewhat lower than these minimum values, but below 70 rpm oil lift pumps which raise the motor and fan shafts off the bearing surfaces are required to provide a lubrication film. The lift pump system was not designed for continuous use and overheating can limit run duration at low rpm's. Motor speed with Freon in the tunnel is limited to the low range because of possible fan stall. The maximum design power available throughout the speed range is shown on the curve at the right. The motor is also capable of overload operation, within carefully controlled limits, as will be discussed in the next paragraph. An additional limitation is overheating of the electrolyte in the liquid rheostat (see diagram under speed control) for power conditions near 50 to 65 percent maximum rpm where a considerable percentage of the total energy is expended in the rheostat. The maximum allowable electrolyte temperature of 80°C can be monitored only in the electrical control room. Lowering the temperature of the cooling water sump in advance of such runs will considerably delay excessive temperature rise in the liquid rheostat. The cooling water sump temperature, however, must be coordinated with Freon processing operations.

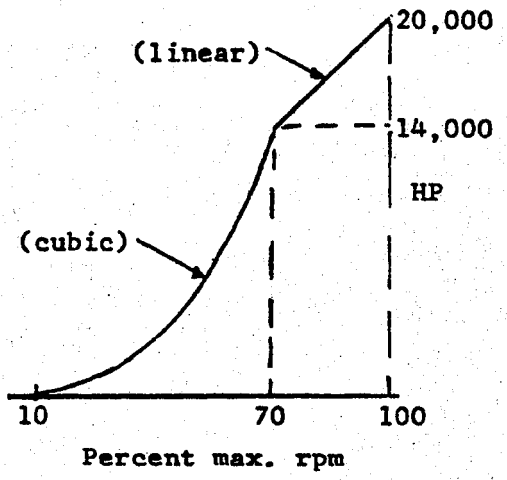

The Electrical Systems Division established the following maximum limits for overload operation of the main drive motor:

Stator current	2350 amp
Rotor current	1650 amp
Stator and rotor temperatures	230°F
(220°F limit recommended to allow for overshoot)	

These currents and temperatures read out only in the electrical control room and during such operations must be constantly monitored by the electrician in charge. Operation at overpower may be time-limited because of heating and must be terminated immediately upon the electrician's request since temperature rise can be quite rapid at maximum current conditions. Operation above rated power may considerably decrease the life of the main drive motor; therefore, such operation is not recommended as a regular practice. Running time above rated power should be kept to a minimum.

Speed control.- The motor speed control is illustrated in the following block diagram:

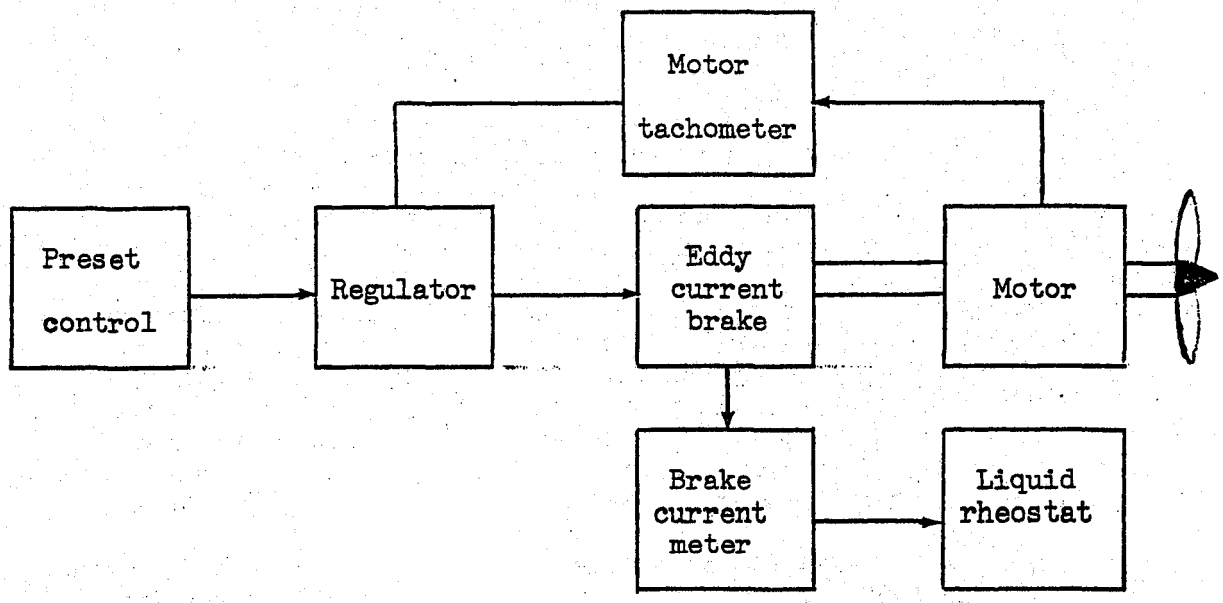

The preset rpm control signal is compared by the regulator with a feedback signal from the motor tachometer. If it differs, the controller causes the eddy current brake to extract either more or less energy and thus change rpm. If the brake current goes beyond specified upper and lower limits, the liquid rheostat setting automatically changes to provide a coarse incremental change in motor rpm. The nominal brake current setting is sufficient to maintain rpm to $\pm$ 0.25 percent. In order to provide reasonably fast response, the control system is not highly damped; as a result the rpm tends to overshoot the set point by as much as one percent but settles out in one cycle. If an overshoot in test section Mach number cannot be tolerated (i.e., critical flutter tests) the motor speed control can be used to arrive at a condition just below the desired value and then the prerotation vane angle decreased to get on point. Motor speeds slightly higher than the design maximum speeds will actuate the overspeed control which will automatically "kickdown" the motor speed to a lower value.

APPENDIX III

TUNNEL CALIBRATION

Mach number distribution.- Static pressures were measured at intervals, longitudinally along the sidewalls, the top, and at the centerline throughout the length of the test region and beyond. Typical distributions of static pressure, in terms of local Mach numbers, are shown in figure 32 for the top, centerline, and for the sidewalls. Reference Mach numbers based on test chamber static pressure are also noted. Comparing the longitudinal distributions for the centerline and the sidewalls at corresponding Mach numbers, for air, shows the difference to be generally small (of the order of the accuracy of the data), indicating the probability of satisfactory uniformity across the stream. Although no centerline pressures were measured where Freon was used, it is presumed that differences of the same order would also exist. Distributions for the top were about the same as those shown for the sidewalls.

Figure 33 shows maximum variations of local Mach numbers from average values, over the length from station 64 feet to 78 feet for the typical distributions shown in figure 32. For the 14-foot length considered, variations of the local Mach number from average values are generally less than $\pm$ 0.005 for Mach numbers below 1.0 and not greater than $\pm$ 0.014 in the worst range around $M = 1.15$. The average value of Mach number depends, of course, on the location and length considered; thus, variations smaller than those shown in figure 33 are possible. The variations shown may reflect Mach number inaccuracies in data reduction of as much as $\pm$ 0.001, and also unknown inaccuracies due to a number of possible manometer effects, local shocks, etc. An effort has been made, however, to eliminate obviously questionable points from the data used in preparing figures 32 and 33.

The deviation from a reference Mach number of the above-mentioned average values of Mach number between stations 64 feet and 78 feet is shown in figure 34. The reference Mach number is based on test chamber static pressure as measured by the Ideal manometer. This figure shows the average Mach number to be slightly lower than the reference Mach number. These curves were, however, faired near the extreme values of plotted data having considerable scatter, indicating uncertainties in the average Mach numbers (and possibly to some degree in the reference Mach numbers) from the values shown to slightly positive values. This region of scatter is indicated by cross-hatching on figure 34. In view of the scatter of these data and the relatively small magnitude of the deviation, no correction factor is applied for the usual test. For additional accuracy, however, reduction of the reference Mach number by about 1/2 percent would probably be a reasonable correction.

Figure 32 also shows the effect of having too large a reentry flap opening at subsonic Mach numbers. The gradient in Mach number between stations 68 and 80, indicated for the $M = 0.673$ distribution, is typical of a number of measurements and observations of the manometer, when the flaps were opened appreciably more than the amount recommended.

Wall boundary layer survey.- Surveys of the boundary layer profiles at station 69.5 feet on the center of the east sidewall of the test section were made for a few conditions with air and with Freon-12 as a test medium. Representative results of these surveys are shown in figures 35 and 36 to indicate the approximate extent of the boundary layer.

Turbulence.- A preliminary survey of tunnel turbulence at one station on the tunnel centerline using a hot-wire anemometer was made for one tunnel pressure using Freon-12 as a test medium. Figure 37 shows the results expressed as $\sqrt{\overline{u^2}}/U$ vs. Mach number, where $\sqrt{\overline{u^2}}$ is the root-mean square of the longitudinal velocity fluctuation and U is the average velocity. These results indicate a "medium" level of turbulence compared with some other wind tunnels.

Bypass valve operation.- Figure 38 shows the change in Mach number and dynamic pressure resulting from operation of the bypass valves. Curves shown for 2, 3, and 4 valves were not well defined by data points and for parts of the Mach number range are estimated values. There is some amount of scatter in the data anyway; therefore, it is felt that the estimates are consistent with the data and sufficiently accurate for the intended purpose. There also seemed to be no consistent difference between air and Freon operation. Time history measurements of Mach number and dynamic pressure decrease with operation of the valves showed that about 50 percent of the total decrease occurs in about 3 seconds and about 99 percent of the final value is reached in 10 seconds. Measurements made at a station upstream of the slots indicate little change in Mach number and dynamic pressure at this station with operation of the bypass valves.

Airstream oscillator characteristics.- The aerodynamic effect of the oscillating vanes on the test section flow results from cross-stream flow components induced by the trailing vortices from the vane tips. These vortices extend downstream through the test section (near the sidewalls) as rather discrete vortex cores. These vortices alternate in sign as the vanes oscillate, and the system passes downstream through the test section with a spacing (wavelength) depending upon the frequency and the stream velocity. When the vanes are "in sync" the principal oscillating component over the middle portion of the airstream is directed vertically. If the vanes are "out of sync" both lateral and vertical components produce a kind of rolling gust about the tunnel centerline.

Surveys have been made at one streamwise station in the test section at positions over the center portion of the stream from the centerline to 5 feet in a horizontal direction and to 4 feet in a vertical direction. Both hot-wire anemometers and fast-response pressure probes have been used to measure the oscillating flow components in terms of variation in stream angle. Complete surveys have not yet been obtained for all test conditions and positions of interest because of the large number of variables involved and difficulties in test techniques and data reduction. Data shown in figures 39 and 40 are, however, thought to be representative for purposes of program planning. It is expected that for any new gust program, additional surveys will be made at conditions applicable to the particular investigation.

For the vanes on the two sides synchronized, the variation of magnitude of the vertical amplitude of oscillation across the stream at centerline height out to spanwise distances of 40 inches on either side of the centerline is shown in figure 39(a) for several values of the frequency parameter ω/V (where ω is the frequency and V the stream velocity). Figure 39(d) gives the amplitudes at two spanwise stations at vertical distances up to 16 inches from the center. The cause of the large variation in amplitude across the stream and the difference in character of the two sides shown in figure 39(a) is not understood at this time. It is presumed that with this obviously complicated flow field, considerable effort will be required for a better understanding of this phenomenon. The distribution is felt to be usable for gust response studies, however, and analytical procedures for accounting for this variation are thought to be adequate. Since the variation in amplitude becomes much greater beyond the range shown, it is thought advisable to limit model wing semispans for gust response studies to about three feet at this time.

Figure 39(b) shows that the variation in phase across the stream is very small up to ω/V of about 0.20 but becomes quite large at ω/V values above about 0.40. Some of the irregularity shown in this figure, however, may be due to data reduction techniques. The complication of large phase variations at the higher values of ω/V might perhaps be avoided by limiting the range of test conditions since values of amplitude at these higher values of ω/V are so small as to be of questionable usefulness. Amplitude and phase measurements at higher Mach numbers were made in somewhat less detail and with less satisfactory data reduction techniques. These data indicate, however, that at Mach numbers up to about 0.80 the characteristics are similar to those shown in figure 39 with perhaps a slight decrease in the average amplitude with increasing Mach number at the lower values of ω/V. Somewhat incomplete data at $M = 1.1$ suggest a more uniform spanwise variation but with lower average amplitudes.

The average amplitudes shown in figure 39(c) were measured at $M = 0.22$ in Freon-12 and thus were at a relatively low velocity. The frequencies represented in the range of ω/V shown were below about 9 Hz. Some evidence of sharply tuned resonance effects have been observed at frequencies of about 14 Hz during some other runs at higher Mach numbers. Although these effects have not been fully explored at this time, it is thought that frequencies in this resonance range should probably be avoided in gust response investigations.

Surveys shown in figure 39 are for an oscillator vane angle of about $\pm 6^{\circ}$. Limited surveys at vane angles of $\pm 3^{\circ}$ and $\pm 9^{\circ}$ indicate that vertical amplitudes of oscillation are roughly proportional to vane angle but that there are slight differences in the spanwise distributions. Adjustment of the vane angle is, of course, a useful means of varying input excitation to suit the degree of response desired.

Surveys have also been made with the vanes out of synchronization to see if a usable rolling gust is generated. Typical characteristics are shown in figure 40 of the horizontal and vertical components of gust angle for one value of ω/V with the vanes 180° out of synchronization with a vane angle

of $\pm 6^{\circ}$. The vector diagram in the center of the figure illustrates schematically the idea of the rolling gust. The plot on the left shows the variation in components with vertical distance from the centerline while the plot on the right shows the variation with horizontal distance.

TABLE I.- LENGTH OF TIME REQUIRED TO PERFORM VARIOUS PUMPING OPERATIONS UNDER NORMAL CONDITIONS.

FREON IN TUNNEL

(a) Convert tunnel (excludes test chamber) from air at atmospheric pressure to Freon.

Final tunnel total press. (psf)	Time req'd. (hr)
2100	--
2000	3-1/2 hr.
1800	--
1600	--
1400	3 hr.
1200	--
1000	2-1/2 hr.
800	--
600	--
400	1-3/4 hr.
200	--
100	1-1/2 hr.

(b) Start tunnel after model change completed.

Tunnel total pressure (psf)	Time req'd. (min)
2100	80
2000	75
1800	70
1600	65
1400	60
1200	55
1000	50
800	50
600	50
400	50
200	50
100	50

(c) Make entry to test section after tunnel shutdown.

Tunnel total pressure (psf)	Time req'd. (min)
2100	70
2000	65
1800	60
1600	55
1400	50
1200	45
1000	45
800	50
600	55
400	60
200	65
100	70

(d) Time required to vary total pressure in tunnel (includes test chamber).

*Freon operators require 5 min. alert to prepare equipment.

Present total pressure (psf)	Time (min) req'd. to obtain final total pressure (psf)											
	2100	2000	1800	1600	1400	1200	1000	800	600	400	200	100
2100		5	15	25	35	45	60	75	90	120	130	150
2000	10		10	20	30	40	55	70	85	105	125	145
1800	25	15		10	20	30	45	60	75	95	115	135
1600	40	30	15		10	20	35	50	65	85	105	125
1400	55	45	30	15		10	25	40	55	75	95	115
1200	70	60	45	30	15		15	30	45	65	85	105
1000	85	75	60	45	30	15		15	30	50	70	90
800	100	90	75	60	45	30	15		15	35	55	75
600	115	105	90	75	60	45	30	15		20	40	60
400	130	120	105	90	75	60	45	30	15		20	40
200	145	135	120	105	90	75	60	45	30	15		20
100	160	150	135	120	105	90	75	60	45	30	15	

AIR IN TUNNEL

(a) Convert tunnel (excludes test chamber) from Freon to air at atmospheric pressure.

Initial tunnel total pressure (psf)	Time req'd. (hr)
2100	--
2000	3 hr.
1800	--
1600	--
1400	2-1/4 hr.
1200	--
1000	1-3/4 hr.
800	--
600	--
400	1 hr.
200	--
100	--

(b) Start tunnel after model change completed.

Tunnel total pressure (psf)	Time req'd. (min)
2100	15
2000	15
1800	15
1600	20
1400	20
1200	20
1000	25
800	25
600	30
400	30
200	35
100	35

(c) Make entry to test section after tunnel shutdown.

Tunnel total pressure (psf)	Time req'd. (min)
2100	15
2000	15
1800	20
1600	20
1400	25
1200	30
1000	35
800	40
600	45
400	50
200	55
100	60

(d) Time required to vary total pressure in tunnel (includes test chamber).

*Freon operators require a 5 min. alert to prepare equipment.

Present total pressure (psf)	Time (min) req'd. to obtain final total pressure (psf)											
	2100	2000	1800	1600	1400	1200	1000	800	600	400	200	100
2100		5	10	15	20	30	40	50	65	80	100	120
2000	15		5	10	15	25	35	45	60	75	95	115
1800	20	15		5	10	20	30	40	55	70	90	110
1600	25	20	15		5	15	25	35	50	65	85	105
1400	30	25	20	15		10	20	30	45	60	80	100
1200	35	30	25	20	15		10	20	35	50	70	90
1000	40	35	30	25	20	15		10	25	40	60	80
800	50	45	40	35	30	25	20		15	30	50	70
600	55	50	45	40	35	30	25	20		15	25	55
400	60	55	50	45	30	35	30	25	20		20	40
200	65	60	55	50	45	40	35	30	25	20		20
100	70	65	60	55	50	45	40	35	30	25	20	

Drier Operation

Air drier #3 - permits 4 entries to test section before reactivation (reactivation time = 2-1/2 hr.)
Freon drier #1 - permits 3 hrs. of Freon reclaiming operation before reactivation (reactivation time = 3 hr.)

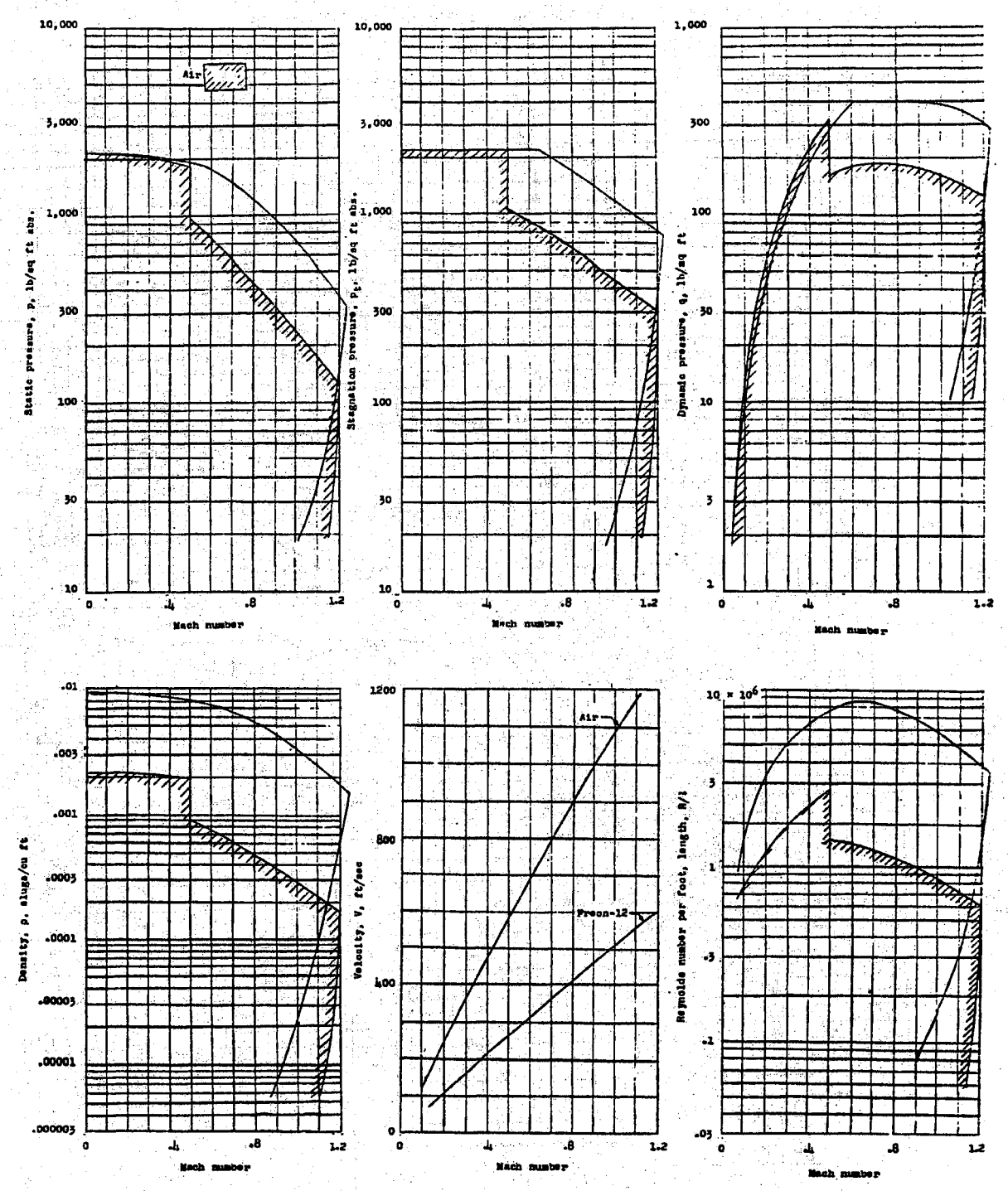

(a) Operating envelope using air or Freon-12. Limits based on $T_t = 130^{\circ}$ F with no model in the test section.

Figure 1.- General operating characteristics of the Langley transonic dynamics tunnel.

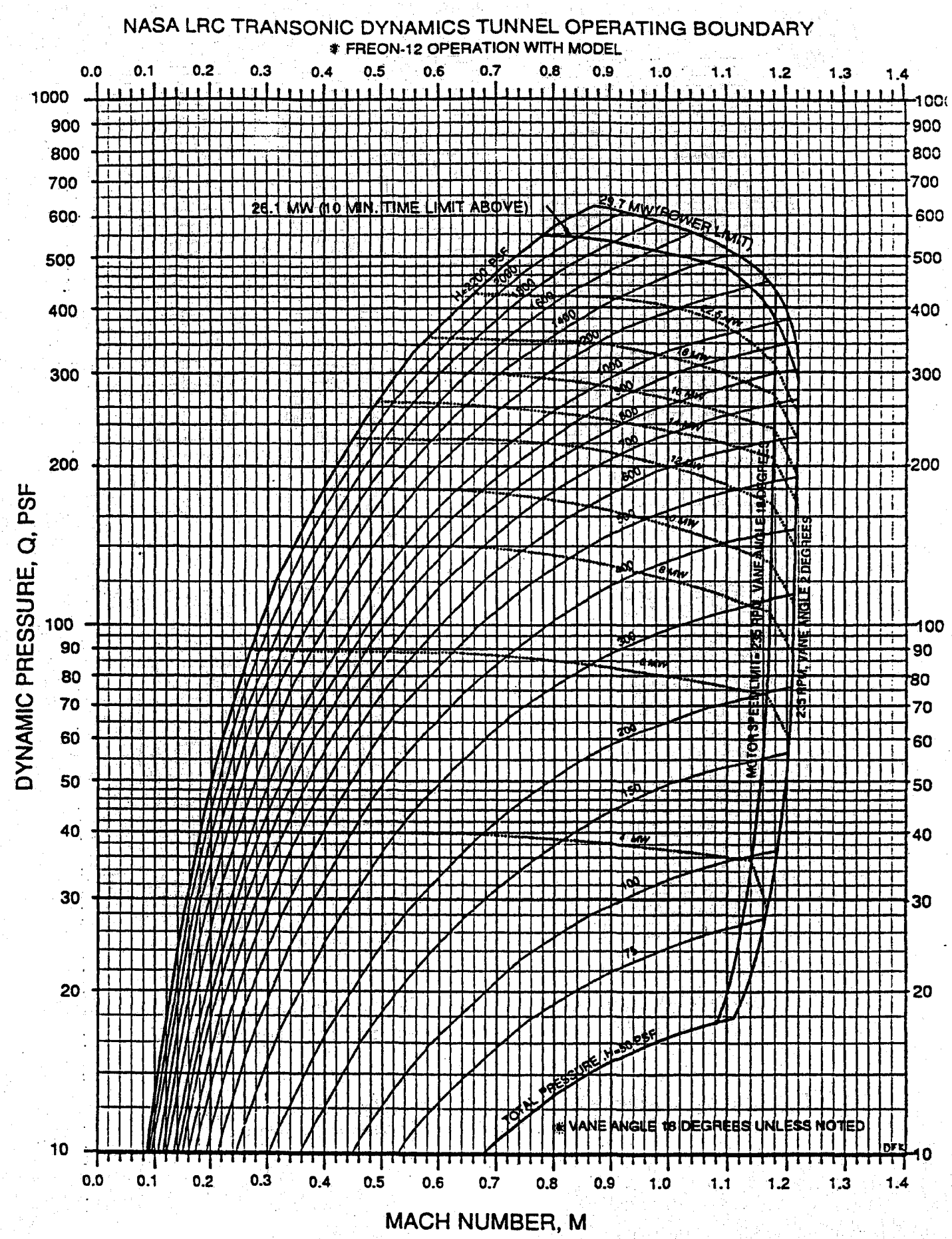
NASA LRC TRANSONIC DYNAMICS TUNNEL OPERATING BOUNDARY
* FREON-12 OPERATION WITH MODEL
26.1 MW (10 MIN. TIME LIMIT ABOVE)
29.7 MW POWER LIMIT
H=200 PSF
1000
1500
(AIR)
1400
200
1000
300
600
700
500
300
200
8 MW
10 MW
12 MW
6 MW
4 MW
300
200
120
100
75
MOTOR SPEED LIMIT = 235 RPM, VANE ANGLE 18 DEGREES
235 RPM, VANE ANGLE 2 DEGREES
TOTAL PRESSURE, H=50 PSF
* VANE ANGLE 18 DEGREES UNLESS NOTED
DYNAMIC PRESSURE, Q, PSF
MACH NUMBER, M

NASA LRC TRANSONIC DYNAMICS TUNNEL

OPERATING BOUNDARY IN AIR

• VANE ANGLE 18 DEGREES UNLESS NOTED•

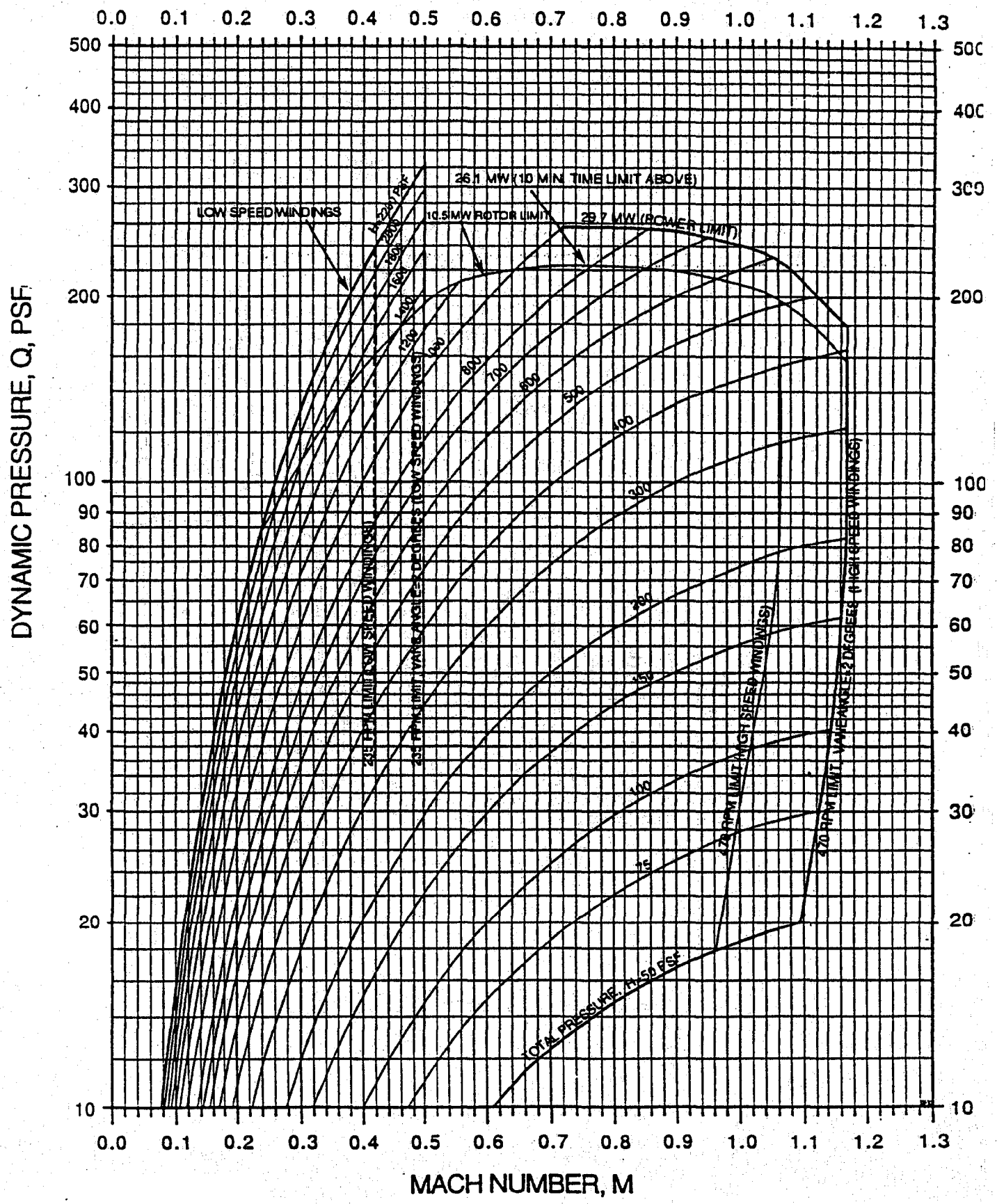

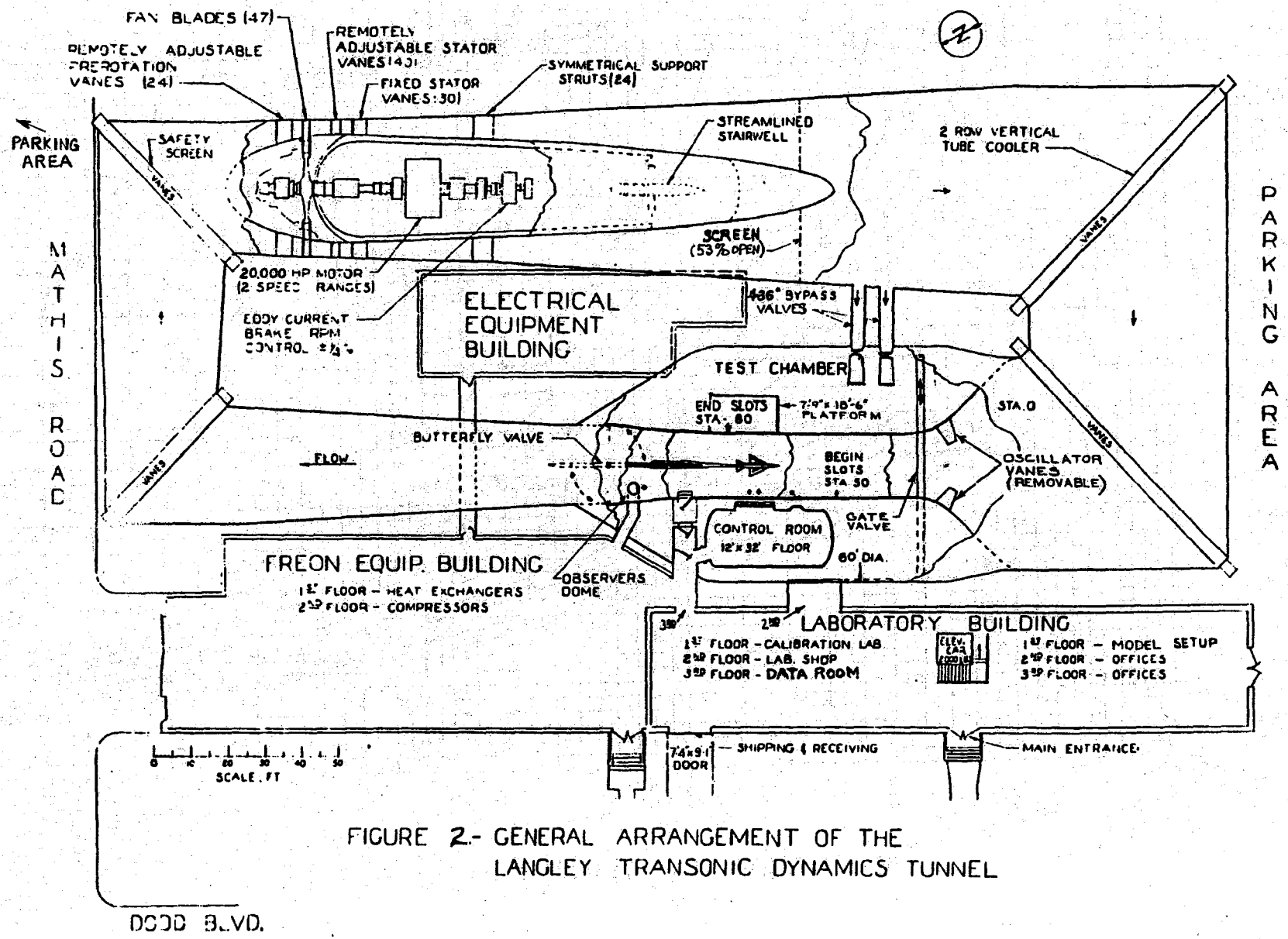

FIGURE 2.- GENERAL ARRANGEMENT OF THE LANGLEY TRANSONIC DYNAMICS TUNNEL

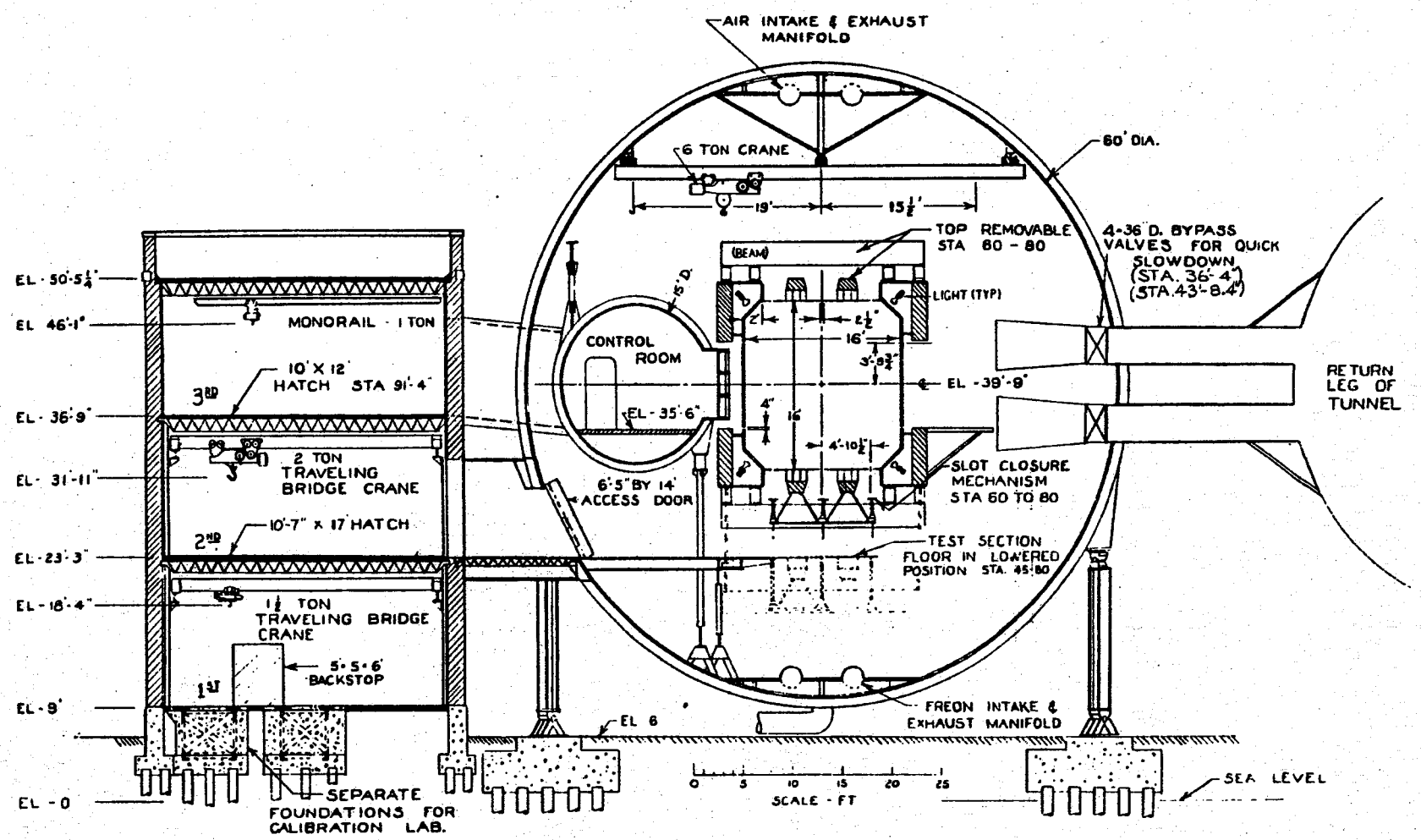

FIGURE 3.- CROSS SECTION THROUGH LABORATORY BUILDING, TEST CHAMBER, CONTROL ROOM AND TEST SECTION.

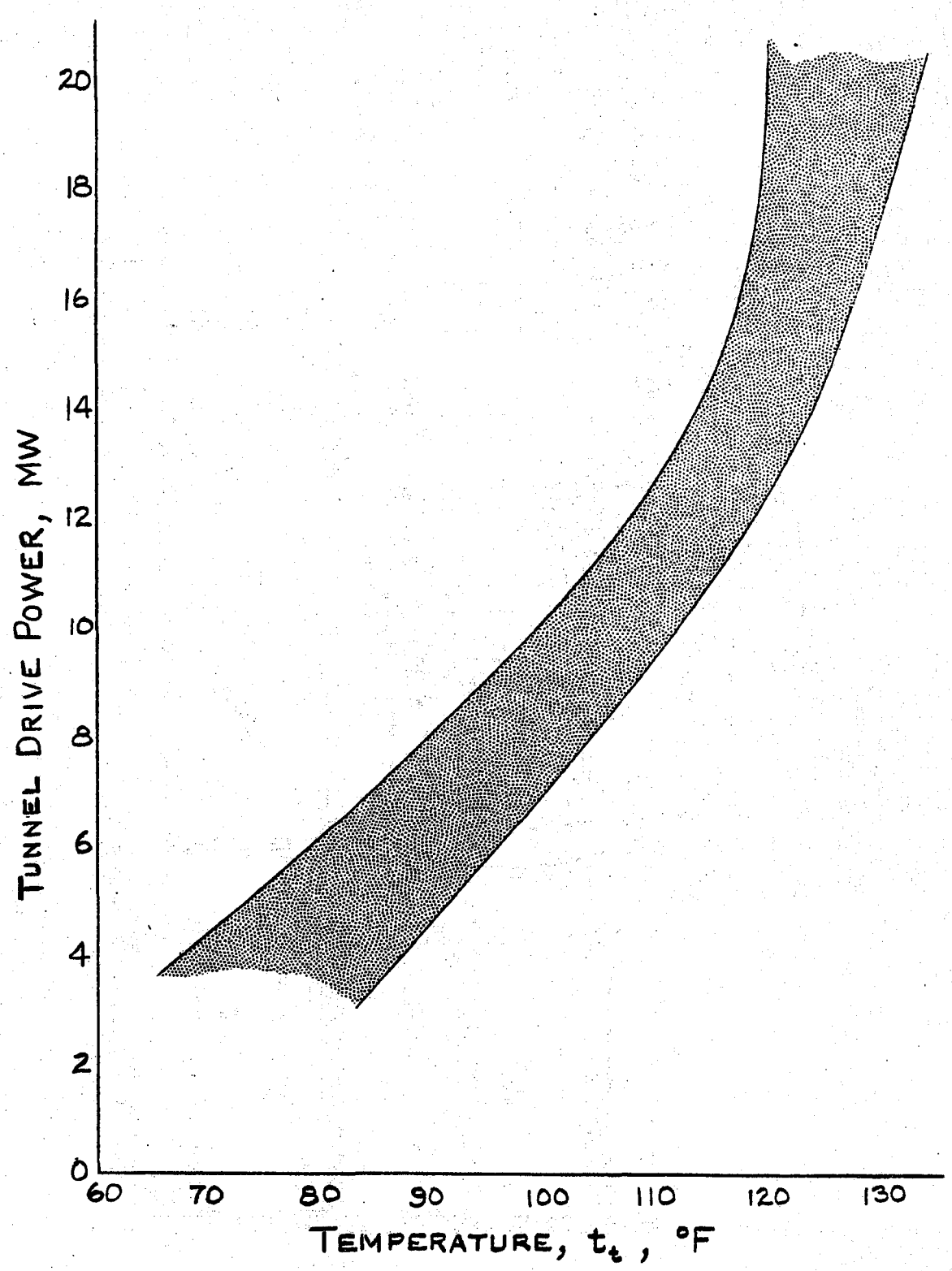

Figure 4.- Representative variation of tunnel stagnation temperature with drive system power. Cooling system on above 100° F.

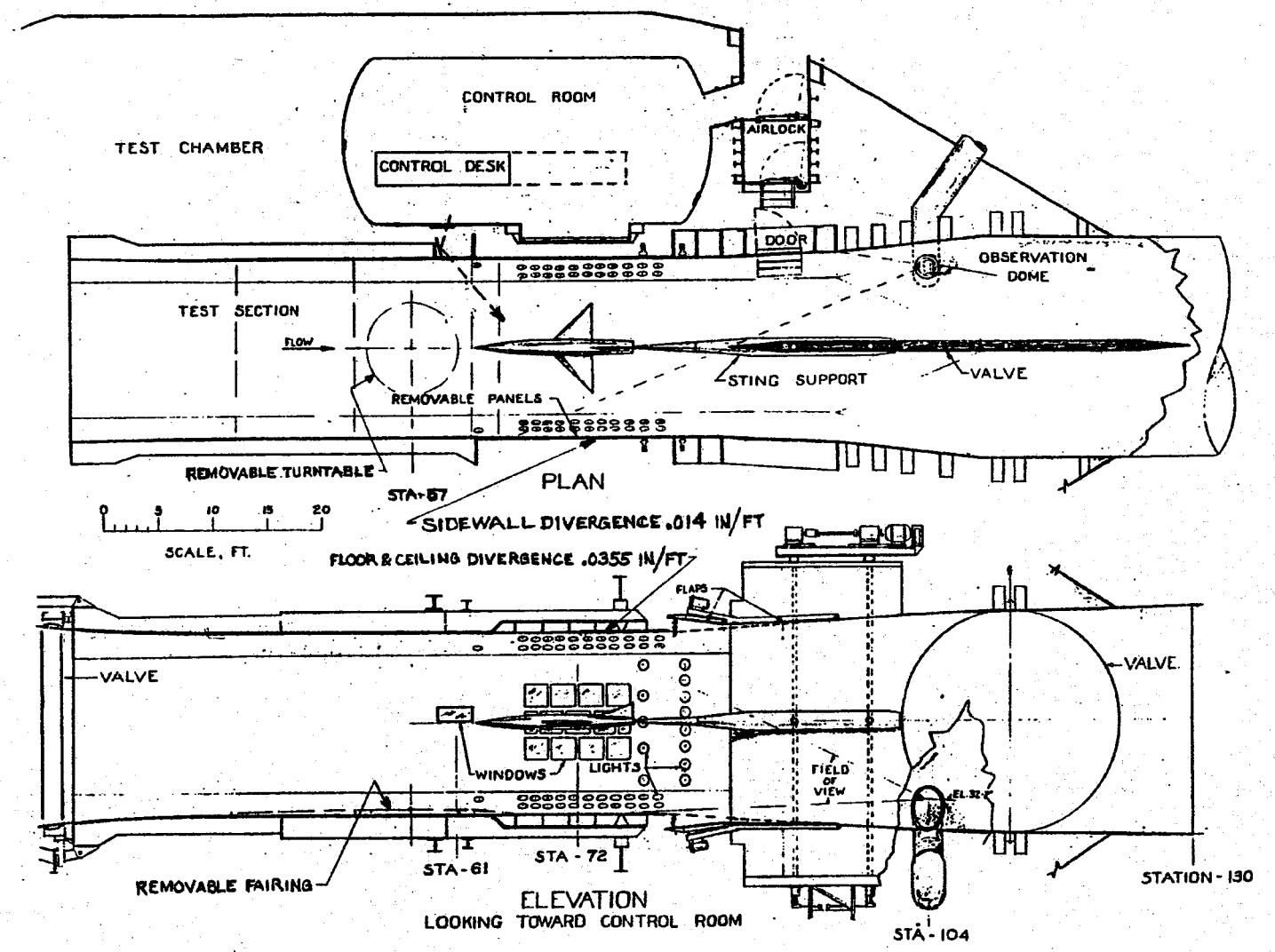

FIGURE 5.- GENERAL ARRANGEMENT OF TEST SECTION

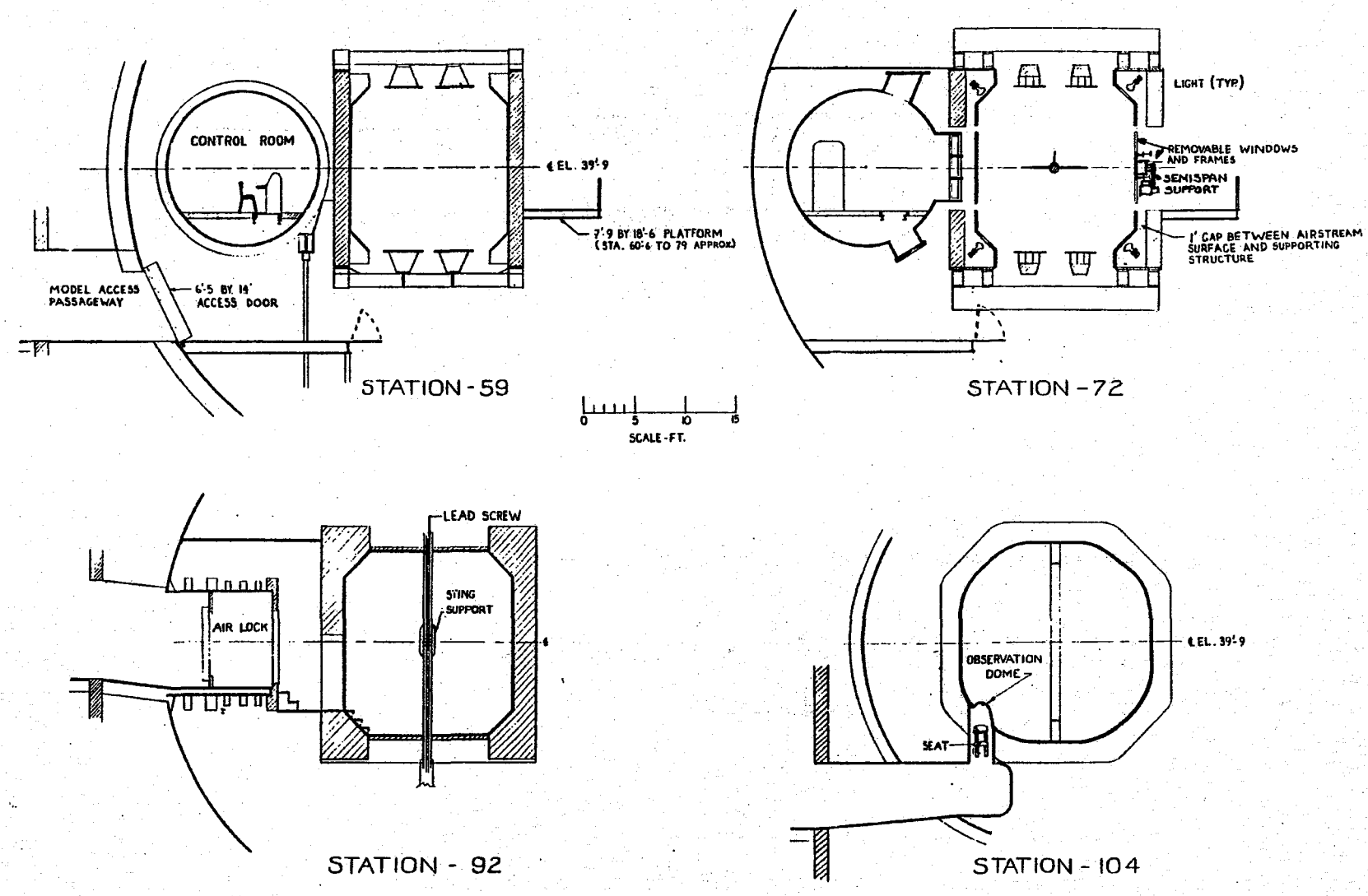

FIGURE 6.- CROSS SECTION VIEWS THROUGH TEST CHAMBER AND TEST SECTION

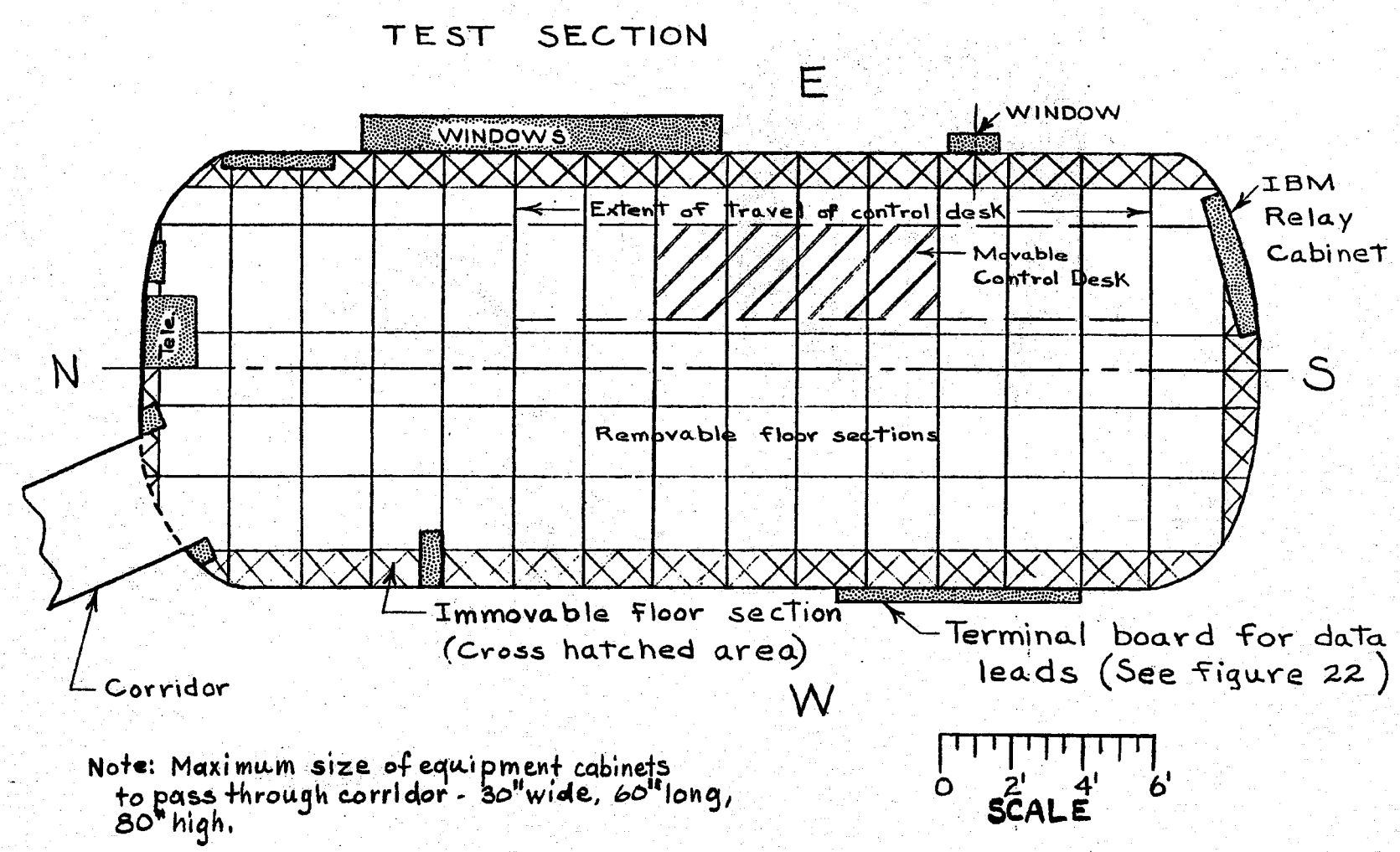

Note: Maximum size of equipment cabinets to pass through corridor - 30" wide, 60" long, 80" high.

Figure 7.- Control room floor plan.

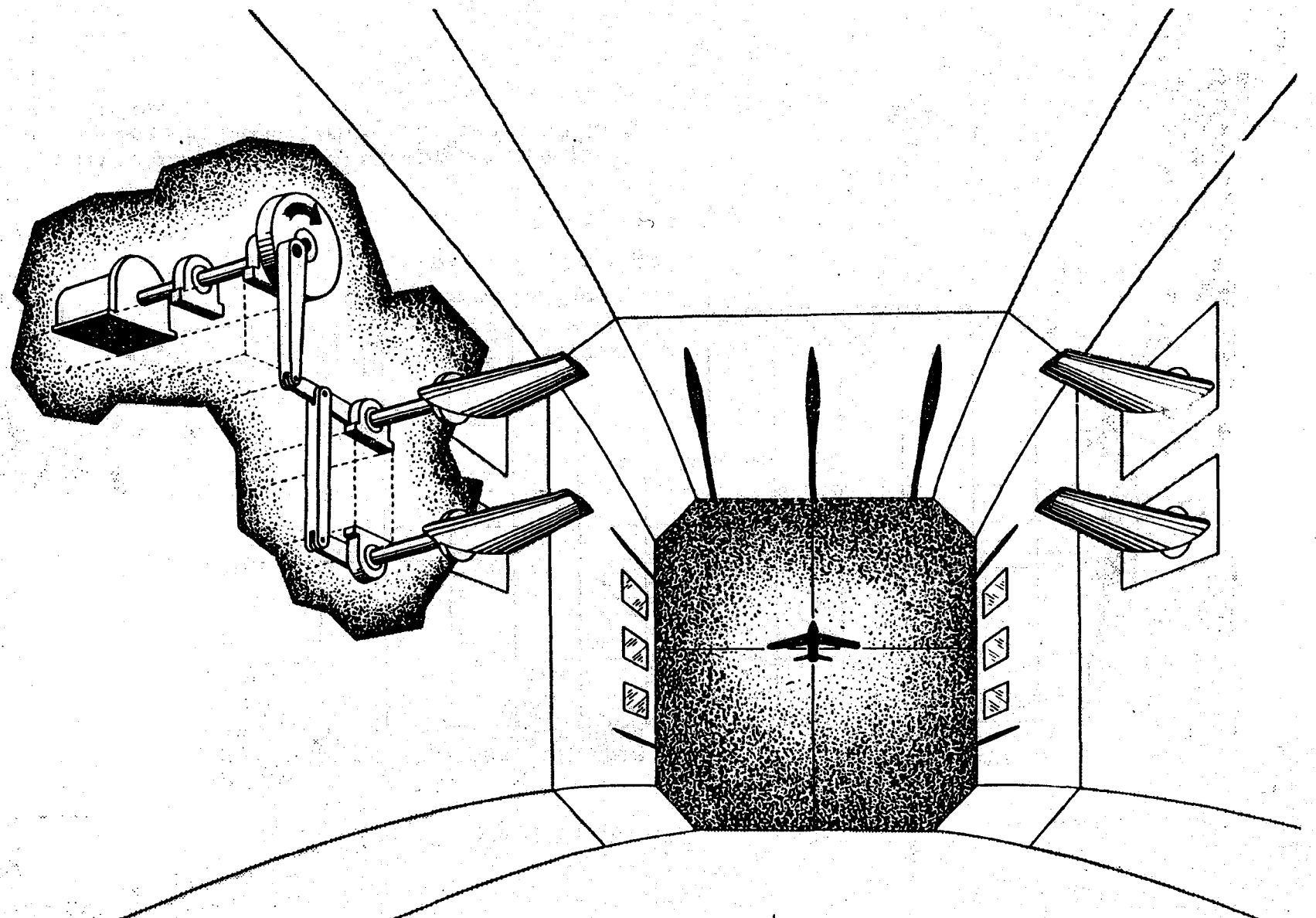

Figure 8 .- Sketch of airstream oscillator vanes and model, with cutaway showing schematic of mechanism.

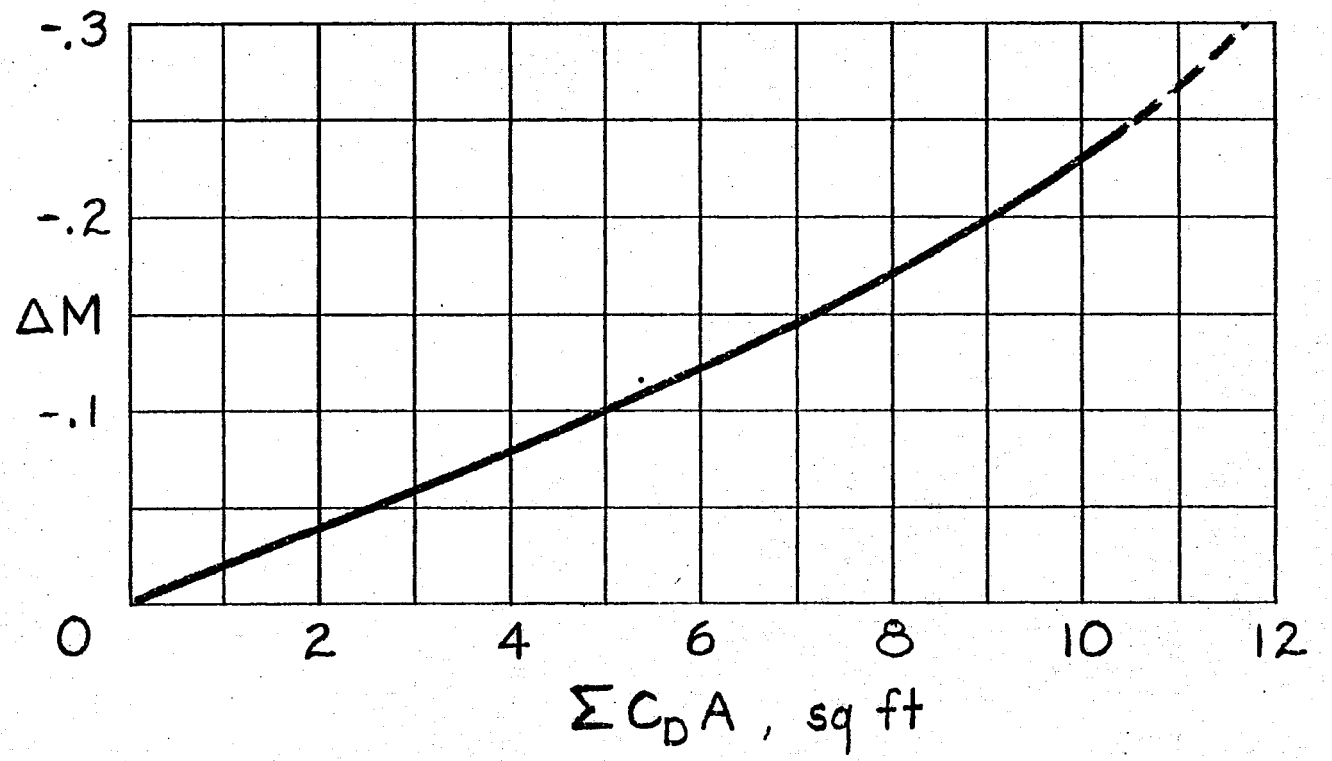

Figure 9.- Approximate Mach number decrease caused by models, struts, and other objects in test section.

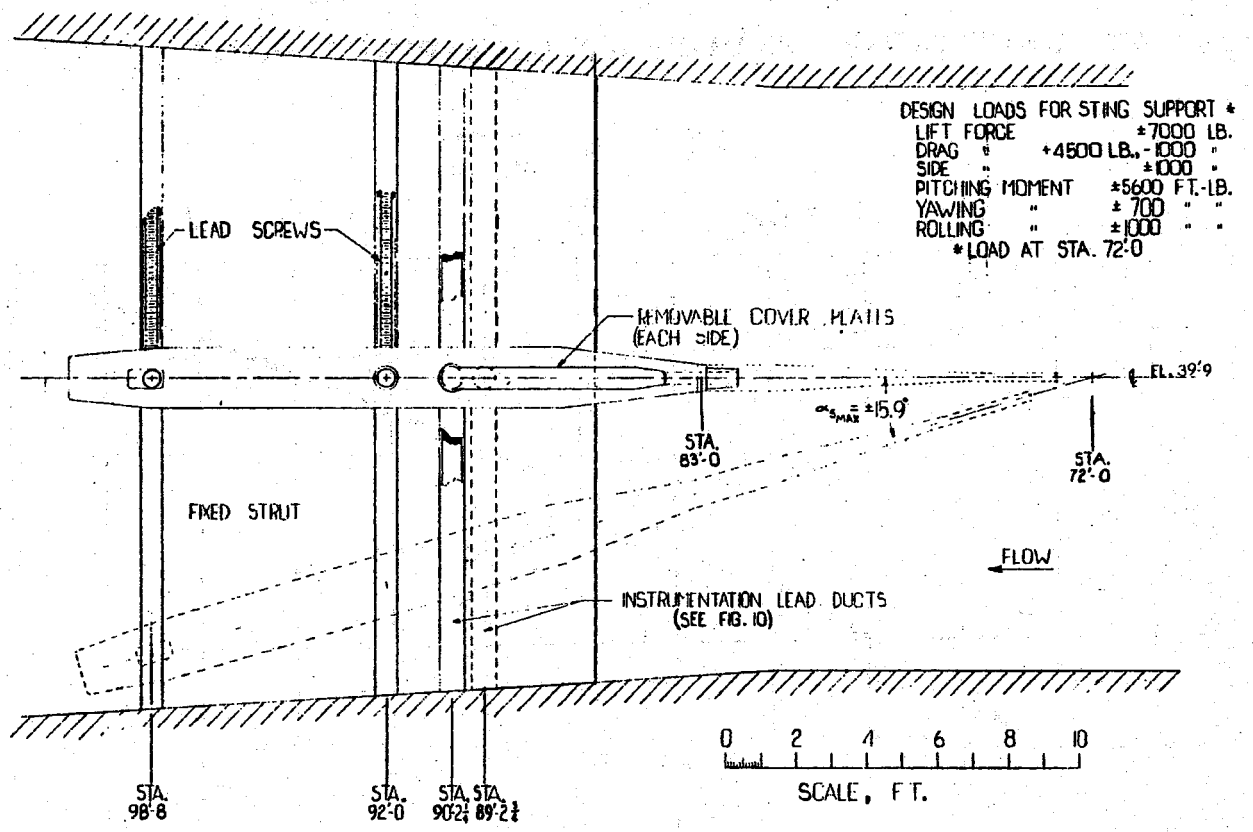

Figure 10 .- Sting support system.

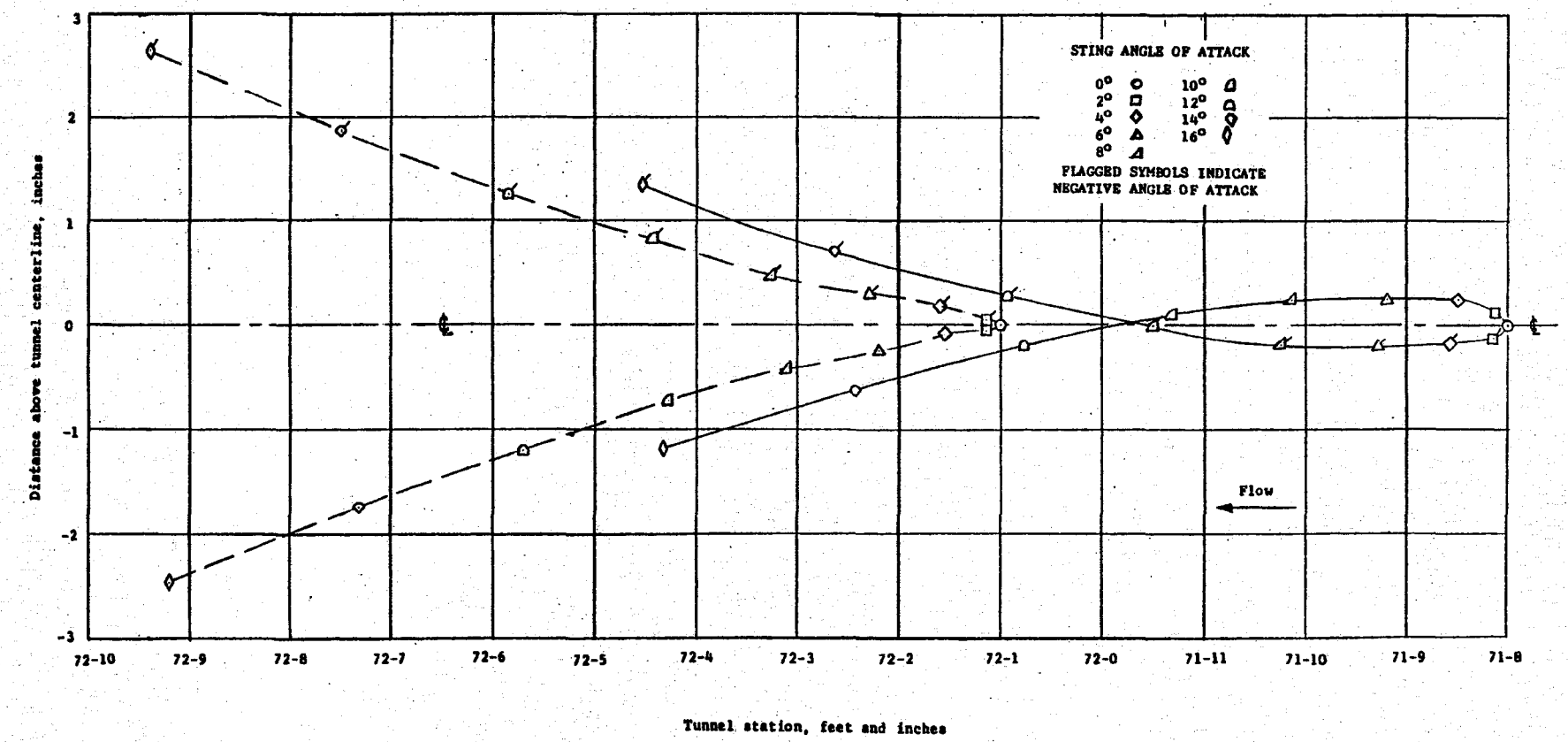

Figure 11 .- Path of travel with angle of attack of two stations on a sting.

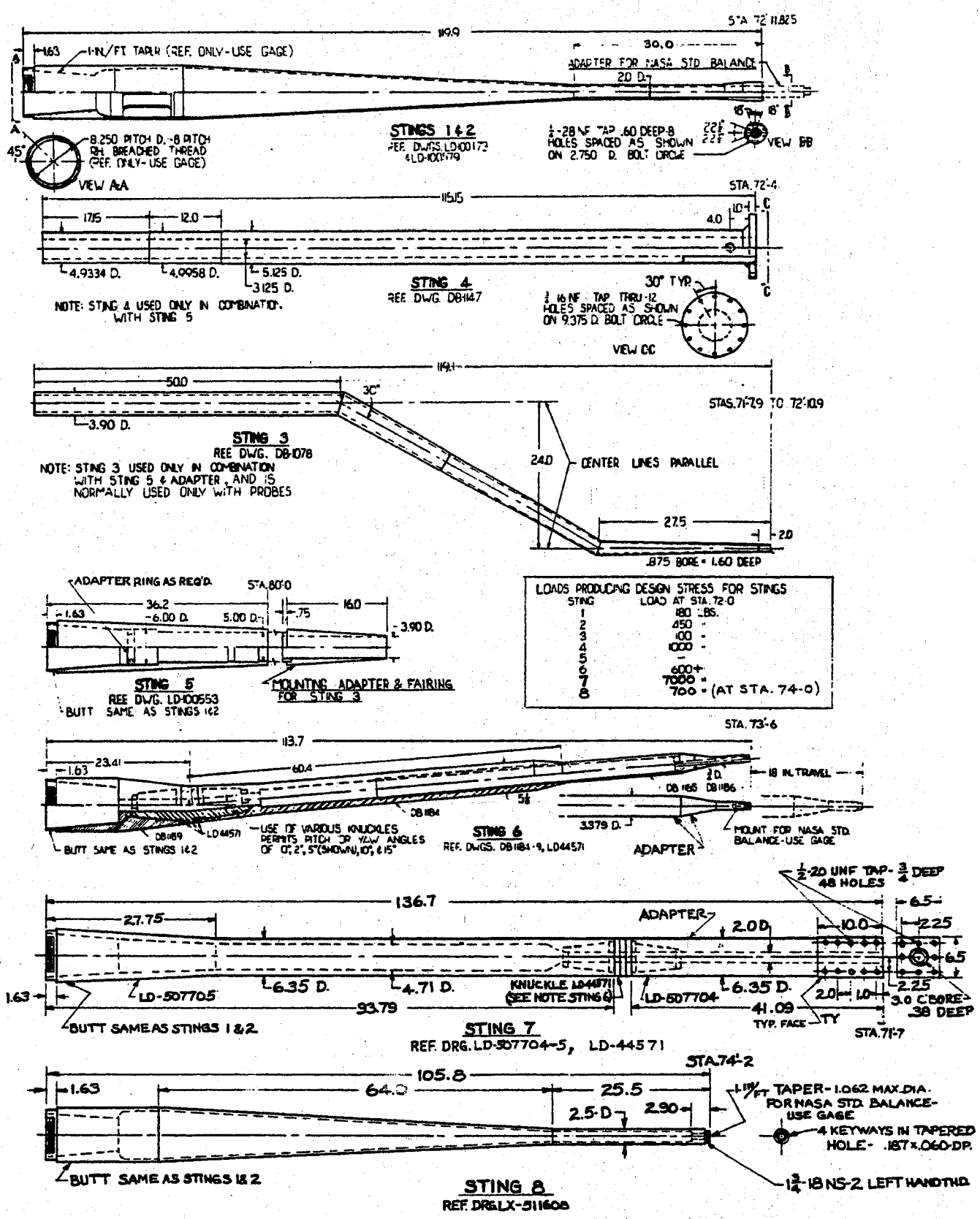

Figure 12 .- Stings and adapters.

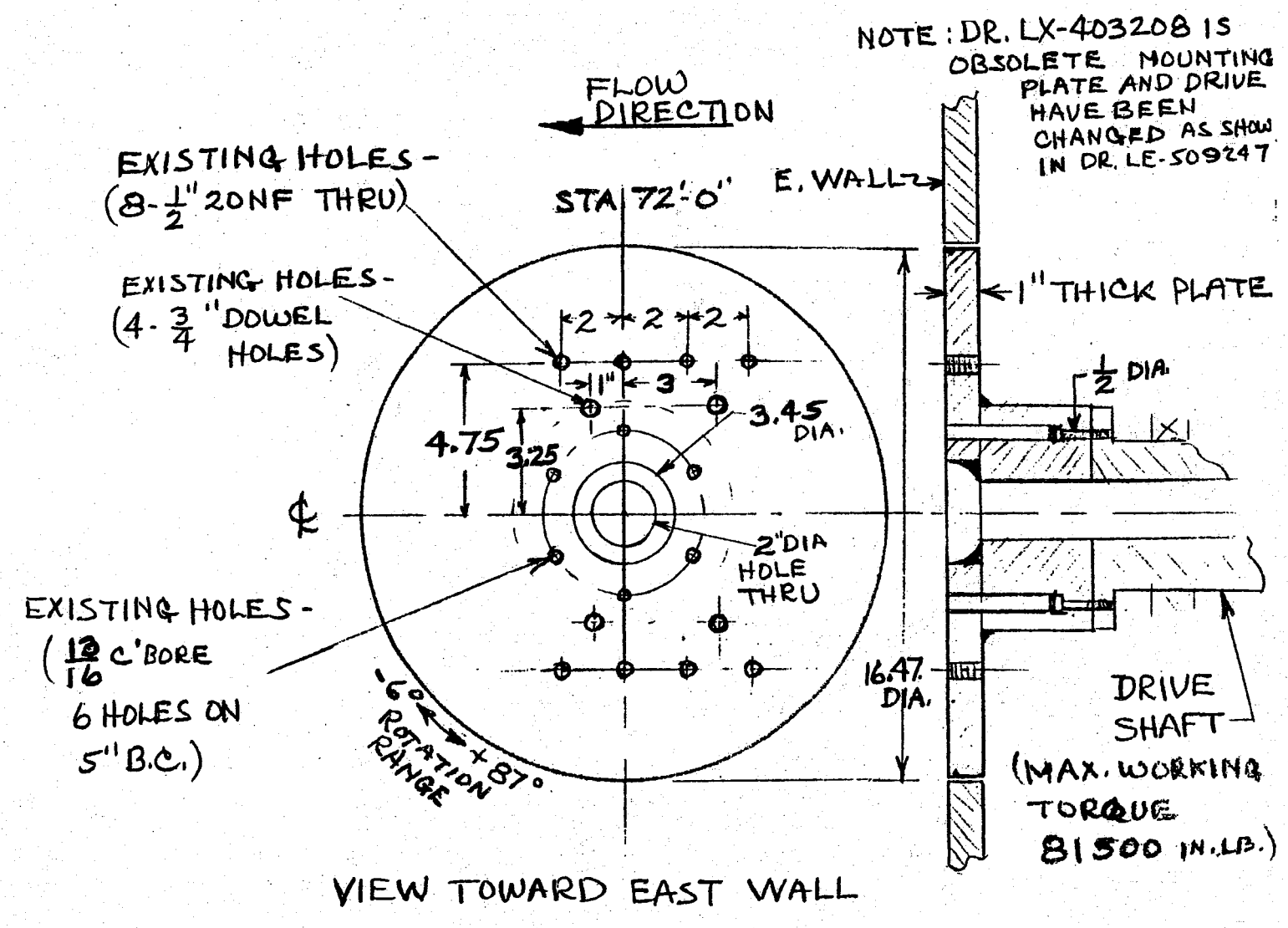

Figure 13.- Sidewall mounting plate.

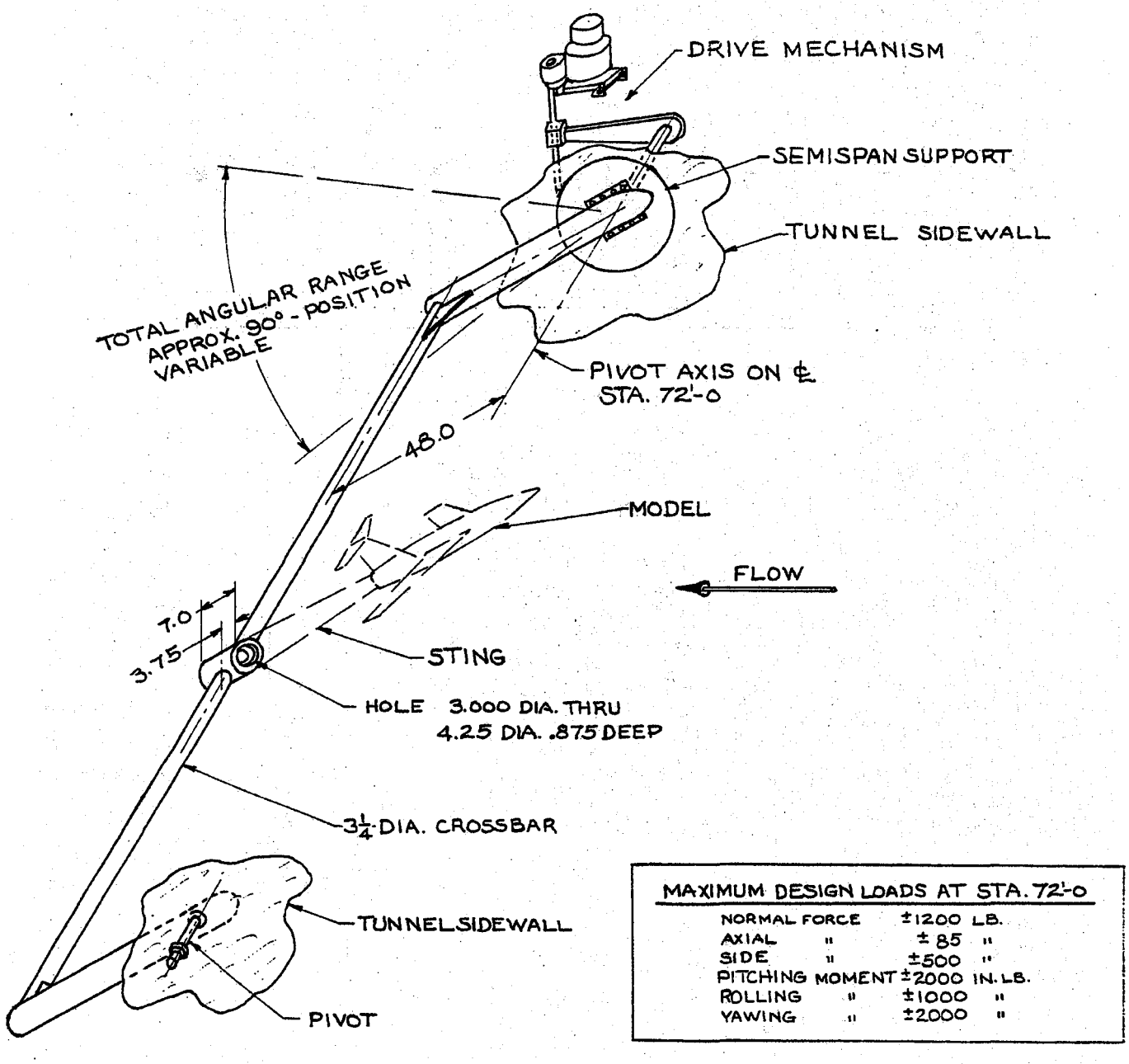

Figure 14.- Crossbar support.

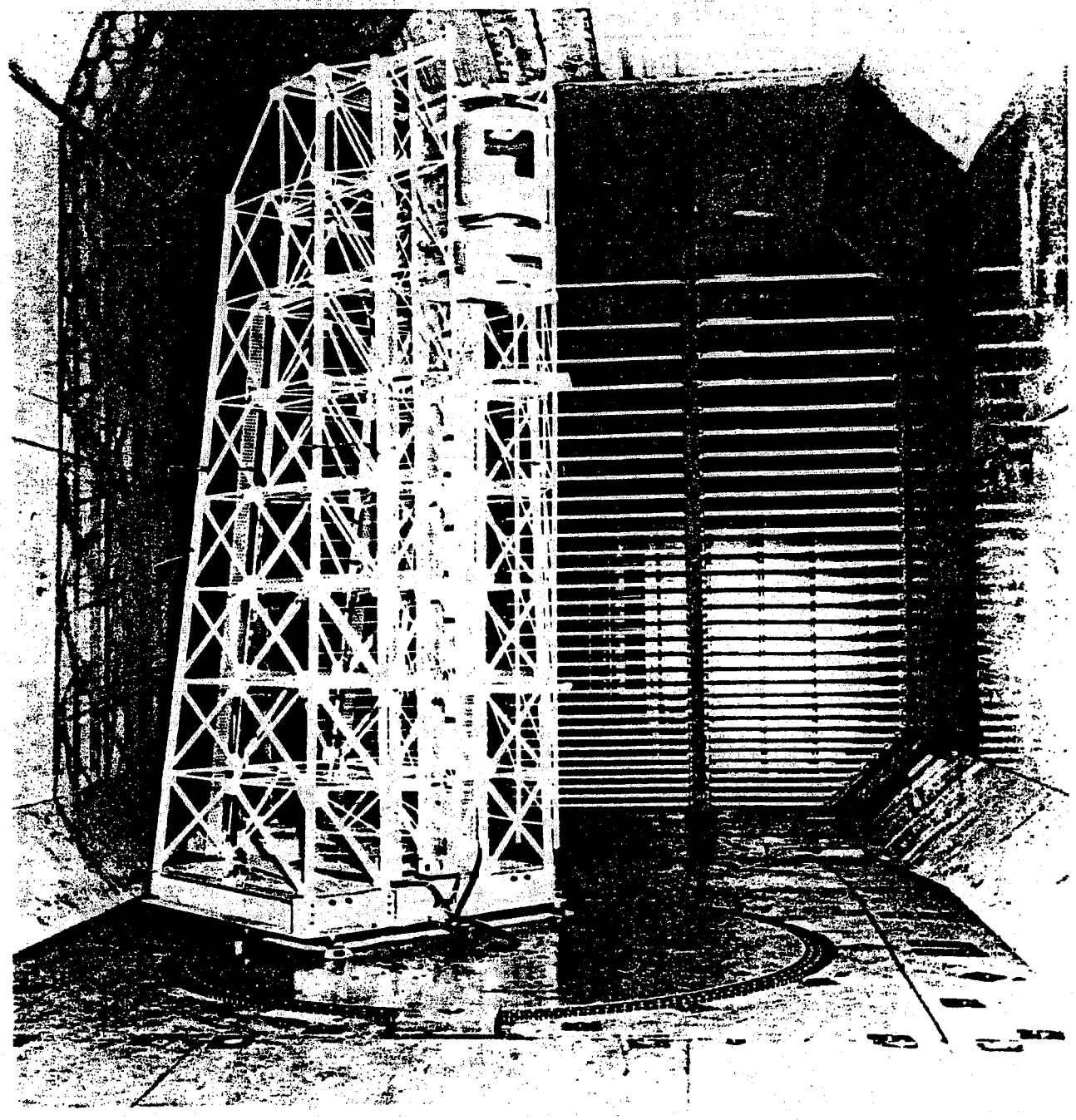

Figure 15.- Turntable with tower model installed.
(Velocity profile bars shown in background.)

A	3/4 - 10
B	1/2 - 20
C	1/2 - 13
D	1 - 8
E	1-1/8 - 12
F	5/8 - 11
G	5/8 - 18
H	1 - 14
I	3/8 - 16

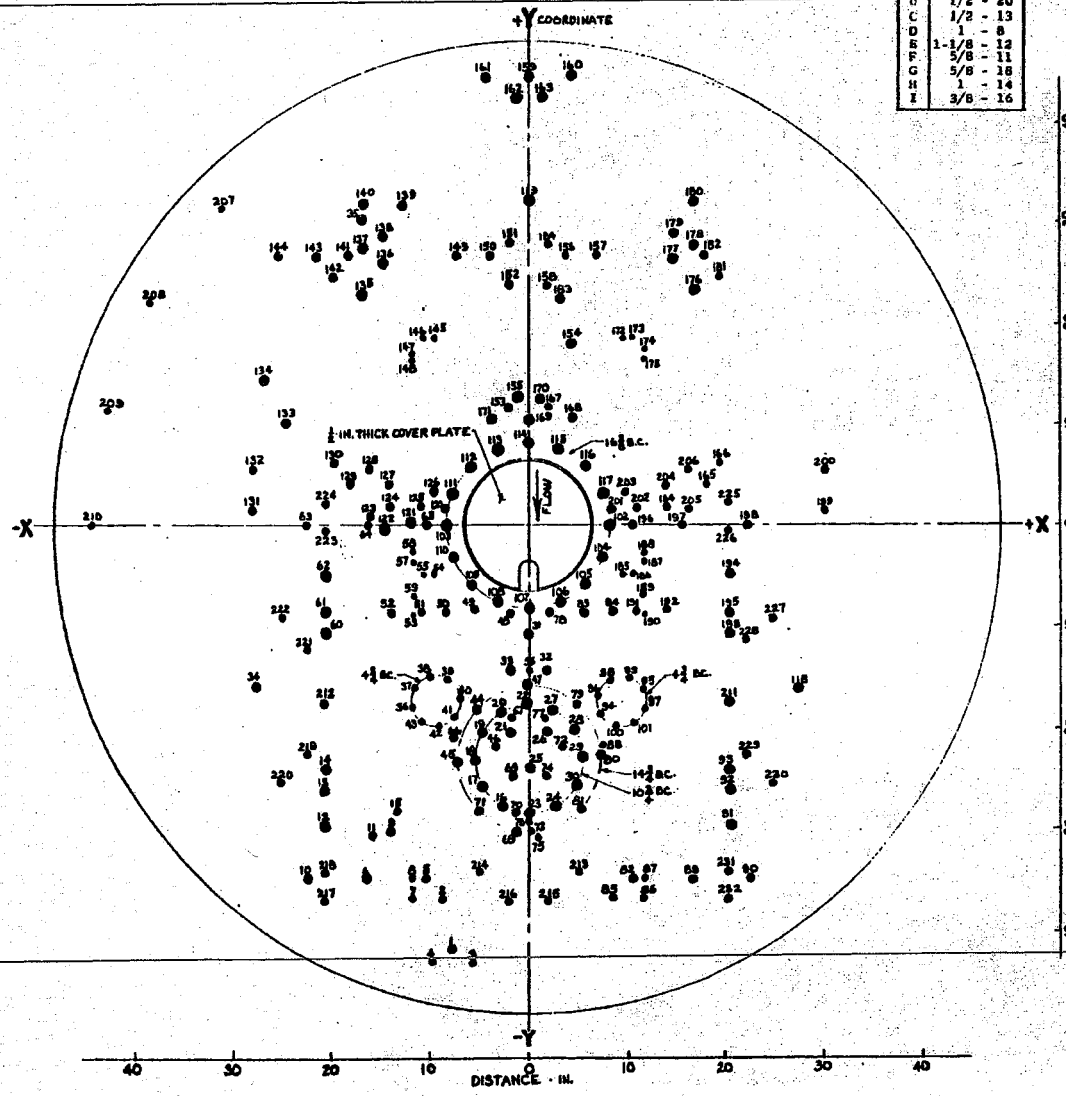

HOLE NO.	COORDINATES X, in	COORDINATES Y, in	HOLE SIZE*	HOLE NO.	COORDINATES X, in	COORDINATES Y, in	HOLE SIZE*	HOLE NO.	COORDINATES X, in	COORDINATES Y, in	HOLE SIZE*
1	-7.69	-41.66	A	81	5.32	-28.96	A	161	-4.44	44.44	D
2	-8.63	-36.77	B	82	10.65	-34.89	A	162	-1.26	42.40	D
3	-5.94	-43.09	C	83	5.61	-8.64	A	163	1.25	42.39	D
4	-9.61	-42.95	C	84	8.47	-8.49	A	164	14.17	1.75	A
5	-10.44	-34.83	A	85	8.57	-36.72	B	165	18.16	4.01	A
6	-16.48	-34.80	A	86	11.73	-36.74	B	166	19.74	6.14	A
7	-11.77	-36.77	B	87	11.76	-34.73	B	167	2.03	11.85	A
8	-11.75	-34.75	B	88	7.52	-21.78	G	168	-4.51	10.66	D
9	-13.86	-30.44	A	89	16.82	-34.89	A	169	0.07	10.62	D
10	-22.48	-34.85	A	90	22.79	-34.84	A	170	1.33	12.69	D
11	-16.03	-30.79	C	91	20.77	-29.73	D	171	-4.22	10.56	D
12	-20.70	-29.86	D	92	20.70	-26.14	D	172	9.58	18.14	B
13	-20.66	-26.16	D	93	20.72	-24.09	D	173	10.63	18.77	B
14	-20.64	-24.11	D	94	7.43	-18.60	F	174	11.75	17.61	B
15	-13.35	-28.72	C	95	11.57	-16.24	F	175	11.74	16.62	B
16	-2.62	-27.81	D	96	EQUALLY SPACED ON 8.5		F	176	16.91	23.28	D
17	-4.66	-25.88	D	97			F	177	14.80	26.40	D
18	-5.53	-23.19	D	98			F	178	16.90	27.64	D
19	-4.83	-20.49	D	99			F	179	14.85	28.93	D
20	-2.92	-18.44	D	100			F	180	16.91	32.01	D
21	-1.89	-20.39	D	101			F	181	19.74	24.60	A
22	-0.31	-17.62	D	102	8.18	0.00	H	182	18.02	26.72	A
23	0.14	-28.43	D	103	-8.18	0.00	H	183	3.20	22.53	D
24	2.83	-27.56	D	104			H	184	2.03	27.80	A
25	0.00	-24.20	D	105			H	185	9.64	-4.81	B
26	1.87	-20.40	D	106			H	186	10.58	-4.80	B
27	2.46	-18.27	D	107	EQUALLY SPACED ON 8.0 BOLT CIRCLE		H	187	11.74	-3.62	B
28	4.49	-20.16	D	108			H	188	11.73	-2.65	B
29	5.34	-22.82	D	109			H	189	11.57	-6.84	B
30	4.70	-25.53	D	110			H	190	11.71	-8.82	B
31	-0.04	-10.59	D	111			H	191	10.97	-8.48	A
32	1.85	-14.38	D	112			H	192	14.06	-8.43	A
33	-1.88	-14.36	D	113			H	193	20.69	-10.59	D
34	-27.72	-15.94	E	114			H	194	20.69	-4.84	D
35	-17.03	30.27	D	115			H	195	20.68	-8.61	D
36	-11.88	-17.87	F	116			H	196	10.62	0.00	A
37	-11.14	-16.08	F	117			H	197	16.66	0.00	A
38	-9.99	-15.09	F	118	27.66	-16.09	E	198	22.64	0.00	A
39	-8.21	-15.41	F	119	0.10	32.05	E	199	30.38	1.33	A
40	-6.92	-16.92	F	120	-8.50	1.74	A	200	30.39	5.39	A
41	-7.54	-18.74	F	121	-11.96	0.30	D	201	8.44	1.59	A
42	-9.04	-19.70	F	122	-14.66	-0.42	D	202	10.98	1.62	A
43	-10.84	-19.36	F	123	-16.17	1.53	A	203	9.76	3.22	A
44	-5.46	-17.99	A	124	-14.11	1.66	A	204	14.11	4.02	A
45	-7.48	-23.30	A	125	-10.46	1.76	A	205	16.35	1.45	A
46	-3.37	-21.88	A	126	-9.72	3.32	A	206	16.41	5.50	A
47	-0.34	-15.62	A	127	-14.18	4.10	A	207	-31.42	31.42	B
48	-1.94	-8.70	A	128	-16.21	5.50	A	208	-38.45	22.25	I
49	-5.45	-8.43	A	129	-18.16	4.06	A	209	-42.93	11.51	I
50	-8.36	-8.62	A	130	-19.88	6.11	A	210	-44.51	0.00	I
51	-10.90	-8.57	A	131	-28.20	1.46	A	211	-20.70	-17.35	D
52	-14.07	-8.63	A	132	-28.20	5.45	A	212	-20.63	-17.35	D
53	-11.70	-8.84	B	133	-24.78	10.06	D	213	-4.95	-34.08	A
54	-9.63	-4.79	B	134	-26.95	14.39	D	214	-4.95	-34.08	A
55	-10.64	-4.82	B	135	-16.91	22.99	D	215	-1.95	-36.88	A
56	0.00	-14.30	G	136	-14.80	26.12	D	216	-1.95	-36.88	A
57	-11.77	-3.66	B	137	-16.90	27.38	D	217	-20.69	-36.88	A
58	-11.77	-2.63	B	138	-14.77	28.65	A	218	-20.69	-34.12	A
59	-11.69	-6.85	B	139	-12.75	31.45	A	219	-22.43	-22.51	A
60	-70.62	-10.62	D	140	-17.04	30.26	A	220	-25.22	-25.51	A
61	-20.61	-8.62	D	141	-18.28	26.72	A	221	-22.43	-12.19	A
62	-20.65	-4.92	D	142	-19.92	24.57	A	222	-25.22	-9.19	A
63	-22.59	0.00	A	143	-21.58	26.64	F	223	-20.69	-0.58	A
64	-16.94	0.00	A	144	-25.47	26.67	F	224	-20.69	2.18	A
65	-10.35	0.08	A	145	-9.64	18.69	C	225	20.69	2.18	A
66	-7.49	-21.86	G	146	-10.65	18.69	C	226	20.69	-0.58	A
67	-1.67	-18.90	A	147	-11.82	17.60	B	227	25.22	-9.36	A
68	-1.40	-30.32	A	148	-11.78	16.60	B	228	22.43	-12.36	A
69	-1.69	-24.77	A	149	-7.18	26.72	A	229	22.43	-22.51	A
70	-1.77	-28.27	C	150	-3.92	26.72	A	230	25.22	-25.51	A
71	-5.08	-28.40	A	151	-2.03	27.85	A	231	20.69	-34.12	A
72	3.37	-21.83	A	152	-2.02	23.82	A	232	20.69	-36.88	A
73	0.24	-30.42	A	153	-1.98	11.83	A				
74	1.65	-24.77	A	154	4.36	18.18	D				
75	0.82	-30.93	C	155	-1.19	12.65	D				
76	0.03	-29.34	G	156	3.65	26.69	A				
77	1.70	-18.92	A	157	6.90	26.69	A				
78	2.10	-8.69	A	158	2.02	23.84	A				
79	4.90	-17.61	A	159	0.00	44.43	D				
80	7.32	-22.69	A	160	4.35	44.49	D				

Figure 16.- Bolt hole locations in turntable.

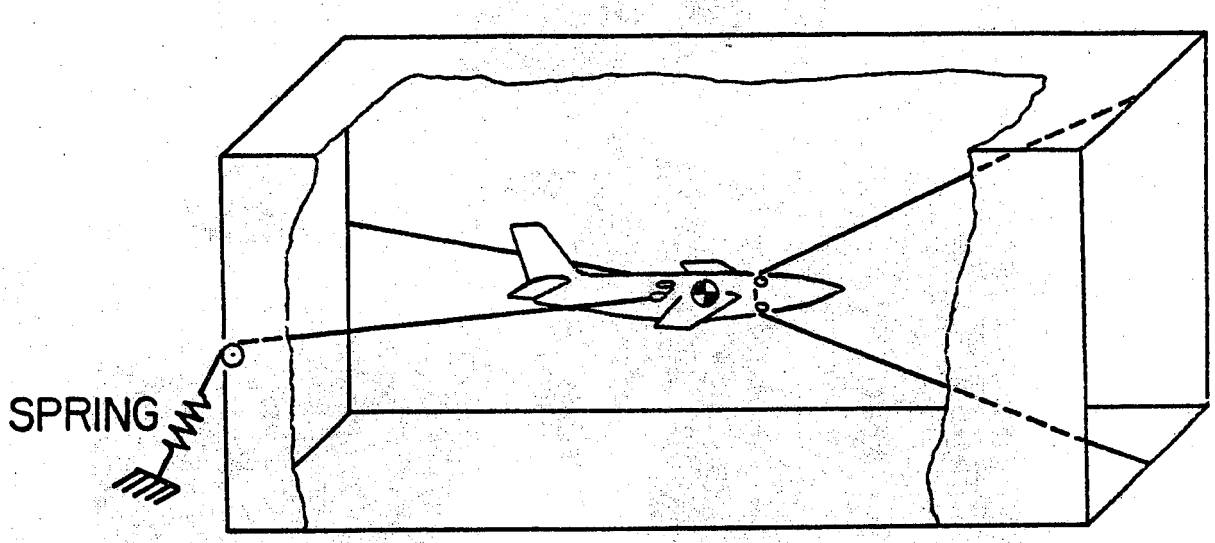

Figure 17.- Two-cable mount.

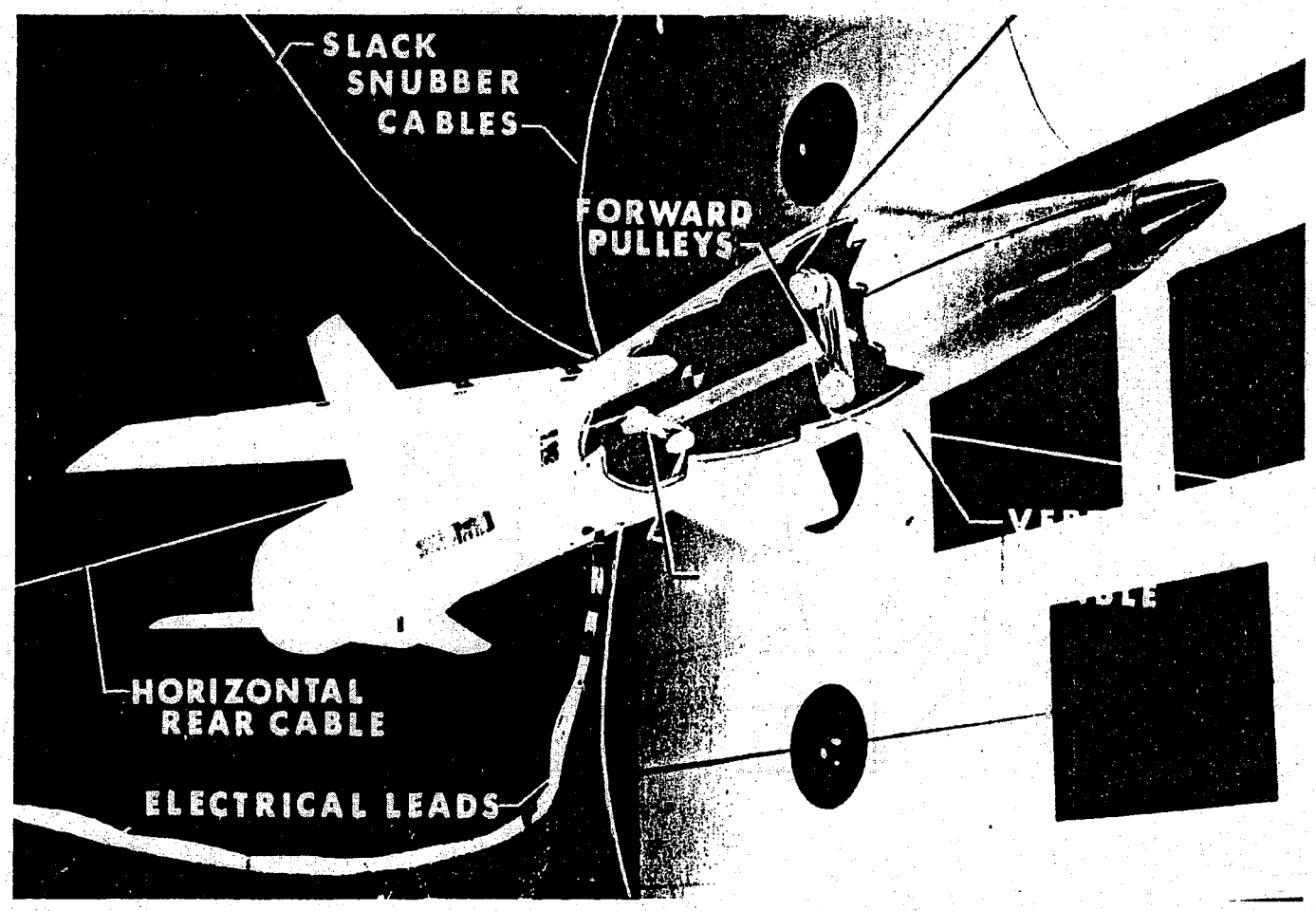

Figure 18 .- Model on two-cable mount.

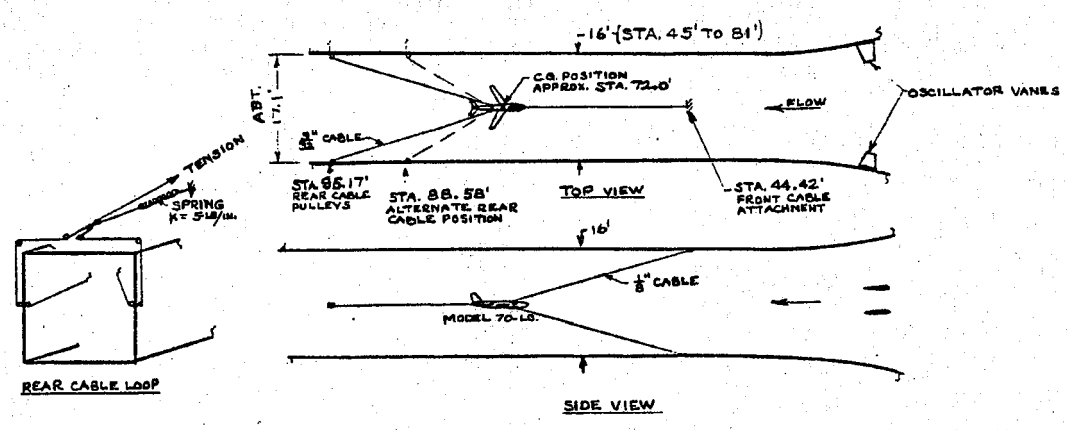

FRONT CABLE VERTICAL - REAR CABLE HORIZONTAL
(SNUBBERS NOT SHOWN)

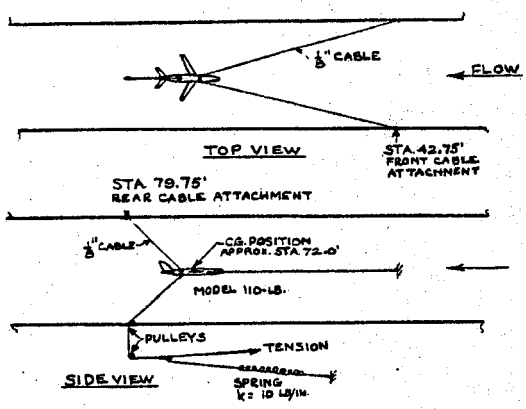

FRONT CABLE HORIZONTAL - REAR CABLE VERTICAL
(SNUBBERS NOT SHOWN)

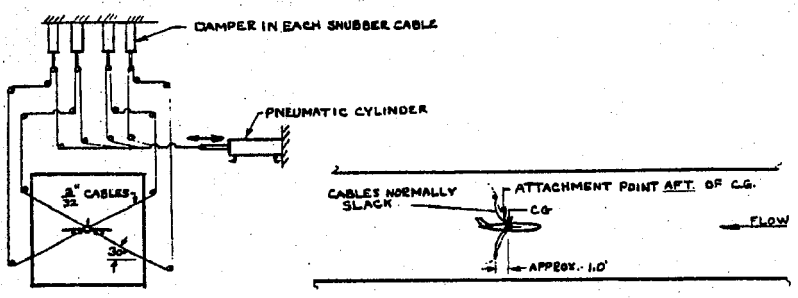

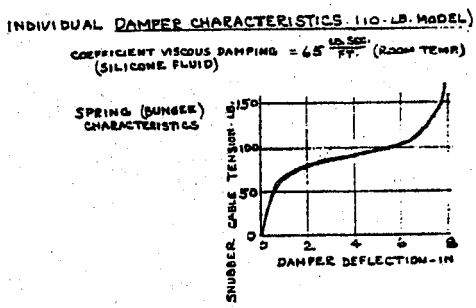

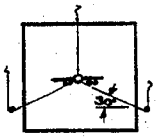

SNUBBER SYSTEM
(MOUNTING CABLES NOT SHOWN)

Figure 19.- Schematic diagram of typical two-cable mount systems and snubbers.

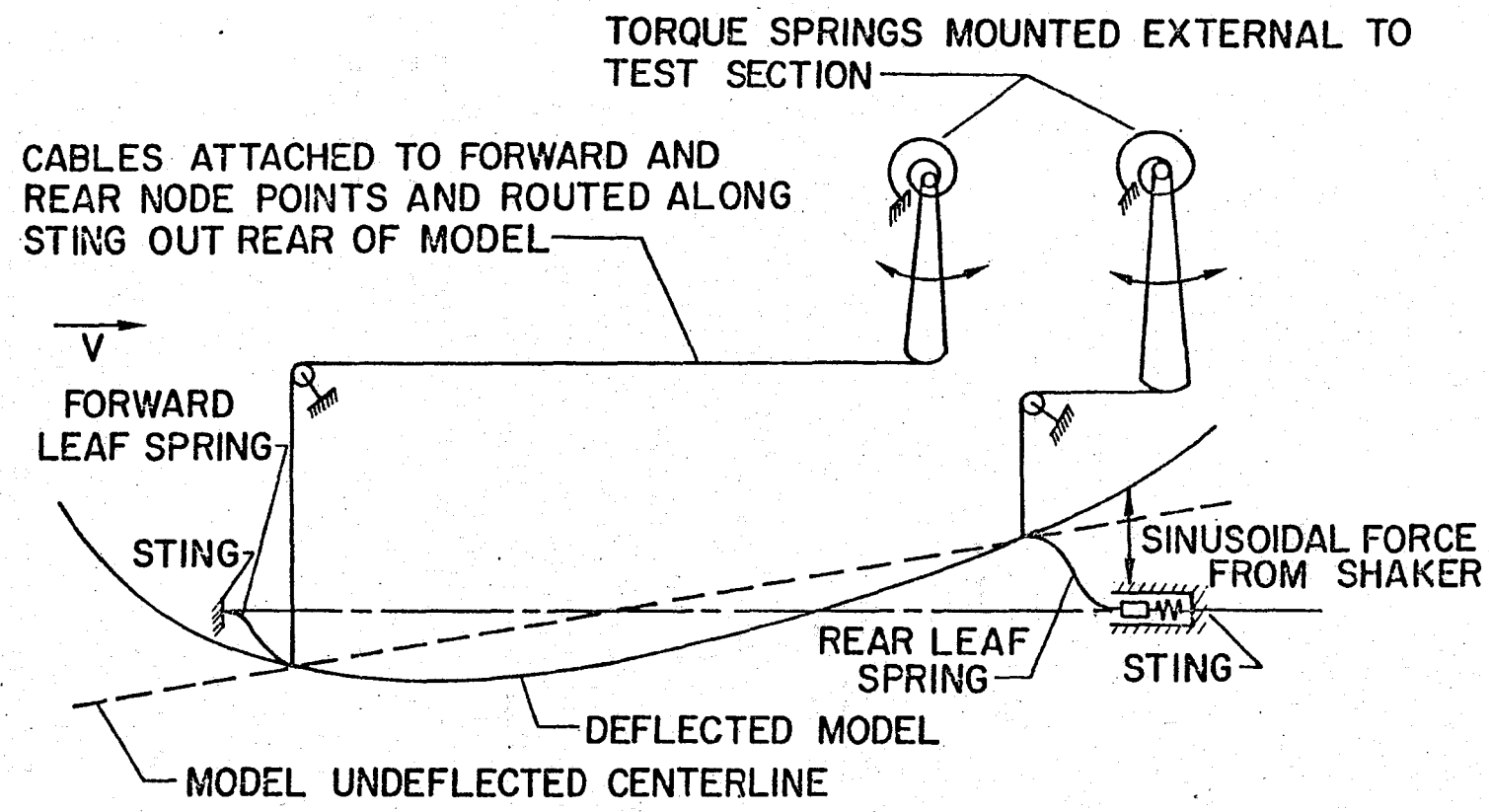

Figure 20 - Schematic diagram of aeroelastic buffet model support system.

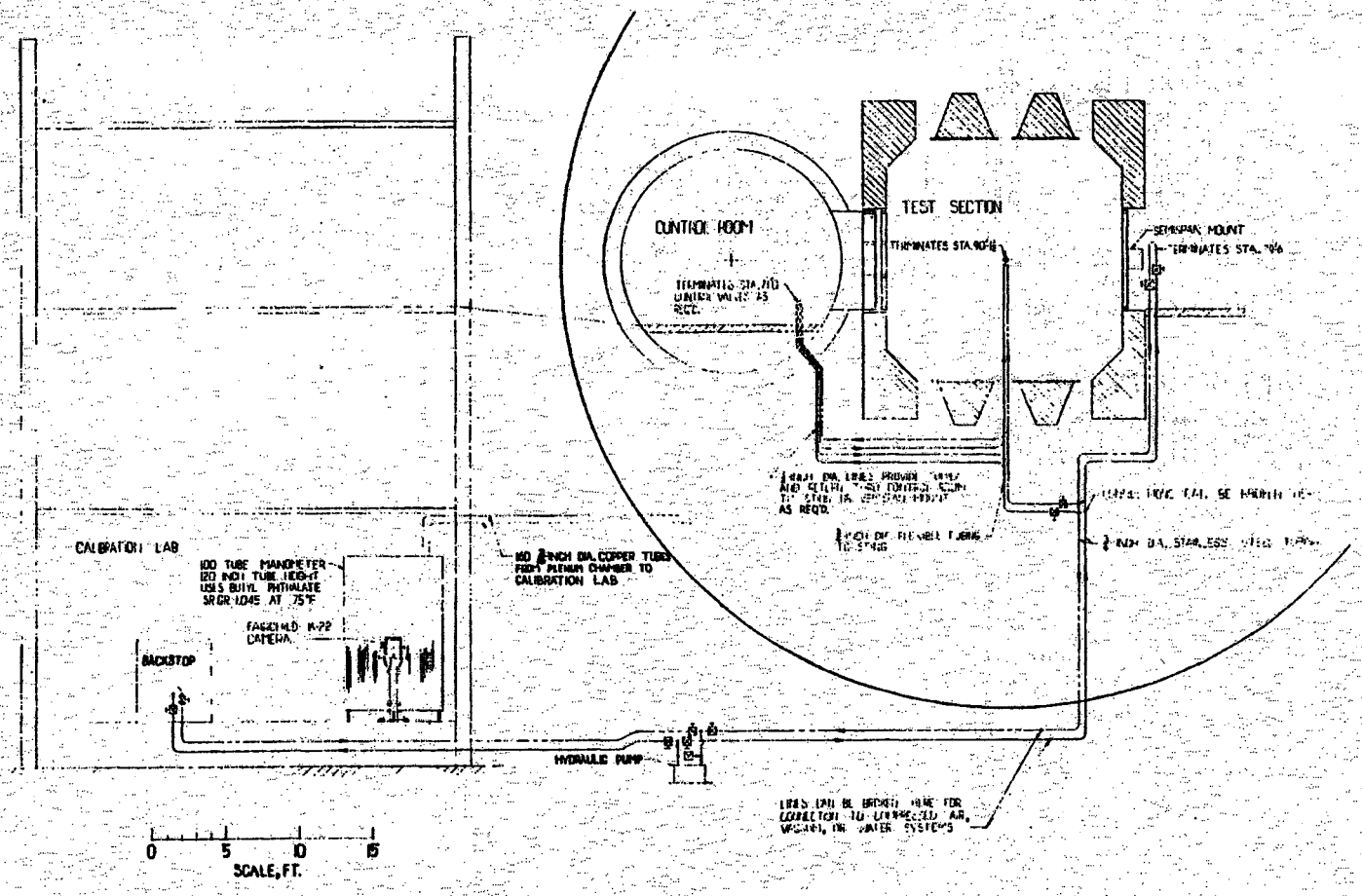

DETAILS OF UTILITIES

	PRESSURE	FLOW RATE
HYDRAULIC*	3000 PSI	12 GPM
WATER	55 PSI	
COMPRESSED AIR (DRY)	60 PSI	20 SCFM
	400 PSI	[illegible]
	600 PSI	600 SCFM
VACUUM	[illegible]	30 CFM (FULL)

*OIL IS MIL.SPEC.5606A, 5 MICRON FILTER

Figure 21 .- Layout of utilities.

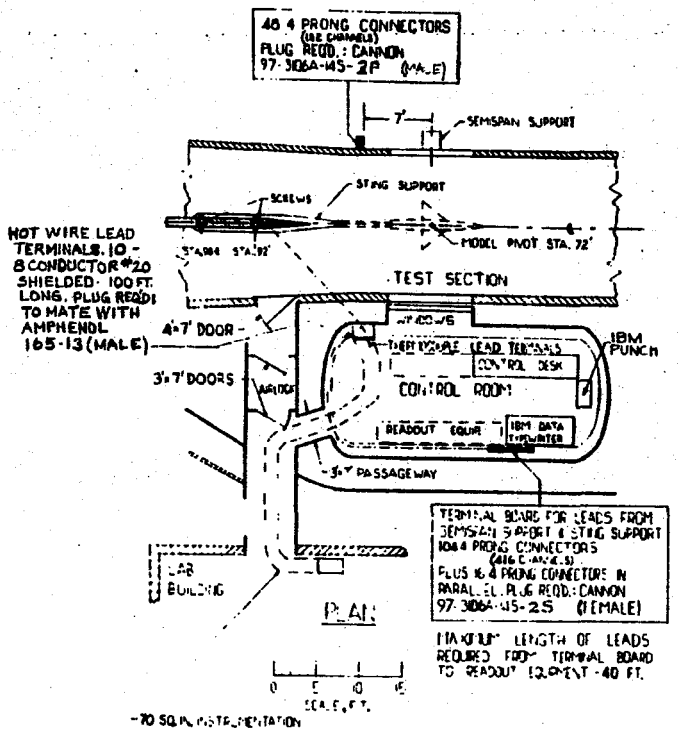

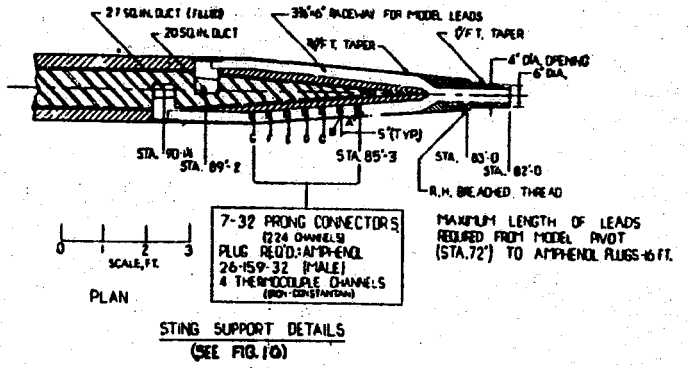

STING SUPPORT DETAILS
(SEE FIG. 10)

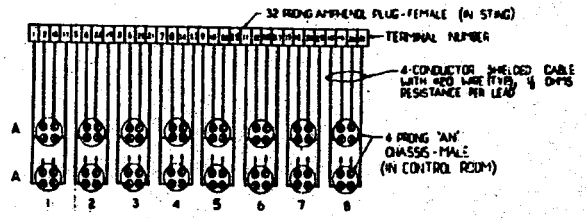

NOTE: GROUP A SHOWN, GROUP B IDENTICAL. GROUPS C THRU G DO NOT HAVE THE PARALLEL PLUGS.

	AMPHENOL PLUG	CANNON PLUG
STING MOUNT (224 CHANNELS)	A	A-1 THRU A-8
		A-1 THRU A-8
	B	B-1 THRU B-8
		B-1 THRU B-8
	C	C-1 THRU C-8
	D	D-1 THRU D-8
	E	E-1 THRU E-8
	F	F-1 THRU F-8
	G	G-1 THRU G-8
	CANNON PLUG	
EAST PLATFORM (16 CHANNELS)	H-1 THRU H-8	H-1 THRU H-8
	J-1 THRU J-8	J-1 THRU J-8
	K-1 THRU K-8	K-1 THRU K-8
	L-1 THRU L-8	L-1 THRU L-8
	M-1 THRU M-8	M-1 THRU M-8
	N-1 THRU N-8	N-1 THRU N-8
P.C. BRICK	P-1 THRU P-8	P-1 THRU P-8

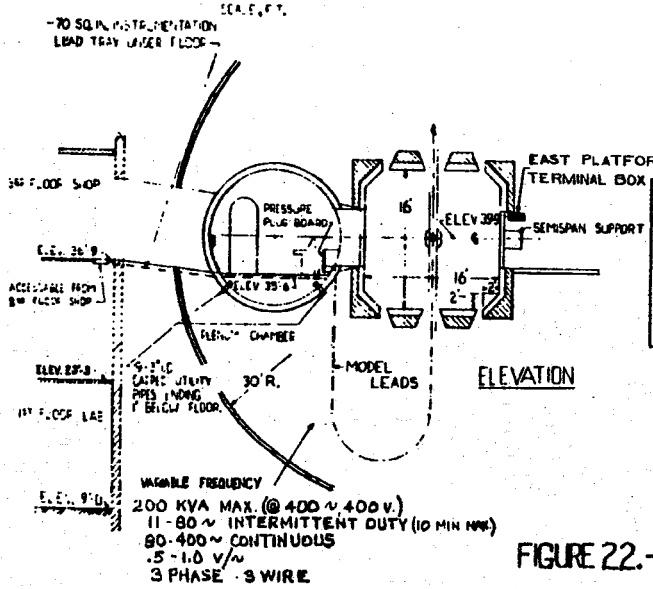

POWER AVAILABLE IN THE CONTROL ROOM

FREQ.		VOLT.	AMP.	CIRCUITS
60~		110	140	REGULATED - NIGHT - 5
60~		110	60	UNREGULATED - 3
60~		110	179	NIGHT - UNREGULATED - 8
60~	3φ	440	30	UNREGULATED - 1
400~	3φ	120/208		5 KW
60~		220	30	NIGHT - UNREG. - 1
D.C.				PORTABLE UNITS

FIGURE 22.- MODEL LEADS LAYOUT
DYNAMIC

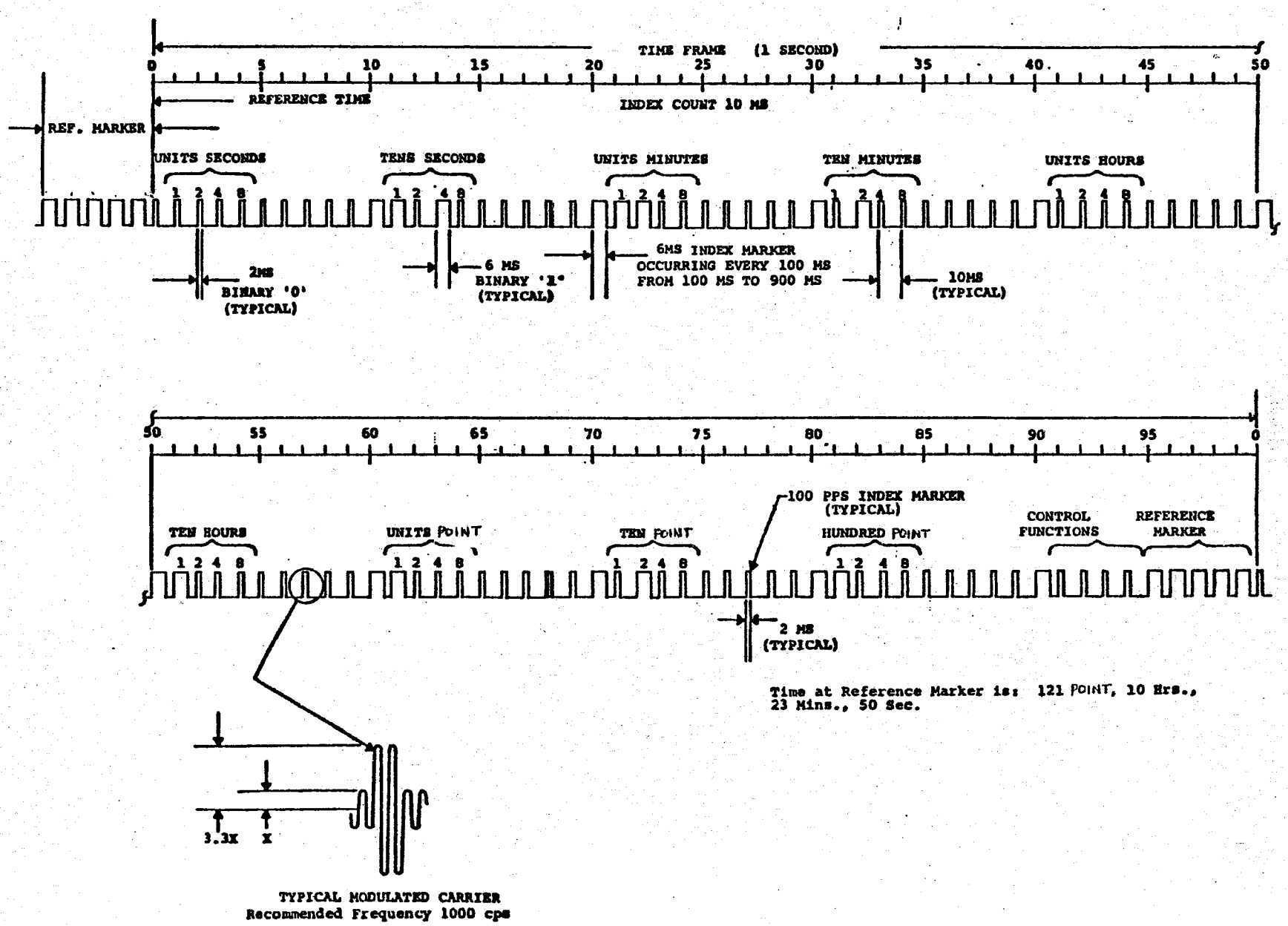

Figure 23.- NASA 36-bit time code (modified for point number).

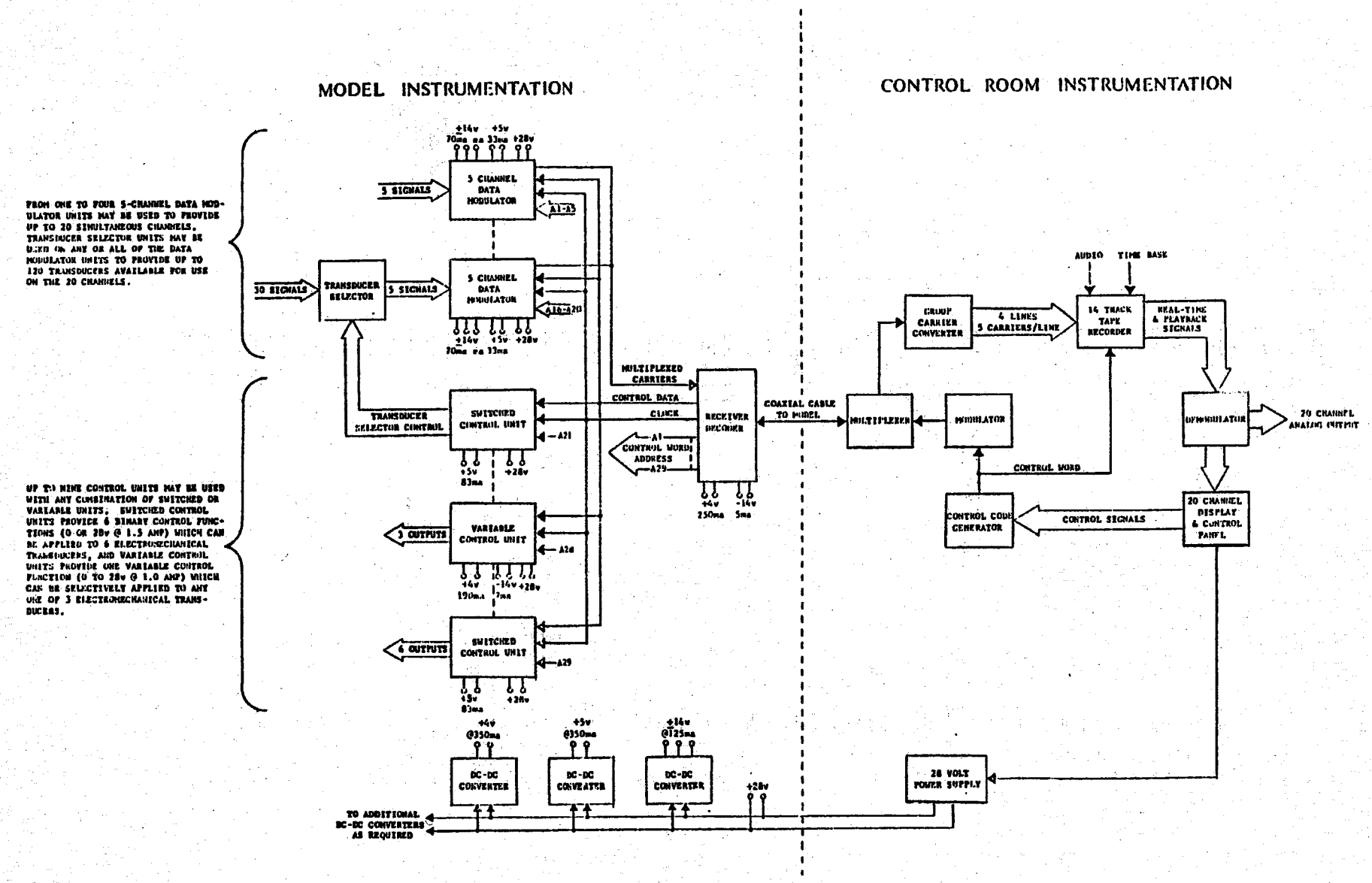

Figure 24 .- General block diagram of telemetry system.

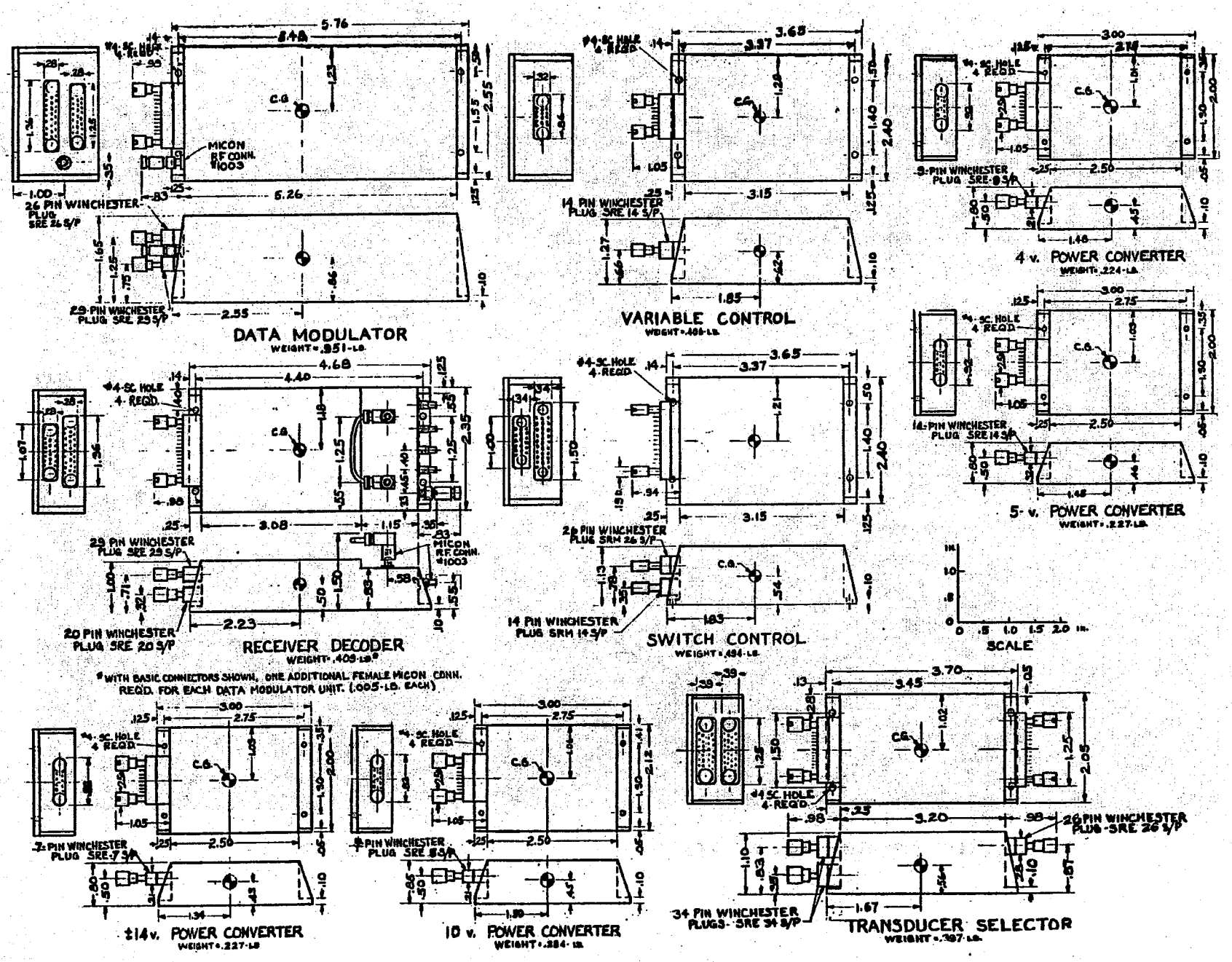

Figure 25 .- Dimensions and mass properties of telemetry components.

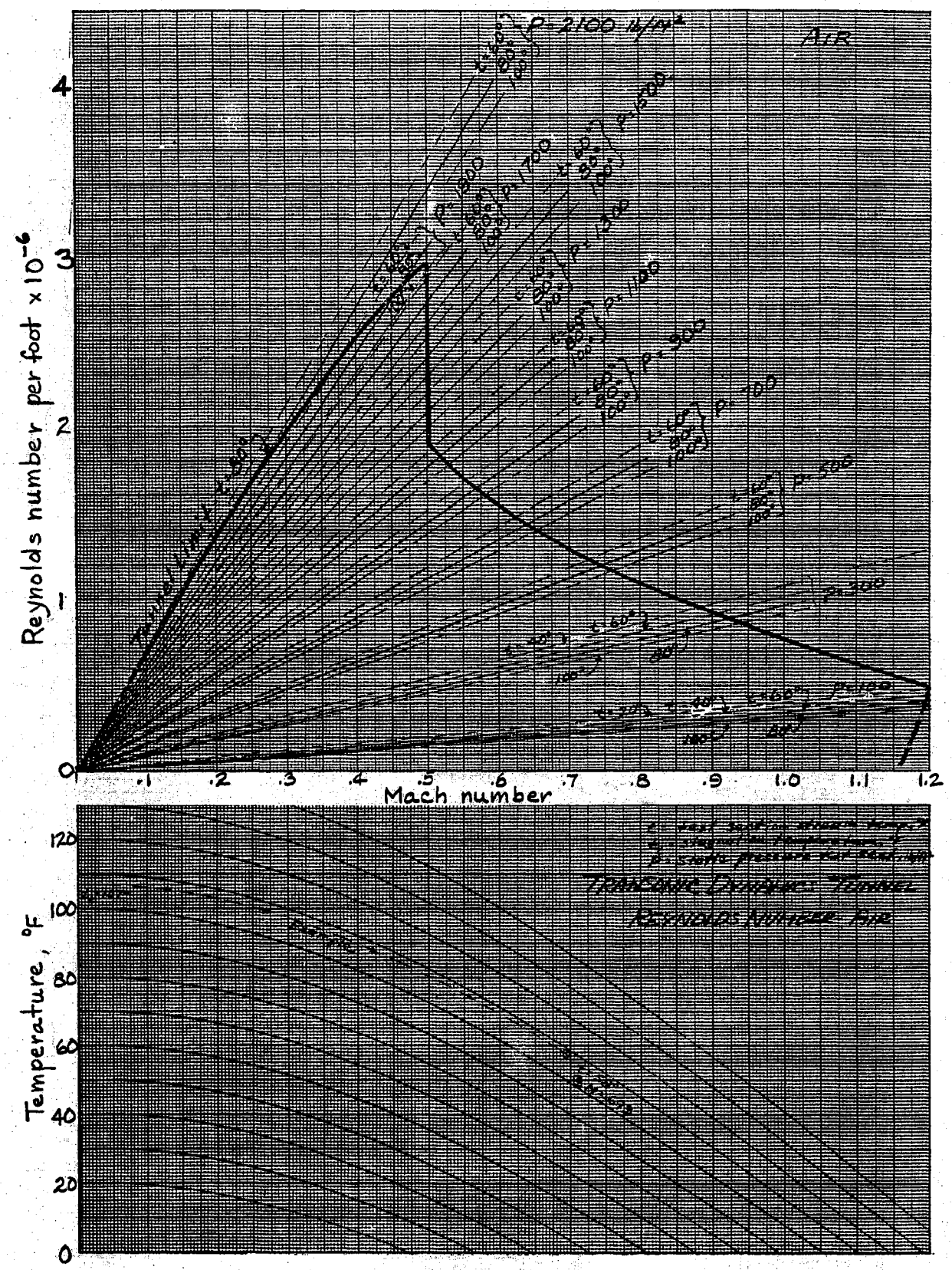

Figure 26.- Variation of Reynolds Number with Mach Number for Air.

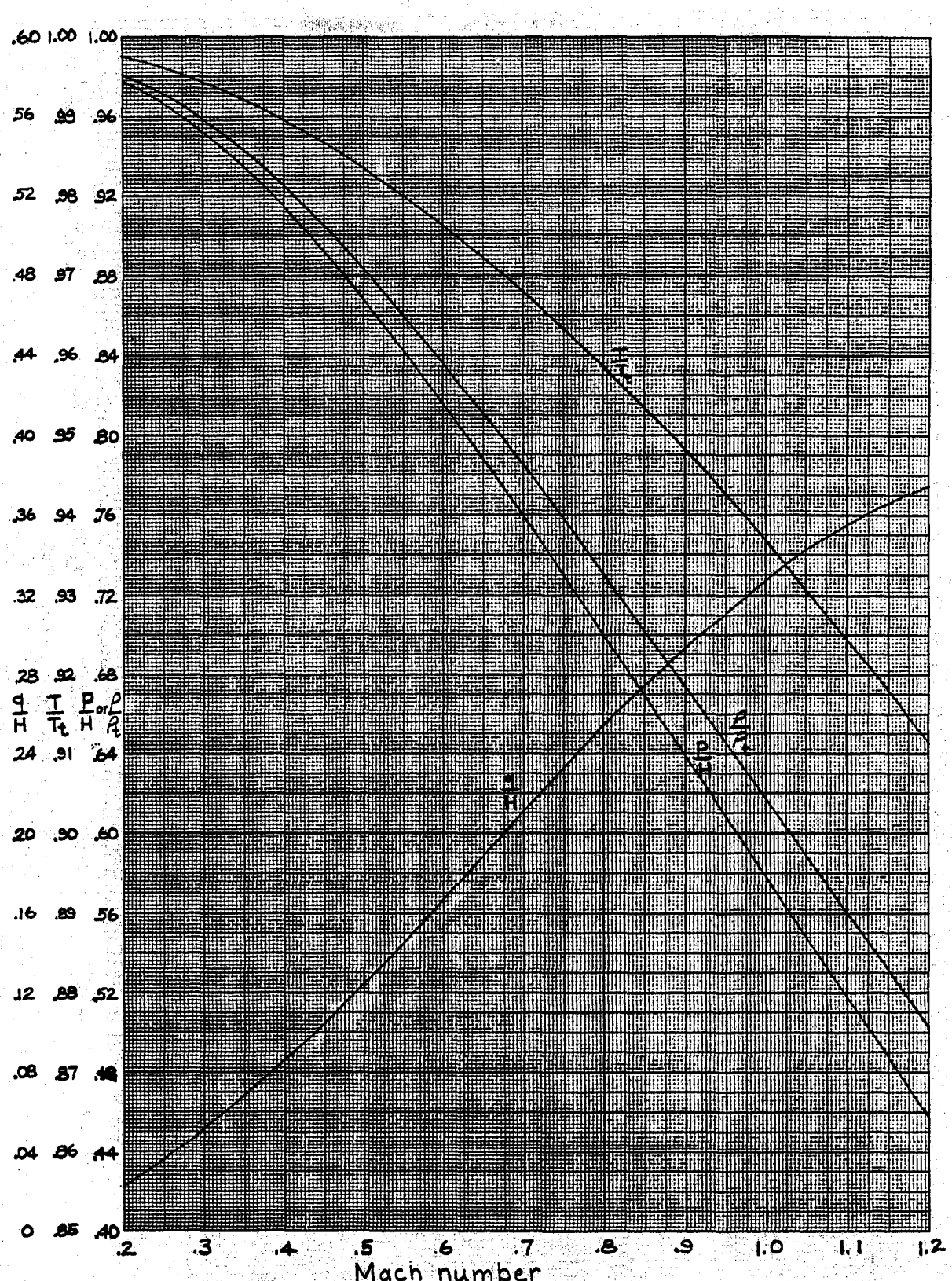

Figure 27.- Compressible flow relations for 95-percent Freon 12-Air mixture.

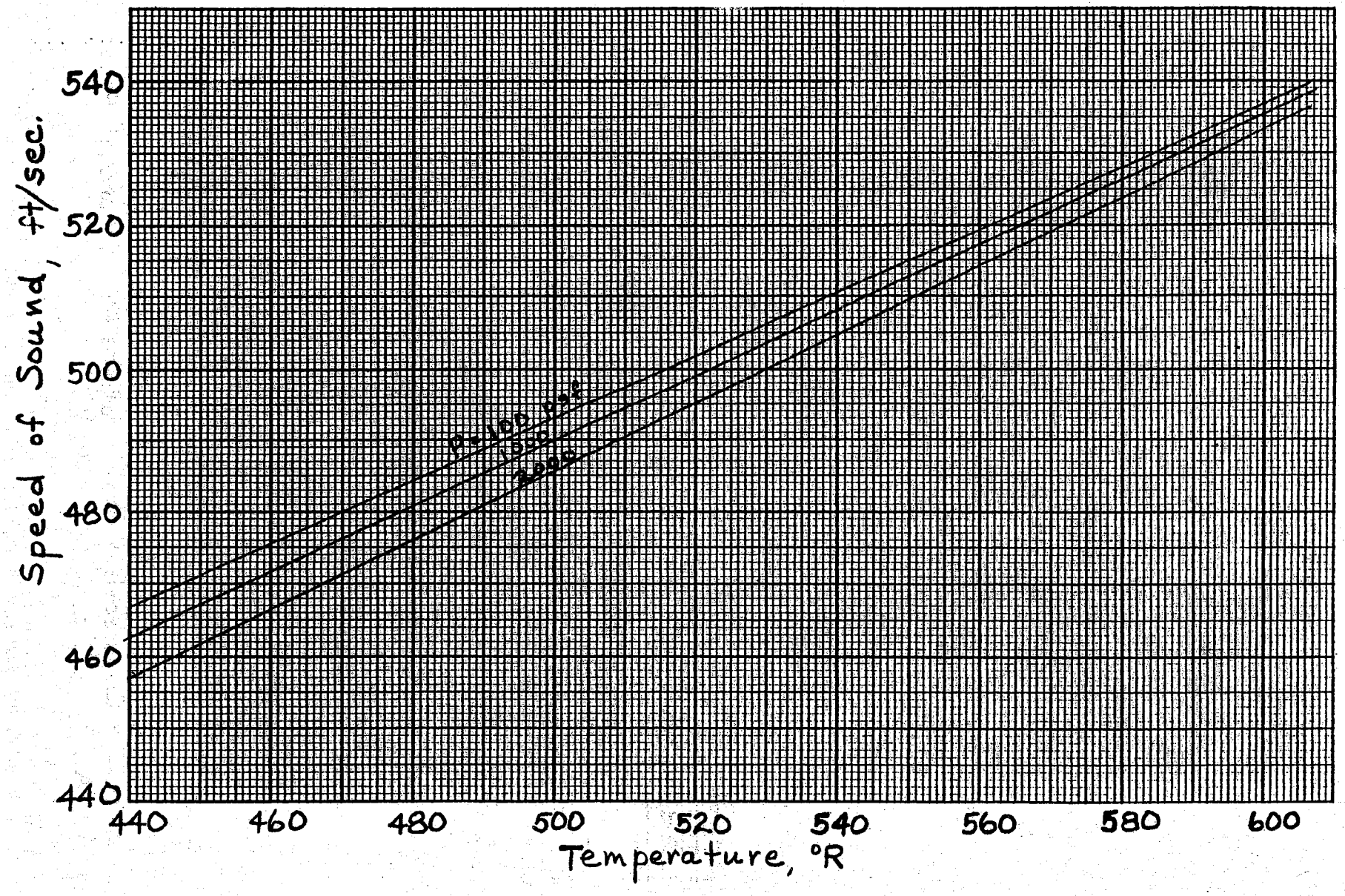

Figure 28.- Speed of sound for 95-percent Freon 12-Air mixture.

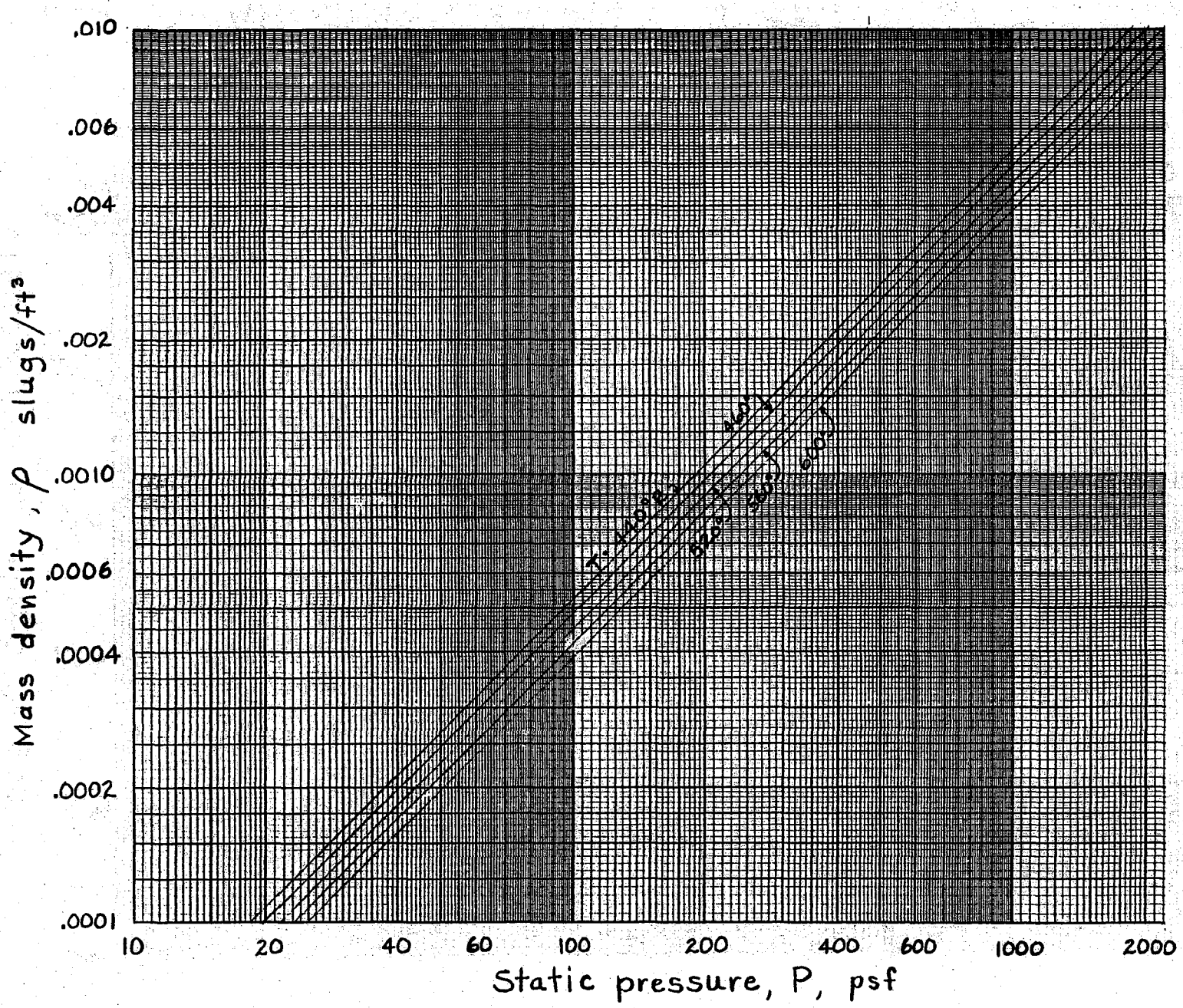

Figure 29.- Mass density of 95-percent Freon 12-Air mixture.

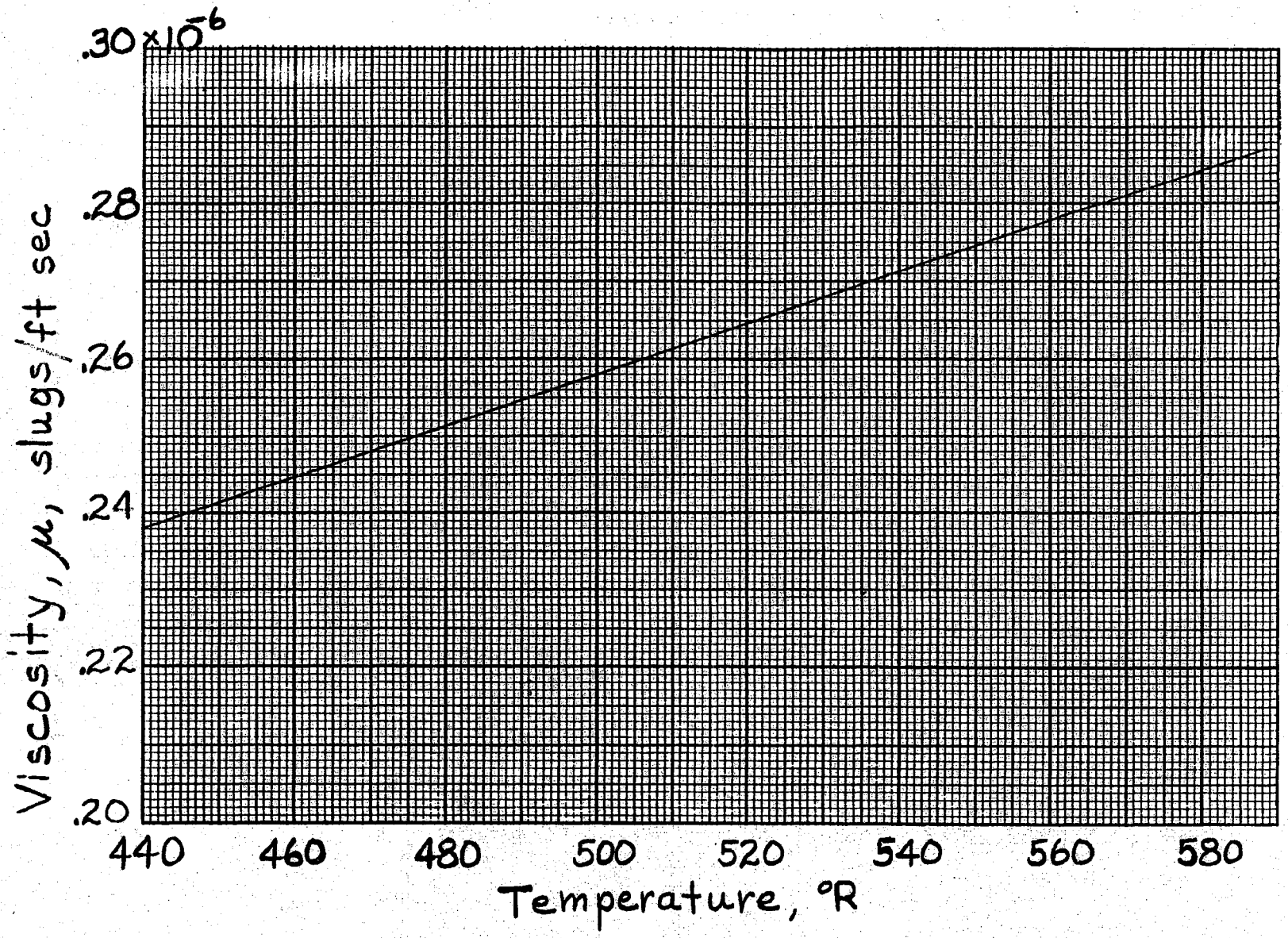

Figure 30.- Absolute viscosity of 95-percent Freon 12-Air mixture.

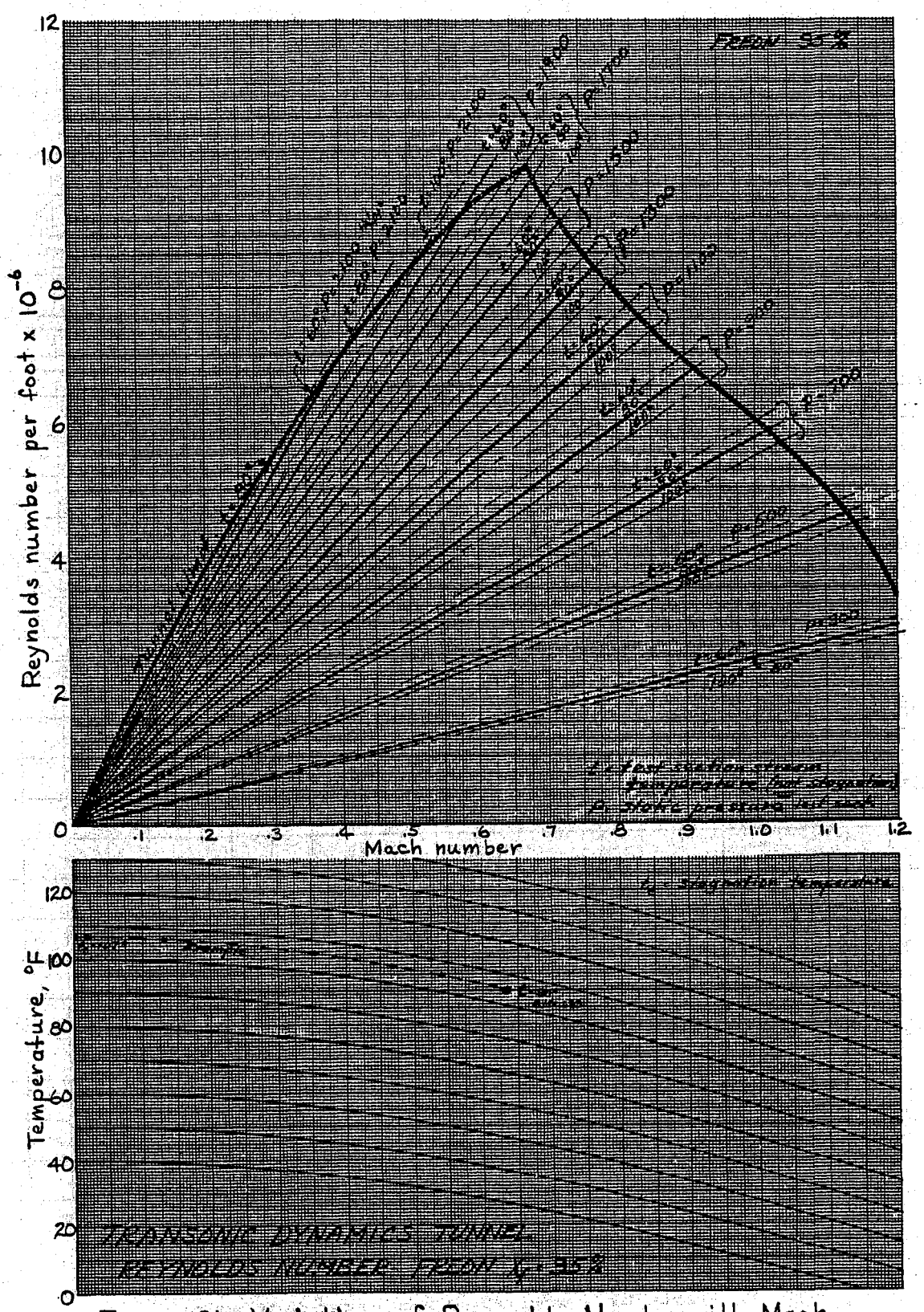

Figure 31.- Variation of Reynolds Number with Mach Number for 95-percent Freon 12- Air Mixture.

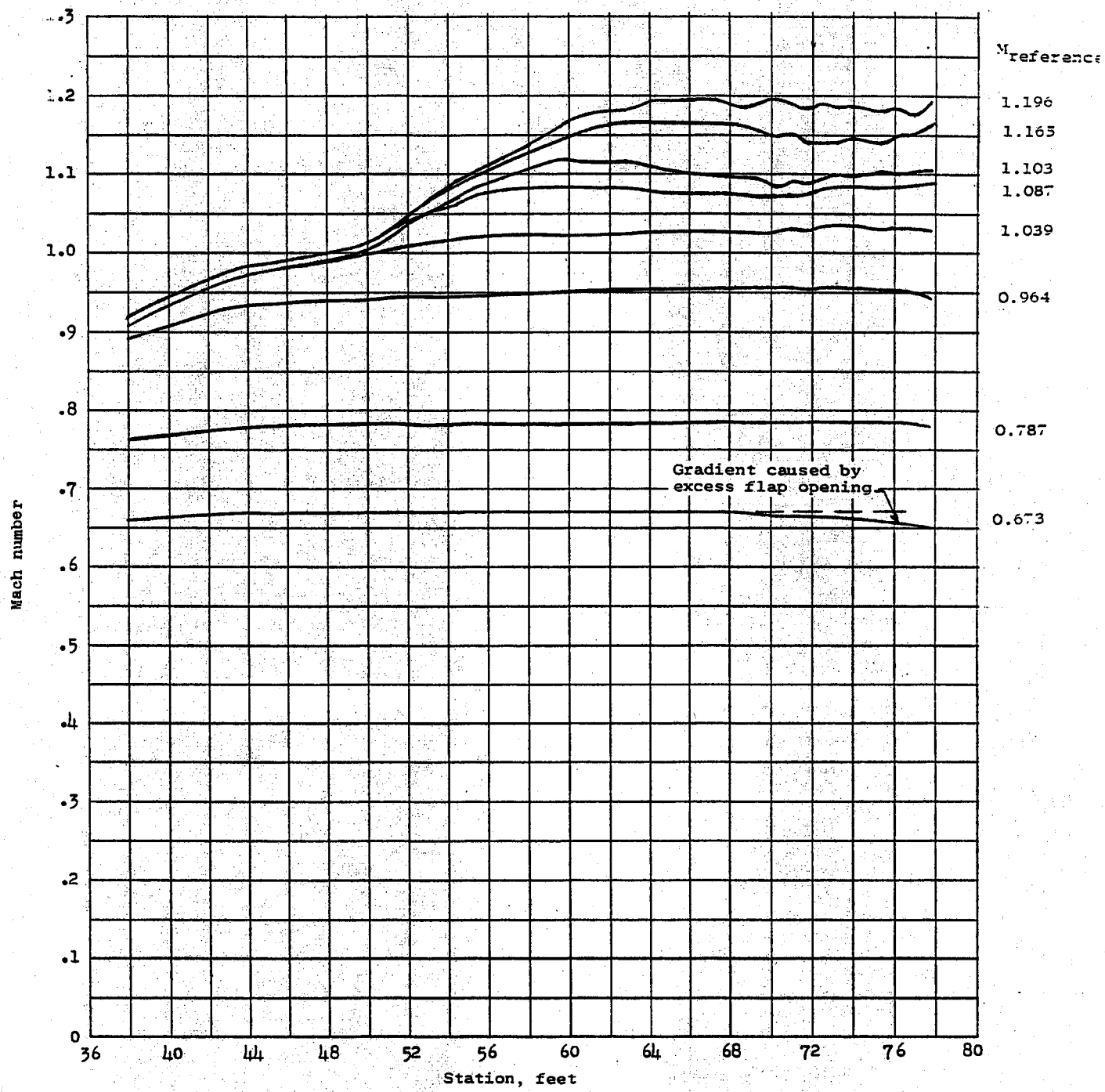

(a) Tunnel centerline. Test medium, air.

Figure 32.- Longitudinal Mach number distribution.

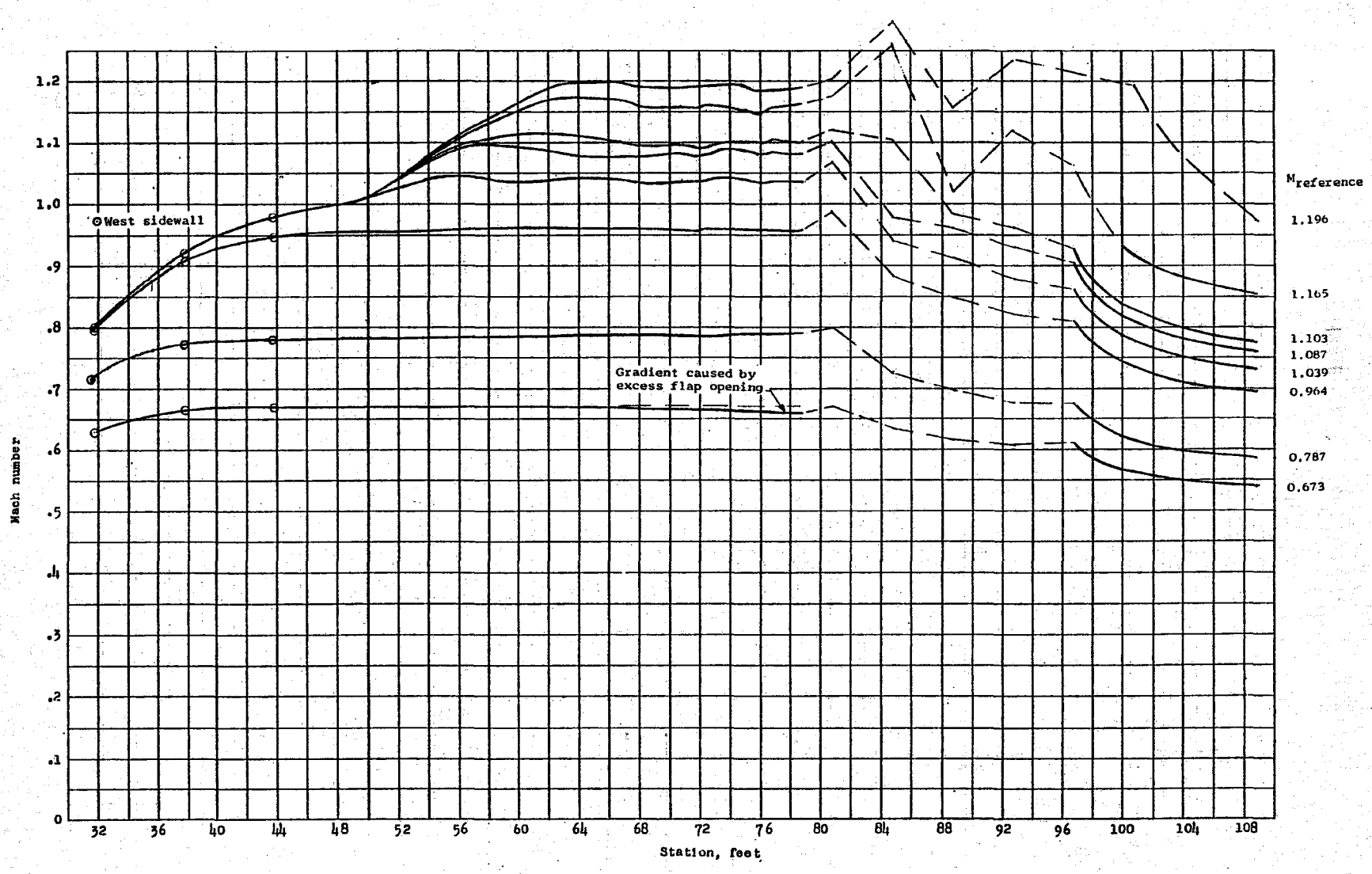

(b) Tunnel sidewalls. Test medium, air.

Figure 32 .- Continued.

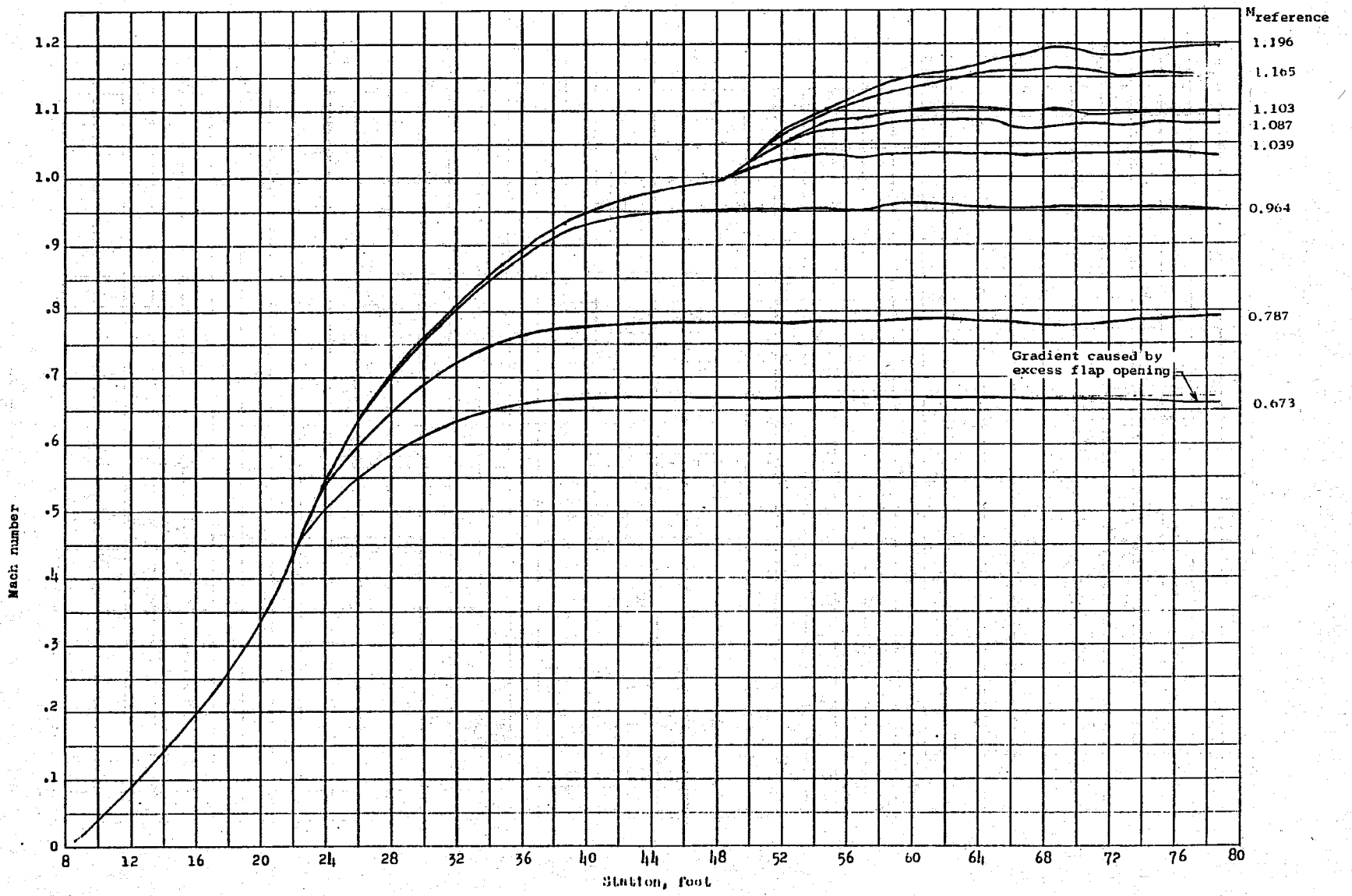

(C) Tunnel top. Test medium, air.

Figure 32 .- Continued.

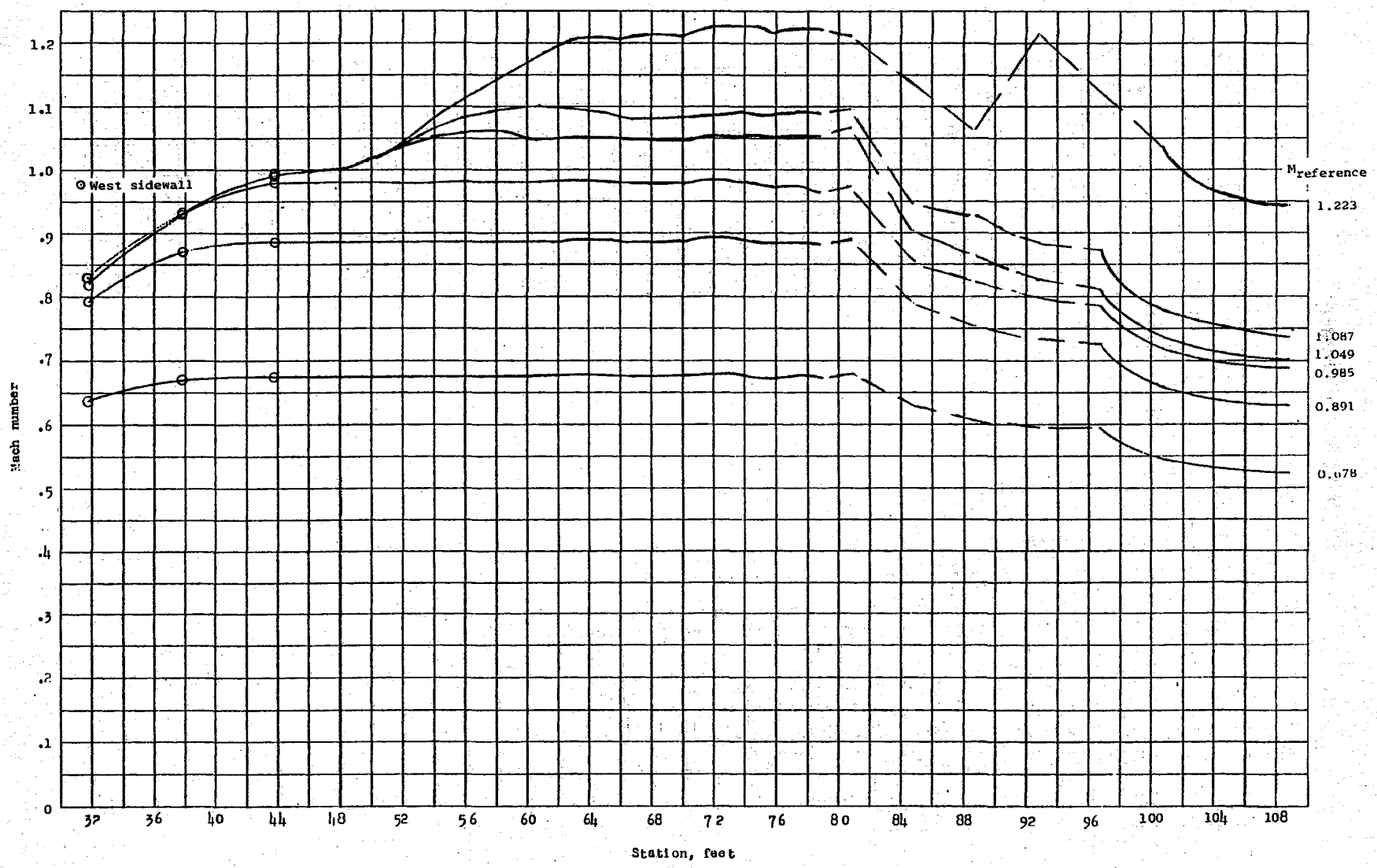

(d) Tunnel sidewalls. Test medium, Freon.

Figure 32.- Continued.

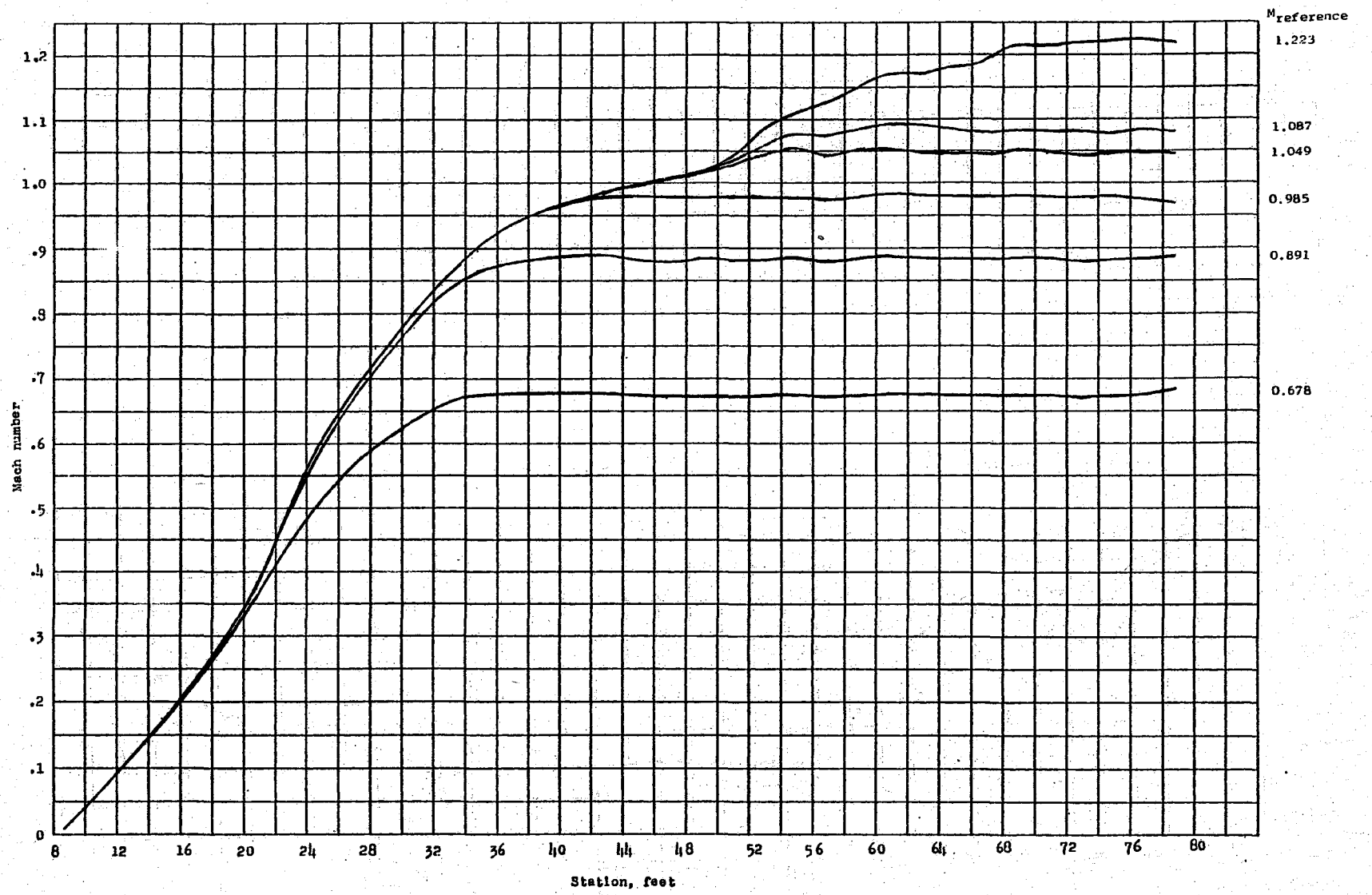

(e) Tunnel top. Test medium, Freon.

Figure 32.- Concluded.

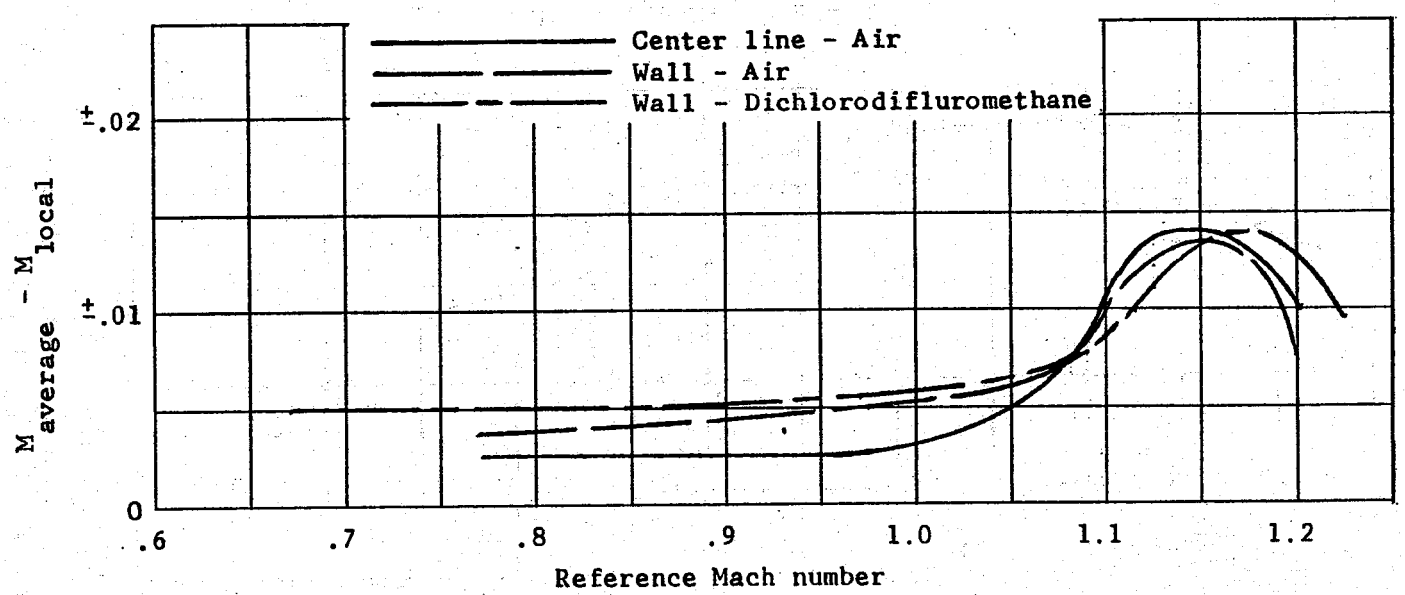

Figure 33.- Maximum static variation from average value of local Mach number between stations 64 feet and 78 feet.

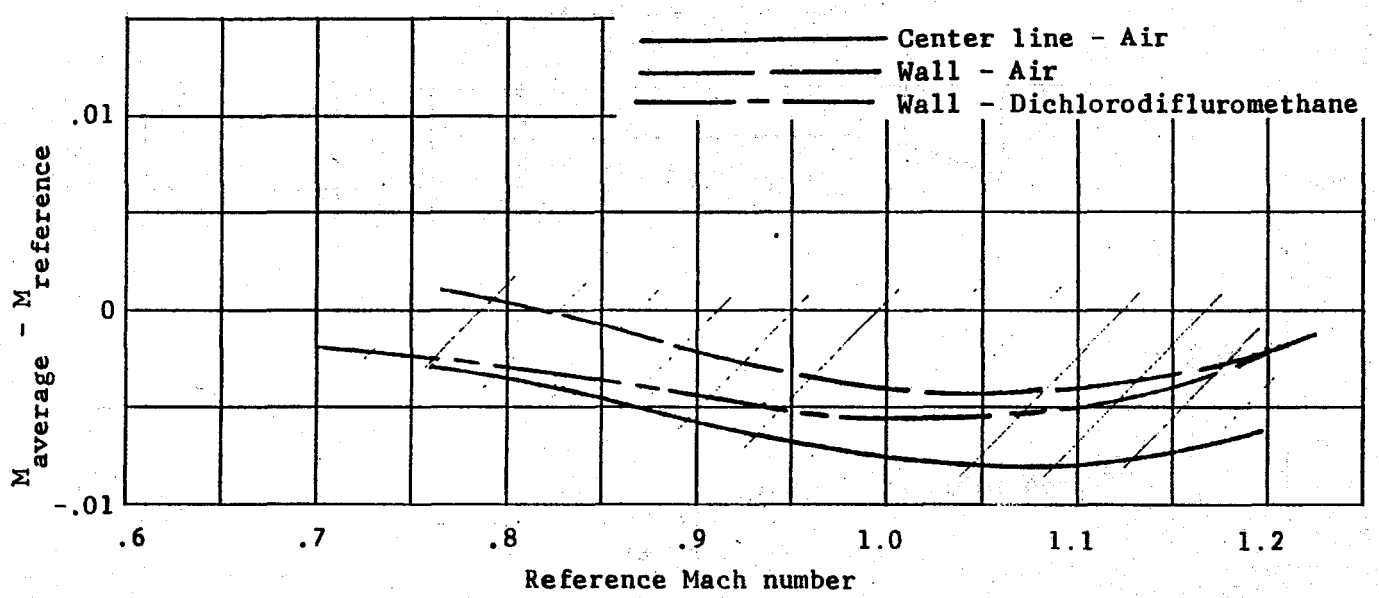

Figure 34.- Approximate maximum deviation from reference Mach number of average Mach number between stations 64 feet and 78 feet.

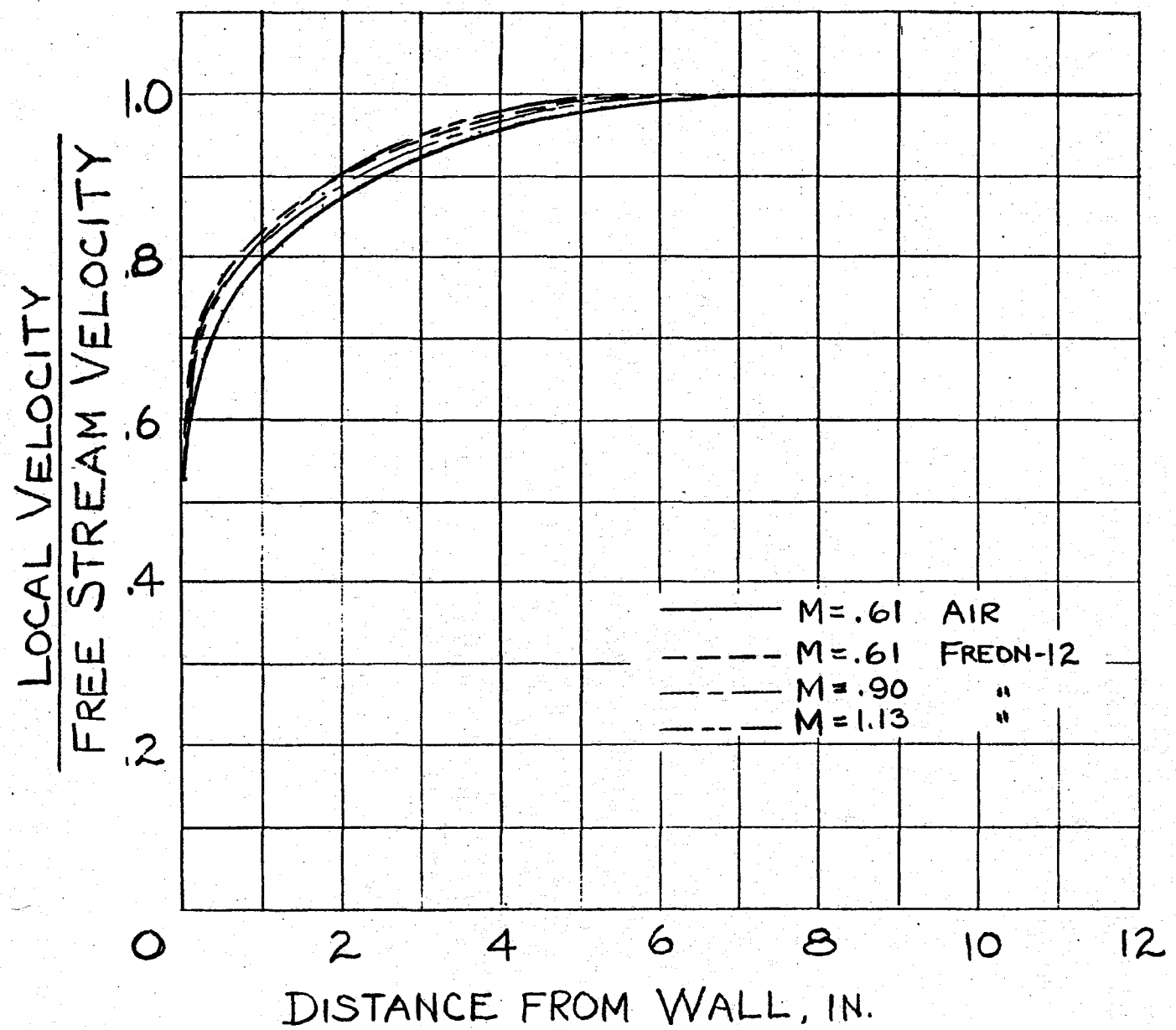

Figure 35.- Sample test section wall boundary layer velocity profiles. (Sta. 69.5 ft., center, east sidewall.)

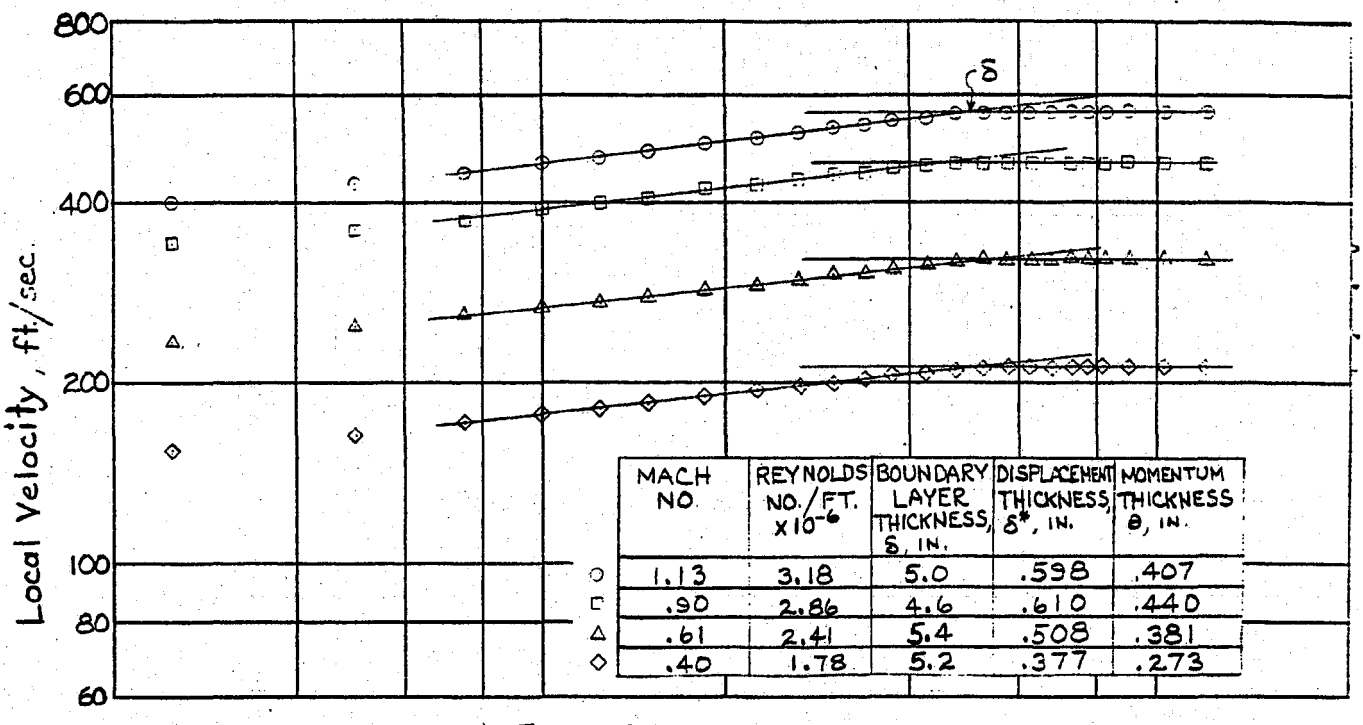

	MACH NO.	REYNOLDS NO./FT. $\times 10^{-6}$	BOUNDARY LAYER THICKNESS, δ, IN.	DISPLACEMENT THICKNESS, δ*, IN.	MOMENTUM THICKNESS θ, IN.
○	1.13	3.18	5.0	.598	.407
□	.90	2.86	4.6	.610	.440
△	.61	2.41	5.4	.508	.381
◇	.40	1.78	5.2	.377	.273

(a) Freon 12

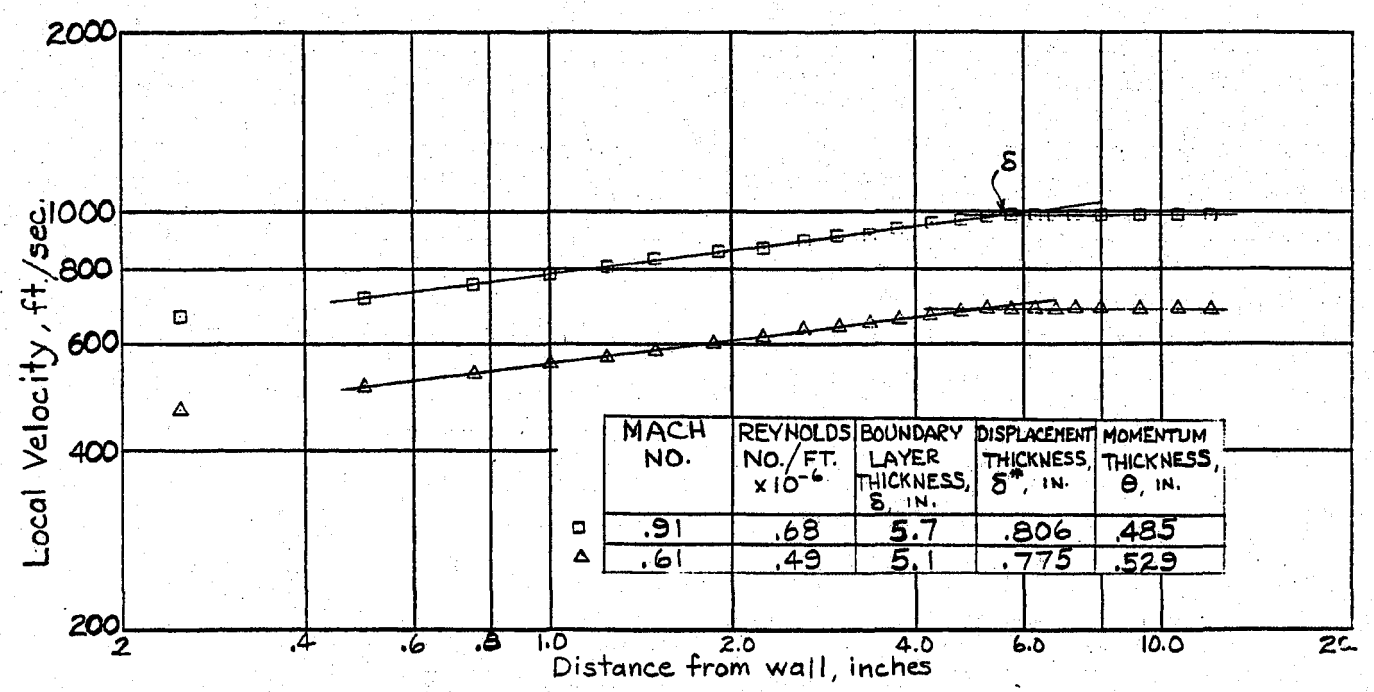

	MACH NO.	REYNOLDS NO./FT. $\times 10^{-6}$	BOUNDARY LAYER THICKNESS, δ, IN.	DISPLACEMENT THICKNESS, δ*, IN.	MOMENTUM THICKNESS, θ, IN.
□	.91	.68	5.7	.806	.485
△	.61	.49	5.1	.775	.529

(b) Air.

Figure 36.- Test section wall boundary layer thickness. (Sta. 69.5 ft center, east sidewall.)

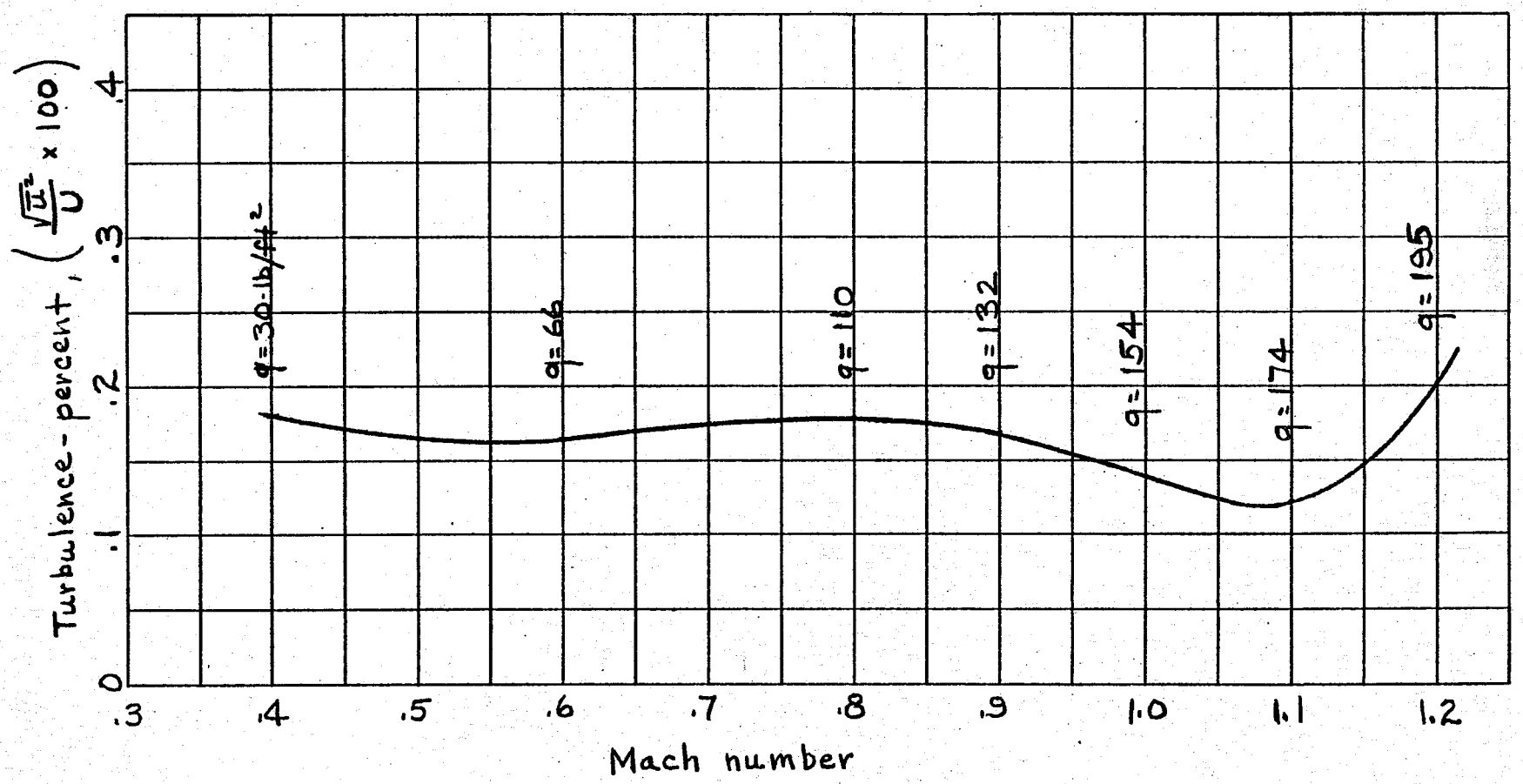

Figure 37.- Preliminary turbulence survey. Sta. 72-0, centerline, Freon. X-hot wire probe.

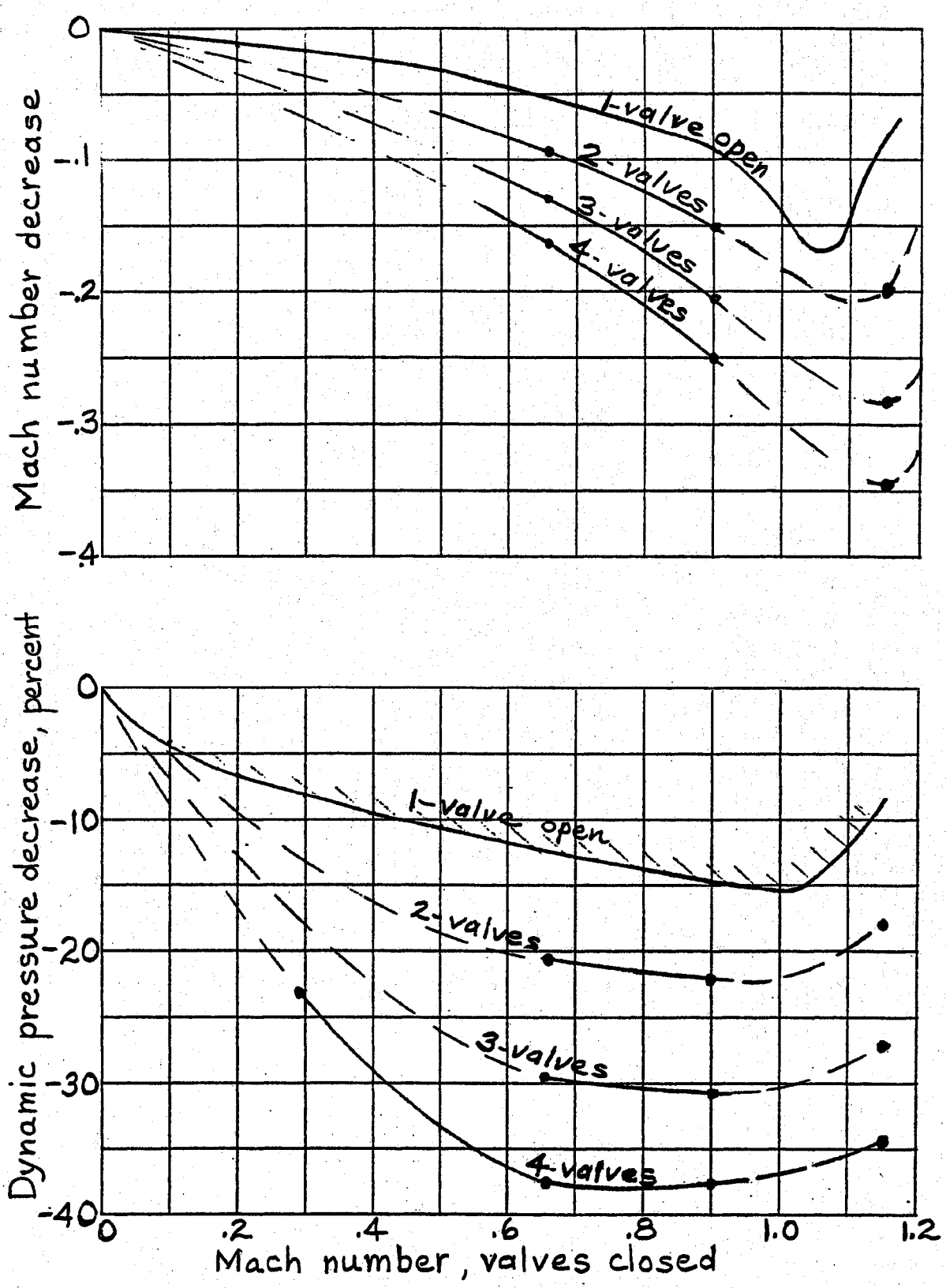

Figure 38.- Effect of bypass valve operation.

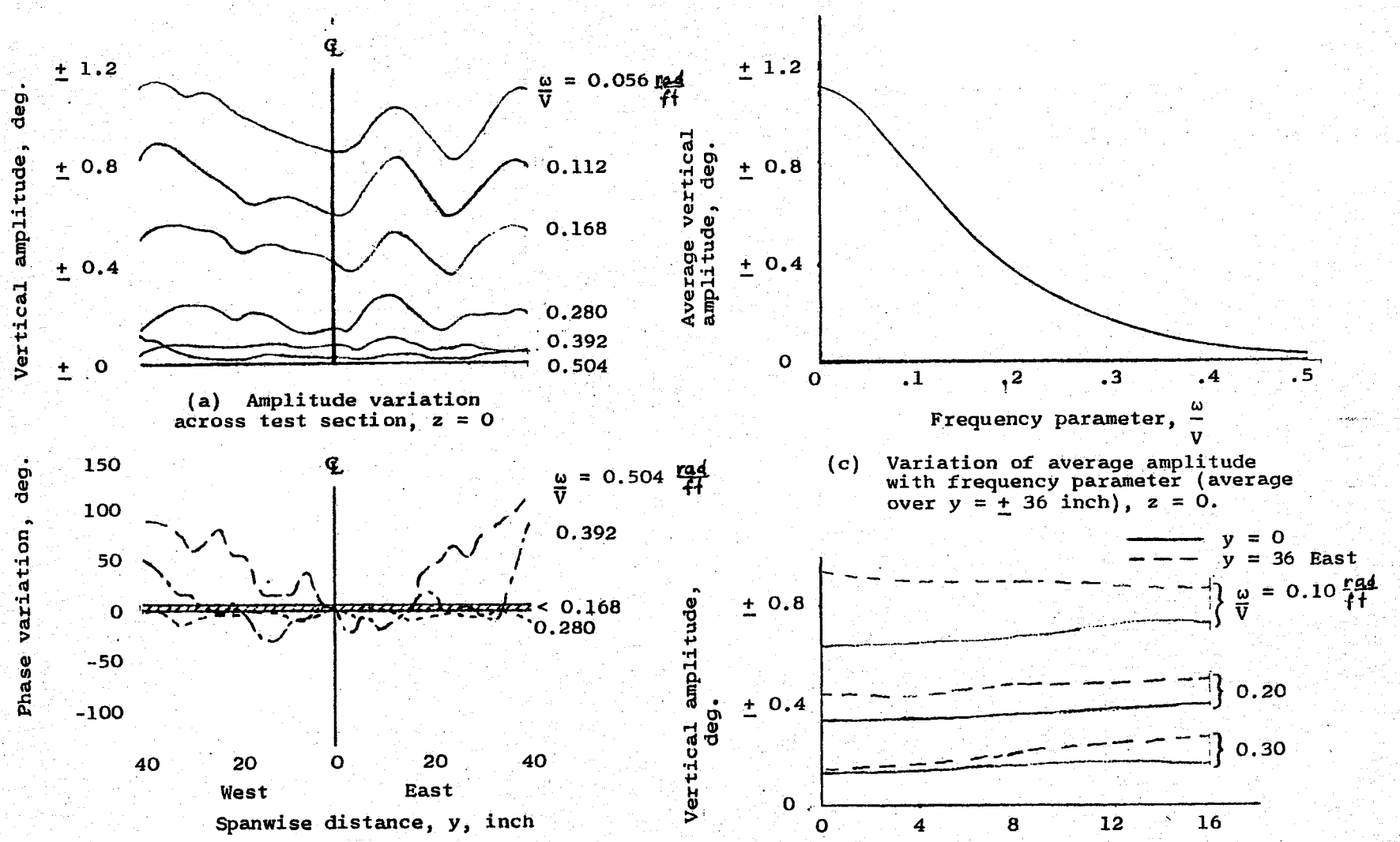

Figure 39.- Representative characteristics of airstream oscillator at Sta. 72.0 ft, M = 0.22, q = 53 psf, Freon-12, oscillator vane angle ± 5.93 deg., vanes in phase.

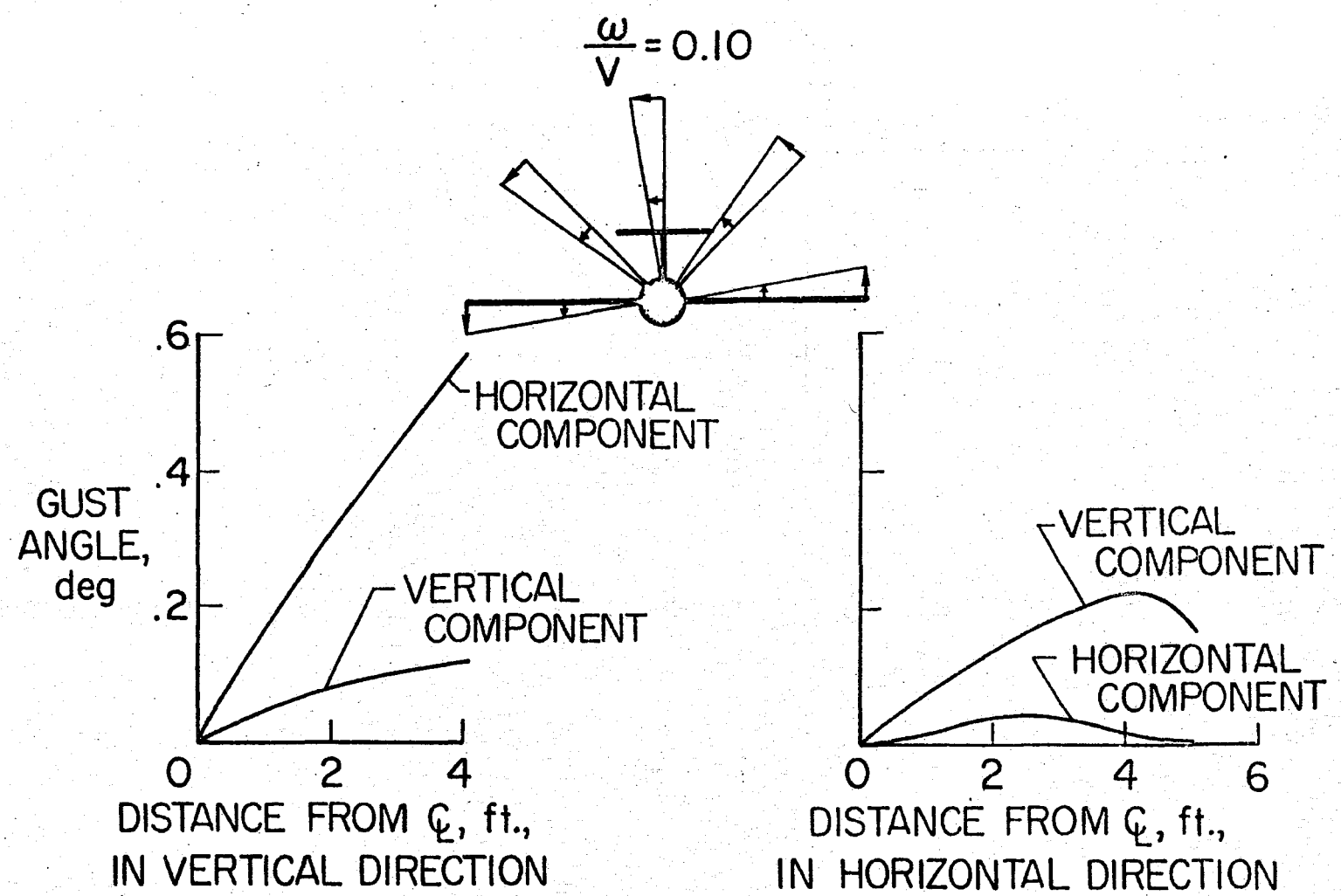

Figure 40.- Variation of vertical and horizontal components of gust angle across stream along axes through tunnel center line. Vanes 180° "out of sync," vane angle ±6°, Mach number 0.23.

NASA-Langley, 1962